Journal of Medicinal Chemistry

Article

Discovery of reversible DNA methyltransferase and lysine methyltransferase G9a inhibitors with antitumoral in vivo efficacy

Obdulia Rabal, Edurne San José - Eneriz, Xabier Agirre, Juan A Sánchez-Arias, Amaia Vilas-Zornoza, Ana Ugarte, Irene De Miguel, Estibaliz Miranda, Leire Garate, Mario Fraga, Pablo Santamarina, Raul Fernandez Perez, Raquel Ordoñez, Elena Sáez, Sergio Roa, Maria Jose Garcia-Barchino, Jose Angel Martinez-Climent, Yingying Liu, Wei Wu, Musheng Xu, Felipe Prosper, and Julen Oyarzabal

J. Med. Chem., **Just Accepted Manuscript** • DOI: 10.1021/acs.jmedchem.7b01926 • Publication Date (Web): 28 Jun 2018

	of Navarra, Small Molecule Discovery

Discovery of reversible DNA methyltransferase and lysine methyltransferase G9a inhibitors with antitumoral in vivo efficacy

Obdulia Rabal,[1,6] Edurne San José-Enériz,[2,6] Xabier Agirre,[2,6] Juan Antonio Sánchez-Arias,[1] Amaia Vilas-Zornoza,[2] Ana Ugarte,[1] Irene de Miguel,[1] Estíbaliz Miranda,[2] Leire Garate,[2] Mario Fraga,[3] Pablo Santamarina,[3] Raul Fernandez Perez,[3] Raquel Ordoñez,[2] Elena Sáez,[1] Sergio Roa,[2] María José García-Barchino,[2] José Angel Martínez-Climent,[2] Yingying Liu,[4] Wei Wu,[4] Musheng Xu,[4] Felipe Prosper[2,5,*] and Julen Oyarzabal[1,*]

[1]Small Molecule Discovery Platform, Molecular Therapeutics Program, [2]Area de Hemato-Oncología, IDISNA, Ciberonc, Center for Applied Medical Research (CIMA), University of Navarra, Avenida Pio XII 55, E-31008 Pamplona, Spain

[3]Nanomaterials and Nanotechnology Research Center (CINN-CSIC)-Universidad de Oviedo-Principado de Asturias, Avenida de la Vega, 4-6, 33940 El Entrego, Spain

[4]WuXi Apptec (Tianjin) Co. Ltd., TEDA, No. 111 HuangHai Road, 4th Avenue, Tianjin 300456, PR China

[5]Departmento de Hematología, Clinica Universidad de Navarra, University of Navarra, Avenida Pio XII 36, E-31008 Pamplona, Spain

[6]These authors equally contributed to this work.

ABSTRACT

Using knowledge- and structure-based approaches, we designed and synthesized reversible chemical probes that simultaneously inhibit the activity of two epigenetic targets, histone 3 lysine 9 methyltransferase (G9a) and DNA methyltransferases (DNMT), at nanomolar ranges. Enzymatic competition assays confirmed our design strategy: substrate competitive inhibitors. Next, an initial exploration around our hit **11**

was pursued to identify an adequate tool compound for *in vivo* testing. *In vitro* treatment of different hematological neoplasia cell lines led to the identification of molecules with clear anti-proliferative efficacies (GI_{50} values in the nanomolar range). Based on epigenetic functional cellular responses (levels of lysine 9 methylation and 5-methylcytosine), an acceptable therapeutic window (around 1 log unit) and a suitable pharmacokinetic profile, **12** was selected for *in vivo* proof-of-concept (ref 53). Herein, **12** achieved a significant *in vivo* efficacy: 70% overall tumor growth inhibition of a human AML (Acute Myeloid Leukemia) xenograft in a mouse model.

INTRODUCTION

Epigenetic regulation of gene expression is controlled by DNA methylation, nucleosome positioning, histone variant exchange and post-translational histone modifications.[1,2] Epigenetic alterations contribute to many human diseases, including cancer, inflammation, brain disorders, and metabolic and cardiovascular diseases. Thus, the development of epigenetic-based therapies has attracted considerable interest in the scientific and pharmaceutical communities, especially after the approval of the first therapies targeting DNA methyltransferases (DNMTs) and histone deacetylases (HDACs) for treatment of hematological malignancies. Thus, among possible epigenetic modifications, methylation has gained increased attention. Methyltransferases, the methyl writers of the histone and DNA code, catalyze the transfer of a methyl group from S-adenosyl-L-methionine (SAM or AdoMet) to its corresponding substrate—histones, nonhistone proteins or DNA—yielding S-adenosyl-L-homocysteine (SAH or AdoHcy). Methyltransferases acting on lysine and arginine

residues of histones and other proteins are referred to as Protein Methyltransferases (PMTs), while those that methylate DNA are known as DNMTs.

G9a (also known as KMT1C (lysine methyltransferase 1C) or EHMT2 (euchromatic histone methyltransferase 2)) is a histone-lysine N-methyltransferase that catalyzes the transfer of one or two methyl groups to the ε-amino group of lysine 9 of histone H3 (H3K9me1 and H3K9me2), a hallmark associated with transcriptional gene silencing. Other protein targets[3] of G9 include the tumor suppressor p53, whose methylation leads to its inactivation.[4] G9a is upregulated in various cancers, and its overexpression has been associated with poor prognosis and metastasis.[5–7] There is mounting evidence that the knockdown or pharmacological inhibition of G9a decreases cell growth,[8–11] delays acute myeloid leukemia (AML) progression[12] and blocks tumor metastasis.[6,7] Beyond cancer, G9a is involved in the maintenance of HIV-1 latency,[13] colitis,[14] cognitive disturbances (mental retardation, cocaine addiction, age-related cognitive decline),[15] embryonic development[16] and stem cell reprogramming, which has been used to produce inducible pluripotent stem cells (iPSCs).[17]

Compound **1** (BIX-01294, Chart 1) was the first selective inhibitor of G9a and GLP (G9a-like protein, its closely related protein, also known as EHMT1), discovered in a screening campaign.[18] As shown in Chart 1, subsequent optimizations of **1** led to the identification of a series of compounds possessing the same quinazoline core. Thus, inhibitor **2** (UNC-0224), around two log units more potent than **1**, was the first G9a-small molecule inhibitor co-crystallized with G9a, demonstrating that these quinazoline-based inhibitors bind at the substrate peptide binding site and are not SAM-competitive inhibitors.[19] Chemical probe **3** (UNC-0638)[20] was the result of an extensive medicinal chemistry effort[19,21] to obtain more potency against G9a and cell-permeable quinazoline derivatives. Finally, compound **4** (UNC-0642), has an optimized pharmacokinetic (PK)

profile for *in vivo* assays,[22] and only very recently its efficacy in a Prader-Willi syndrome mouse model has been proven.[23] Only a few studies have been published aiming to identify new alternative chemotypes of the quinazoline ring: the chemical probe **5** (A-366)[24] having a spiro[cyclobutane-1,3'-indole] ring and, more recently, the 2,4-diamino quinoline **6**, which was found to be a potent G9a inhibitor after exhaustive heterocycle replacement of the quinazoline ring of BIX derivatives.[25] The *in vivo* administration of compound **5** using osmotic mini-pump dosing in an AML flank xenograft model resulted in moderate (45%) tumor growth inhibition.[26] With the exception of **3** (IC_{50} against DNMT1 in the micromolar range),[20,27] all of these compounds are inactive against DNMT1 at concentrations higher than 10 μM or even 50 μM. Other G9a inhibitors with a pharmacophore different from **1** have been reviewed[28–30] or were published very recently.[31,32]

The involvement of DNA methylation in cancer is well acknowledged.[2] DNMTs are responsible for the methylation of the C5-cytosine of DNA. The methylation of promoter CpG islands leads to gene inactivation, as described for tumor suppressors and DNA repair genes in different tumors. DNMTs are grouped into two families: DNMT1 and DNMT3A/DNMT3B, each family being predominantly involved in methylation maintenance (DNMT1) or de novo methylation (DNMT3A/DNMT3B).[33] These three proteins are overexpressed in different cancer types or present mutations, as DNMT3A in leukemia.[34] Additionally, there is recent evidence that DNA methylation may play an important role in various diseases from different therapeutic areas: memory function,[35] Alzheimer's disease,[36] amyotrophic lateral sclerosis,[37] schizophrenia and bipolar disorder,[38] addiction,[39] hypertension,[40] atherosclerosis,[41] type 2 diabetes,[42] systemic lupus erythematosus[43] and fibrosis.[44] As mentioned above, two nucleoside analogs, **7** (Azacytidine) and **8** (Decitabine) (Chart 2), have been approved by the U.S. FDA and

EMA for treatment of hematological malignancies. These drugs incorporate into DNA and inhibit DNMT1 through an irreversible covalent complex.[45] These two drugs show poor bioavailability, chemical instability and metabolic stability,[45] leading to the search for optimized nucleoside analogs, such as **9** (SGI-110), currently being explored in clinical trials.[46] However, due to the toxic side effects associated with its mechanism of action, there is increasing interest in finding potent non-incorporating reversible DNMT inhibitors. Among others (see refs [47,48] for comprehensive reviews), the quinoline-based **10** (SGI-1027) has demonstrated inhibitory activity against DNMT1, DNMT3a and DNMT3b in biochemical assays and its potential to induce hypomethylation of CpG islands of tumor suppressor genes.[49] Interestingly, DNMT1 directly binds G9a and both methyltransferases cooperate during cell division,[50] promoting the transcriptional silencing of target genes,[51] including the reactivation of tumor suppressor genes.[52] Recently, we[53] and others[54] have shown that simultaneous blocking of G9a and DNMT1 exerts a synergistic effect on reducing the growth of cancer cells, either when combining G9a knockdown with pharmacologic inhibition of DNMT[54] or using specific siRNAs against both targets[53] or by inhibiting them with a combination of **5** and **8**.[53] Based on these results, we postulated that small-molecule reversible dual inhibitors of both methyltransferases might represent a novel approach in cancer therapeutics. Our efforts toward the identification of such dual inhibitors commenced with compound **11** (Chart 3), a quinoline-based matched pair of **3**. Subsequent optimization led to the discovery of the lead compound **12** (CM-272), with a suitable PK profile for *in vivo* administration and the ability to prolong the survival of AML, acute lymphoblastic leukemia (ALL) and diffuse large B-cell lymphoma (DLBCL) mice.[53] Here, we report the discovery and an initial exploration leading to the identification of our candidate for *in vivo* proof-of-concept compound **12**.

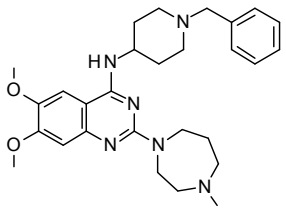

1

BIX-01294

IC_{50} G9a = 1200 nM
IC_{50} DNMT1 > 10000 nM

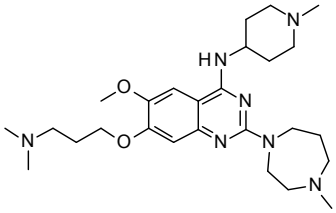

2

UNC-0224

IC_{50} G9a = 15 nM

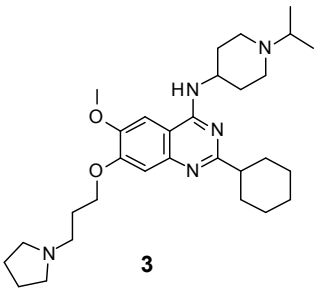

3

UNC-0638

IC_{50} G9a = 55 nM
IC_{50} DNMT1 = 2010 nM

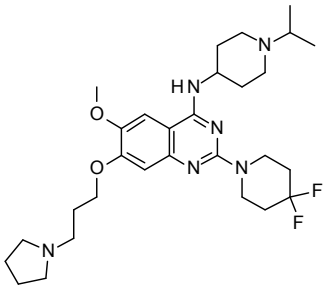

4

UNC-0642

IC_{50} G9a < 2.5 nM
IC_{50} DNMT1 > 50000 nM

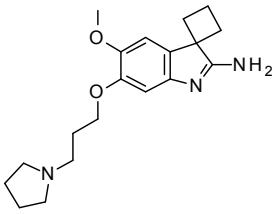

5

A-366

IC_{50} G9a = 3.3 nM
IC_{50} DNMT1 > 50000 nM

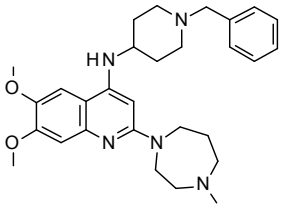

6

IC_{50} G9a = 13 nM
IC_{50} DNMT1 > 50000 nM

Chart 1. Known G9a inhibitors: quinazoline-based derivatives (compounds **1**, **2**, **3, 4**) and two novel alternative scaffolds of quinazoline: compounds **5** and **6**. G9a and DNMT IC_{50} values for **1** and **3** were determined internally (see footnote in Table 1). Alternatively, reported G9a IC_{50} values for **1** are 180 nM (SAHH-coupled assay)[20] and 1900 nM (mass spectrometry-based inhibition assay)[55] and < 15 nM for **3** (SAHH-coupled assay).[20] Concerning DNMT1, a percentage of inhibition of 35%±8% at 100 μM was reported for **1**[56] and an IC_{50} value of 1287 nM was reported for **3**,[27] in both cases using a radioactive methyl transfer assay. Discrepancies with initially reported DNMT1 IC_{50} values for **3** (IC50 = 107,000 nM)[20] have been attributed to a different

assay format.[27] The IC_{50} values for compounds **2**[19], **4**[22], **5**[24], and **6**[25] have been published previously.

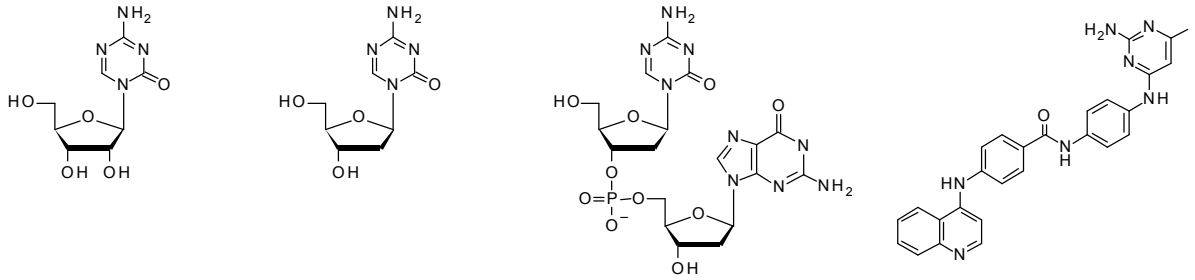

7 5-Azacitidine
IC_{50} G9a > 10000 nM
DNMT1 = 300 nM

8 Decitabine
IC_{50} G9a > 10000 nM
DNMT1 = 30 nM

9 SGI-110

10 SGI-1027
IC_{50} G9a > 10000 nM
IC_{50} DNMT1 = 3550 nM

Chart 2. Known DNMT1 inhibitors: nucleoside (compounds **7**, **8**, **9**) and non-nucleoside (compound **10**). G9a IC_{50} values for **7**, **8** and **10** and DNMT1 IC_{50} values for **10** as determined internally (see footnote in Table 1). Alternatively, DNMT1 IC_{50} values of 12500 nM (Poly(dI-dC)) and 6000 nM (hemimethylated DNA) have been reported for compound **10** using a radioactive methyl transfer assay with two different substrates.[49] For G9a, reported value for **10** is 59 ± 4 μM.[57] DNMT1 values for **7** and **8** have been reported previously and correspond to the lower concentration at which DNA hypomethylation is observed.[45]

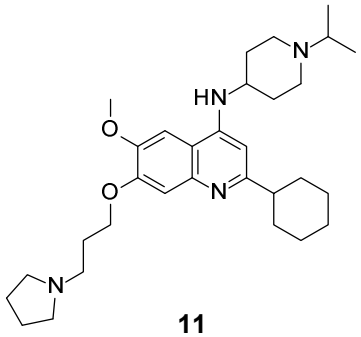

11

IC_{50} G9a = 0.7 nM
IC_{50} DNMT1 = 619 nM

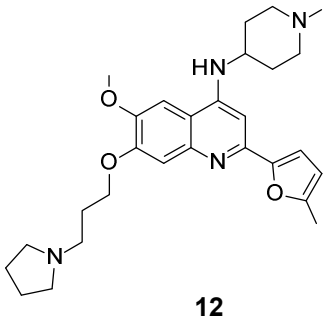

12

CM-272

IC_{50} G9a = 8 nM
IC_{50} DNMT1 = 382 nM

Chart 3. 11, quinoline matched pair of **3**, and lead compound **12** (CM-272). G9a and DNMT1 IC_{50} values determined internally (see footnote in Table 1). Biochemical inhibitory data of **12**, and its close analogue (CM-579), was confirmed by orthogonal biochemical assays as well as by direct binding measurements to DNMT1 using microscale thermophoresis (MST) and by cellular functional response (using pyrosequencing).[53]

RESULTS

Rational Design

We pursued knowledge- and structure-based approaches to design novel G9a and DNMT methyltransferase activity inhibitors; targeting both enzymes. For G9a, the crystal structures of **2** (PDB entry 3K5K)[19] and **3** (PDB entry 3RJW)[20] revealed that these quinazoline-based inhibitors could bind to the histone-binding pocket of G9a.[20] A detailed analysis of the interactions of **3** with the substrate-binding pocket of G9a (Figure 1A) shows that i) the pyrrolidine side chain interacts with the lysine binding channel (hydrogen-bond contact with the carbonyl of Leu1086 and cation-π interaction with the side-chain of Tyr1154); ii) the –NH group at the 4-position of the quinazoline

establishes a hydrogen-bond with Asp1083; iii) the basic nitrogen of the piperidine ring, which is directed toward the solvent region, is in close proximity with Asp1078 (4.5 Å); and iv) the N1 of the quinazoline ring, which is expected to be protonated at physiological pH,[20,55] forms a salt bridge with Asp1088. As observed in Figure 1A, the ring nitrogen atom (N3) of the quinazoline scaffold does not participate in any direct key interaction with the protein, and no conserved water molecules appear proximal to this residue as mediators in a water-mediated hydrogen-bond contact. Thus, from the viewpoint of G9a activity, the replacement of the quinazoline ring by a quinoline would be well tolerated. Thus, we set out to synthesize and test the quinoline-matched pair of **3**, compound **11**, to validate our initial hypothesis for G9a activity. The observation that **3** displayed micromolar activity against DNMT1 (Chart 1) prompted us to use it as our initial starting point for the proof-of-concept of the dual G9a-DNMT inhibitor design. Moreover, during the course of our investigations, Rotili[56] disclosed a series of quinazoline-based compounds (based on chemical exploration around the G9a inhibitor **1**) that inhibit DNMT3A at low micromolar levels without any significant inhibition of DNMT1 and G9a.

For the DNMT1 structure-based ligand design, different crystal structures of DNMT1 in complex with SAH, SAM, sinefungin (a SAM-competitive inhibitor) and/or DNA are publicly available. However, no crystal structures of any DNMT (including DNMT1, DNMT3A and DNMT3B) complexed with small molecule reversible inhibitors such as for example **10** are available, and only modeling studies have been published.[58–61] Thus, the binding mode as well as the binding cavity (SAM or DNA pockets), for most of these compounds, remain unknown. To guide the design of DNMT inhibitors, we carried out docking studies using the productive DNMT1-DNA-SAH complex structure (mouse DNMT1, mDNMT1, PDB entry 4DA4)[62] containing a central hemimethylated

CpG site and lacking the autoinhibitory linker (mDNMT1: 699-733) and zinc-finger-like (CXXC motif, residues 646-692) domains at the N-terminal region of the catalytic domain (mDNMT1, 1140-1602, hDNMT1 1139-1616). This structure was chosen because the catalytic domain of the active DNMT1 undergoes a strong conformational change compared with the autoinhibited structure,[62,63] in which the DNA minor groove is excluded from the catalytic site by the autoinhibitory linker. Thus, to model whether compound **11** would bind to the SAM or the DNA pocket, a protein structure that can accommodate both options was selected. Our docking studies of compound **11** showed that the compound fits within the DNA binding pocket, superimposing well with the hemimethylated CpG (Figure 1B) and the pyrrolidine ring occupying the cytidine-binding pocket, establishing a hydrogen bond with the carboxylate group of the catalytic Glu1269 (Glu1266 in human DNMT1, hDNMT1) (Figure 1C). Additionally, the oxygen directly bonded at the 7-position establishes a hydrogen bond with the guanidine of Arg1315 (Arg1312 in hDNMT1), a guanidine of the conserved motif TRR flanking the entrance of the cytidine. The NH of the 4-position establishes a hydrogen bond with the side chain of Ser1233 (Ser1230 in hDNMT1), and the isopropylpiperidyl group overlays with the guanine of the DNA chain exiting the catalytic pocket and establishing hydrophobic contacts with Met1235 (Met1232 in hDNMT1) (Figure 1C). The methoxy group at the 6-position orients towards the 3' direction of the DNA chain. Finally, the cyclohexyl ring at the 2-position lies in a cavity flanked by Thr1530 (Thr1528, hDNMT1), Gln1230 (Gln1227, hDNMT1), Tyr1243 (Tyr1240, hDNMT1) and Arg1576 (Arg1574, hDNMT1), without making any explicit contact with any residue. Comparing this active DNMT1 structure with the autoinhibited conformation of DNMT1 (PDB entry 3PTA)[63] that has both the CXXC and autoinhibitory domains, it can be seen that the C-terminal end of the CXXC linker (residues 692-700) lies

proximal to the region occupied by the cyclohexyl group (Figure S1). Thus, without any further structural insight concerning the conformation adopted by the CXXC linker in the active form, no clear conclusion can be stated regarding the potential ligand interactions at this site. Similar conclusions were drawn when analyzing in detail a more recently released crystal structure of hDNMT1 with a higher resolution that is also auto-inhibited (PDB entry 4WXX).[64] Concerning the role of the central quinoline scaffold, it seems to act as a mere scaffold, without establishing any key contact with the protein. Thus, the replacement of the quinazoline of **3** by a quinoline **11** will predictably not have a strong influence on the inhibitory activity against DNMT1. In contrast to G9a, no apparent interaction between the nitrogen ring N1 and protein was observed, and no negatively charged residue lies in its neighborhood.

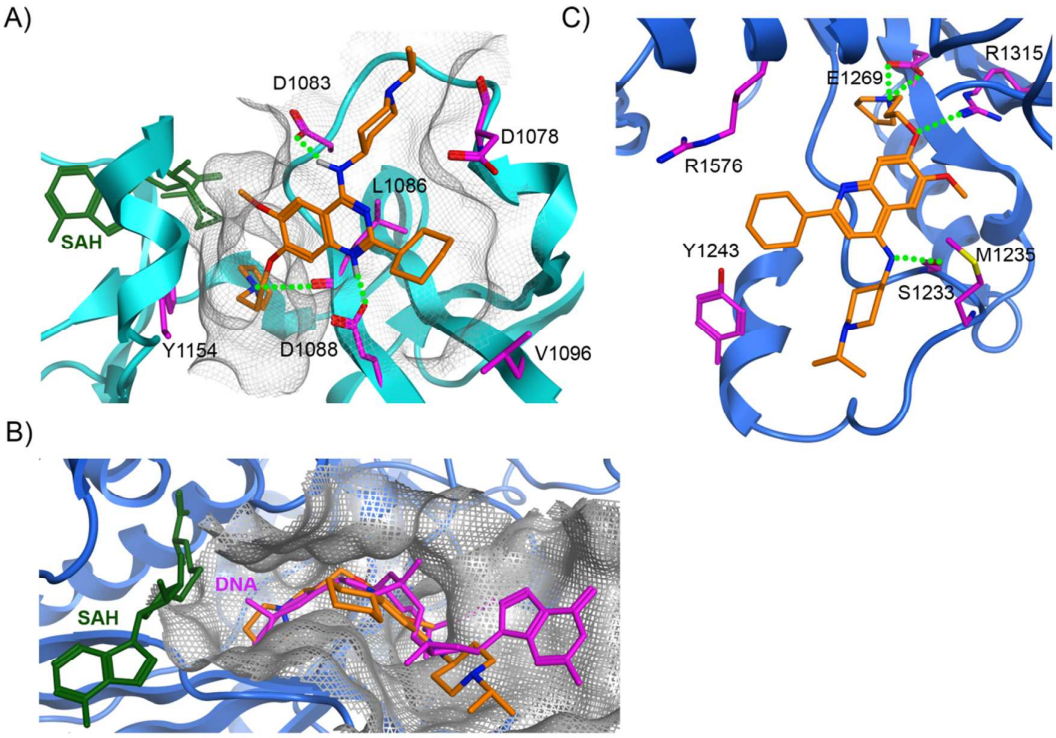

Figure 1. (A) Complex of **3** with G9a (PDB accession code: 3RJW). (B) Docked structure of compound **11** (orange) into DNMT1 (PDB accession code 4DA4) overlaid

with DNA (pink). The cofactor SAH is shown in green. (C) Detailed analysis of the predicted hydrogen bonds between compound **11** and DNMT1.

Scheme 1.

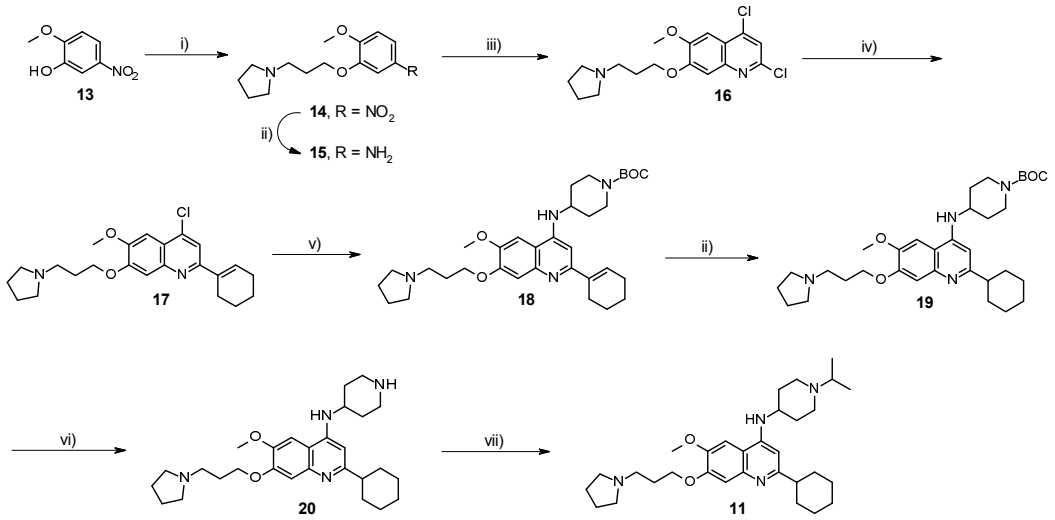

Conditions: i) 3-pyrrolidin-1-yl-propan-1-ol, PPh_3, DEAD, THF, 0 ºC, followed by rt, 5 h; ii) Pd/C, MeOH, H_2 (1 atm), 15-25 ºC, 3-10 h; iii) malonic acid, $POCl_3$, rt, 4 h, followed by 90 ºC overnight; iv) 2-(cyclohex-1-en-1-yl)-4,4,5,5-tetramethyl-1,3,2-dioxaborolane, K_2CO_3, $Pd(PPh_3)_4$, 1,4-dioxane/H_2O (5:1), MW, 120 ºC, 1 h; v) *tert*-butyl 4-aminopiperidine-1-carboxylate, $Pd_2(dba)_3$, BINAP, Cs_2CO_3, 1,4-dioxane, 130 ºC, 36 h; vi) HCl/EtOAc (1.0 M), 16 ºC, 4 h; vii) acetone, AcOH, $NaBH_3CN$, THF, 50 ºC, 15 h.

Compound **11** was synthesized as shown in Scheme 1 from commercially available 2-methoxy-5-nitro-phenol (**13**). This compound was first transformed into amine (**15**) by the Mitsunobu reaction and hydrogenation. Subsequently, 2,4-dichloroquinoline (**16**) was prepared by reaction with malonic acid in $POCl_3$, and intermediate **17** was isolated after Suzuki coupling. Next, the desired substitution at position 4 was installed by reaction with *tert*-butyl 4-aminopiperidine-1-carboxylate obtaining intermediate **18**, which was converted into compound **19** by hydrogenation. Finally, deprotection of the

secondary amine under acidic conditions and reductive amination using acetone led us to the desired compound **11**.

Compound **11** was evaluated for G9a and DNMT1 inhibitory activity using the time-resolved fluorescence resonance energy transfer (TR-FRET) assay. Intriguingly, compound **11** was more potent than **3** against the two targets, with IC_{50} values of 0.7 nM against G9a (1.9 log units of increased potency) and 619 nM against DNMT1 (0.5 log units of increased potency) (Chart 3). Interestingly, in our hands, compound **3** was also a better inhibitor of DNMT1 than compound **10** (Chart 2), a reversible DNMT inhibitor commonly considered a reference compound for the DNMT inhibitor design.

Concerning G9a activity, the higher potency of the quinoline than that of the quinazoline scaffold is in line with the results recently published for the quinoline-matched pair of compound **1** (BIX-01294), compound **6** (Chart 1).[25] In agreement with the conclusions drawn by Srimongkolpithak et al, this improvement in G9a activity can be attributed to the increased basicity of the N1 nitrogen that enhances the ionic interaction with Asp1088, with the Pipeline Pilot[65] predicted pKa values of 6.54 (compound **11**) and 6.32 (compound **6**) for the quinoline series compared with the predicted pKa values of 4.69 (compound **3**) and 4.48 (compound **1**) for their respective quinazolines. Compared with the experimentally determined pKa values of N1 for compound **6** (pKa of 9.50) and compound **1** (pKa of 6.94),[25] the pKa predictor underestimates the pKa values, although the general trend is correctly predicted. Based on the proposed binding mode of compound **11** into DNMT1, no explanation could be stated for the improvement in the DNMT1 activity of compound **11** compared with that of compound **3**.

We next determined the mechanism of action of compound **11** by carrying out enzymatic competition studies varying the concentrations of SAM and the two substrates: histone monomethyl-H3K9 peptide for G9a and poly-deoxy inosine poly-deoxy cytosine (pdI-pdC) DNA for DNMT1 (Figure 2). These competition experiments confirmed that compound **11** is a substrate-competitive inhibitor of both targets, G9a and DNMT1. In fact, the inhibitory potency of **11** is not affected by increasing concentrations of the SAM cofactor (G9a IC_{50} ranging from 2 nM to 0.5 nM in Figure 2A and DNMT1 IC_{50} ranging from 1.4 μM to 2.4 μM in Figure 2C). However, increasing the concentrations of the substrates, histone peptide (G9a, with IC_{50} values spanning 0.7 nM to 29 nM, Figure 2B) and pdI-pdC (DNMT1, IC_{50} values from 1.4 μM to > 10 μM, Figure 2D), have a clear impact on the binding of **11** to these two targets (pIC_{50} differences are greater than 1 log unit). Non-competition with the SAM cofactor is relevant to minimize off-target promiscuity. When compound **11** was assayed at a concentration of 10 μM against a panel of 14 lysine and arginine histone methyltransferases, only GLP, a closely related protein to G9a, was considerably inhibited (IC_{50} of 180 nM, with some selectivity towards G9a); the rest of histone methyltransferases were marginally inhibited, lower than 25% inhibition (Supplementary Table S1). For other DNMTs, only DNMT3A was significantly inhibited by **11** at 10 μM (80%), while had no effect on DNMT3B (Supplementary Table S1).

However, compound **11** had no anti-proliferative response against ALL CEMO-1 (GI_{50} > 10 μM), AML MV4-11 (GI_{50} > 10 μM) and DLBCL OCI-Ly3 and OCI-Ly10 (0% inhibition at 1 μM) cell lines. Interestingly, it showed no cytotoxicity in the healthy hepatic cell line THLE-2 (LC_{50} = 83.8 μM).

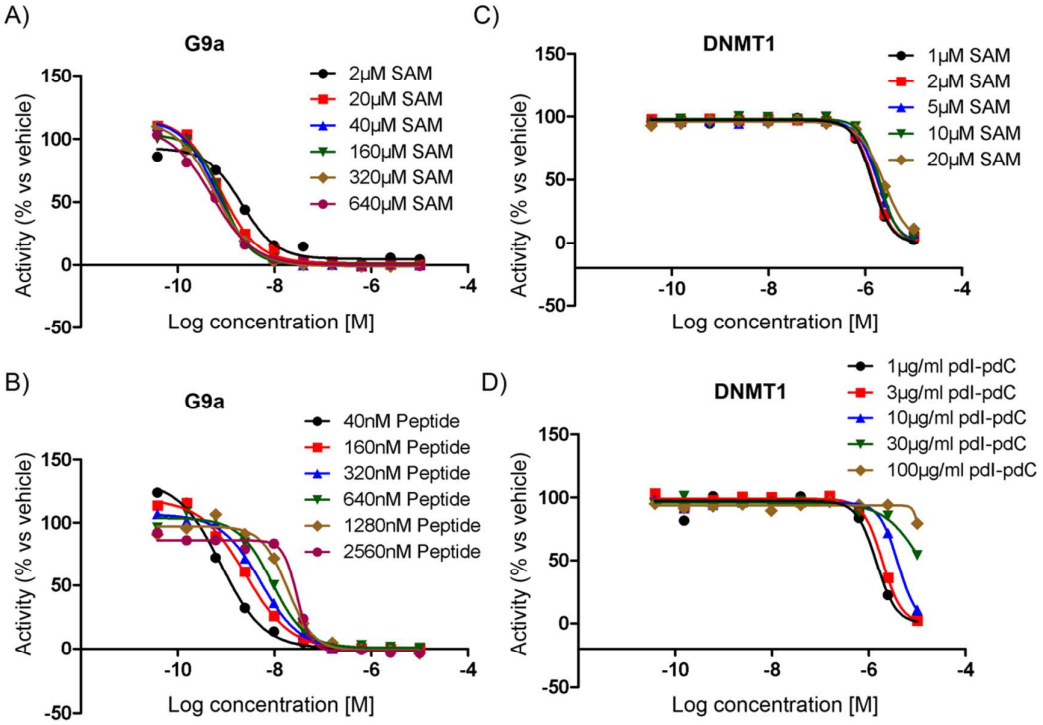

Figure 2. Competition experiments performed with compound **11** on G9a (A, B) and DNMT1 (C, D) by varying the SAM concentrations (A, C), histone monomethyl-H3K9 peptide (B) and pdI-pdC (C). Of note, the difference of 0.35 log units between the determined DNMT1 IC_{50} value for this competition assay (1.4 μM) and the routinely screening (619 nM, Chart 3), was exceptionally accepted for the purpose of the competition assay (accepted difference in routinely screening is 0.3 log units, see footnote in Table 1; requirement is met by **11**).

In light of the high *in vitro* potency of **11** against G9a and DNMT1, we set out to optimize the quinoline series with the first initial goal of enhancing DNMT1 activity with potent anti-proliferative response against different hematological neoplasms and with an adequate ADME profile to be administered *in vivo* (Chart 4). Given, that GLP is

a closely related homologue of G9a, compounds were routinely screened against G9a, and only promising compounds were profiled against GLP.

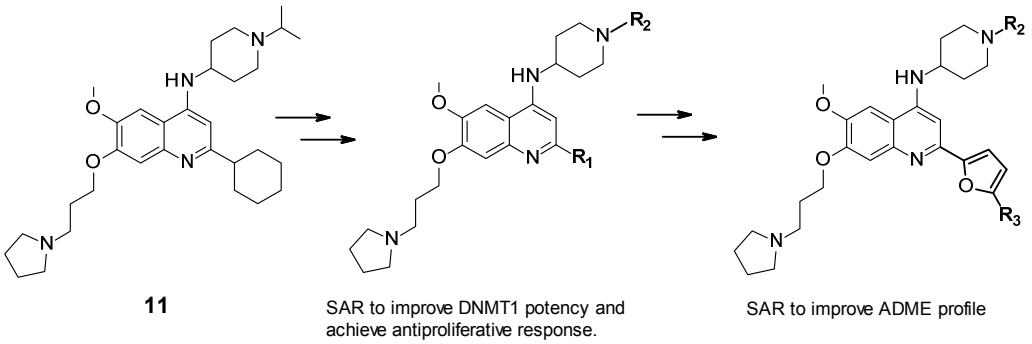

Chart 4. SAR exploration strategy to optimize our initial hit compound **11**.

SAR and antiproliferative response: Exploration of the 2-position (R_1).

Initially, we decided to focus our SAR exploration at the 2-position because i) modifications to the 2-substituent of the quinazoline scaffold are well tolerated from the viewpoint of G9a activity[19,21,66], and ii) we hypothesized that it might have a great impact on the permeability of the compounds to achieve a cellular response. For this exploration, the 1-methylpiperidin-4ylamino substituent was fixed at the 4-position as the N-capping group because this fragment is directed toward the solvent-exposed region of both enzymes (predictably in the case of DNMT1), and it should not strongly influence the *in vitro* potency of compounds while reducing their molecular weight and easing synthetic accessibility. In fact, this fragment was found not to cause any potency loss against G9a compared with the 1-benzylpiperidin-4-ylamino group of compound **1** in the quinazoline series.[19] Thus, compounds **23a-q** and **31** (Table 1) with diverse substituents at 2-position were designed and synthesized as shown in Schemes 2 and 3. The synthesis of compound **12** has been previously reported.[53] Compounds **23a-e** and

23g-q were prepared from intermediate **16**. First, the desired substitution at position 2 was installed by Suzuki coupling (**17**, **22d** and **22g-r**), Buchwald-Hartwig amination (**22c**) or reaction with NaOMe (**22e**). Next, the desired methylpiperidines were isolated by different Pd-mediated coupling reactions. In the case of compound **23f**, the trifluoromethyl group at position 2 was installed through reaction of intermediate **15** with 4,4,4-trifluoro-3-oxobutanoate, and then compound **22f** was prepared by heating in $POCl_3$. Finally, compound **23f** was synthesized by reaction with 1-methylpiperidin-4-amine under Buchwald-Hartwig amination conditions.

Scheme 2.

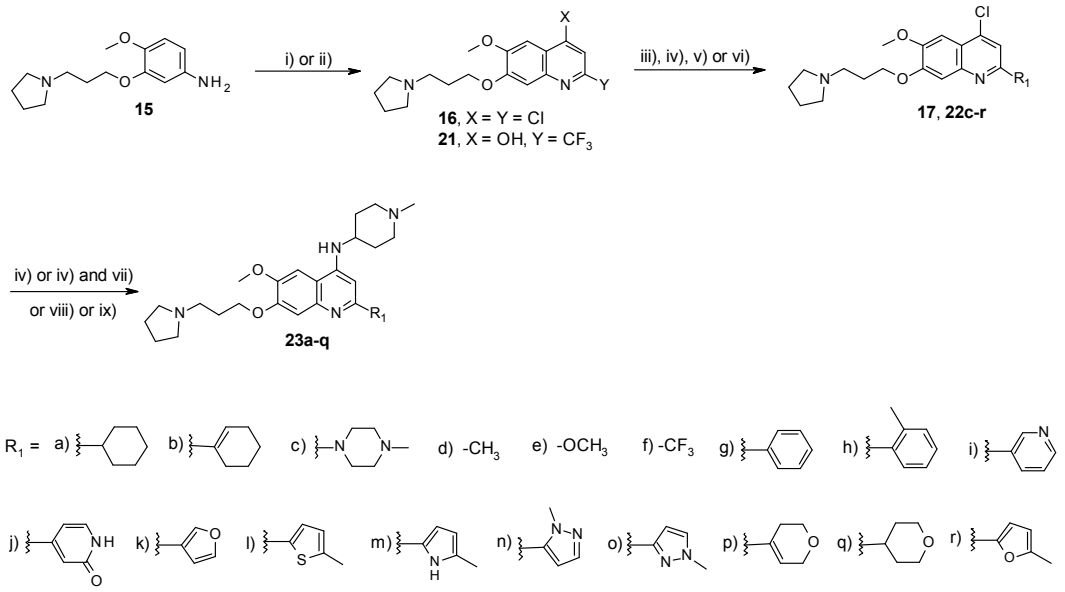

Conditions: i) malonic acid, $POCl_3$, rt, 4 h, followed by heating at 90 ºC overnight; ii) 4,4,4-trifluoro-3-oxobutanoate, phenylpropanolamine, 120 ºC, 12 h; iii) corresponding boronic acid or ester, K_2CO_3 or Na_2CO_3, $Pd(PPh_3)_4$, 1,4-dioxane or 1,4-dioxane/H_2O (5:1 or 15:1), 110-120 ºC, MW or conventional heating, 1-12 h; iv) 1-methyl-piperazine or 1-methylpiperidin-4-amine, $Pd_2(dba)_3$, Cs_2CO_3, BINAP, 1,4-dioxane, 110-130 ºC, MW or conventional heating, 1-12 h; v) NaOMe, rt, overnight; vi) $POCl_3$, 110 ºC, 2 h; vii) Pd/C, EtOH, H_2 (1 atm), 25-35 ºC, 4-15 h; viii) 1-methylpiperidin-4-amine, biphenyl-2-yl-

dicyclohexyl-phosphane, $Pd_2(dba)_3$, K_3PO_4, DME, 110 ºC, MW, 3 h; ix) 1-methylpiperidin-4-amine, *t*-BuOK, xantphos, $Pd_2(dba)_3$, toluene, 130 ºC, MW or conventional heating, 3-10 h.

Scheme 3.

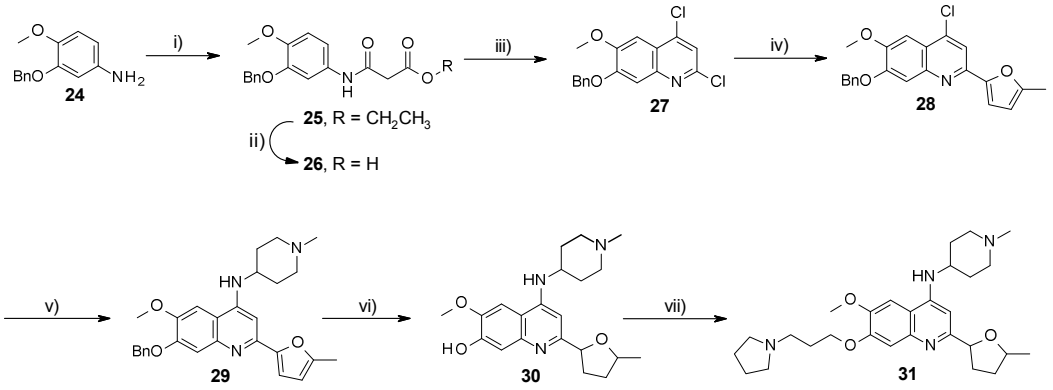

Conditions: i) ethyl 3-chloro-3-oxo-propanoate, Et_3N, CH_2Cl_2, 0 ºC, followed by rt, 12 h; ii) $LiOH{\cdot}H_2O$, THF/MeOH/H_2O (3:3:2), rt, 16 h; iii) $POCl_3$, 90 ºC, 2 h; iv) K_2CO_3, $Pd(PPh_3)_4$, 4,4,5,5-tetramethyl-2-(5-methyl-2-furyl)-1,3,2-dioxaborolane, 1,4-dioxane, 110 ºC, 16 h; v) Cs_2CO_3, BINAP, $Pd_2(dba)_3$, 1-methylpiperidin-4-amine, 1,4-dioxane, 110 ºC, 16 h; vi) Pd/C, H_2 (50 Psi), MeOH, 50 ºC, 16 h; vii) Cs_2CO_3, 1-(3-chloropropyl)pyrrolidine, DMF, 110 ºC, 16 h.

On the other hand, compound **31** (Scheme 3) was prepared from commercially available 3-benzyloxy-4-methoxy-aniline (**24**), which was converted into carboxylic acid **26** by reaction with ethyl 3-chloro-3-oxo-propanoate and ester hydrolysis. Next, 2,4-dichloroquinoline **27** was achieved after heating in $POCl_3$. Subsequent reaction with 4,4,5,5-tetramethyl-2-(5-methyl-2-furyl)-1,3,2-dioxaborolane led to intermediate **28**. As described above, the desired substitution at position 4 of the quinoline was then installed through Buchwald-Hartwig amination. Posterior hydrogenation afforded intermediate **30**, which was finally transformed into the desired compound **31** by reaction with 1-(3-chloropropyl)pyrrolidine in DMF.

According to our initial hypothesis, the replacement of the N-capping group at the 4-position of compound **11** had a minor influence on the *in vitro* potency against both targets (compound **23a**, G9a and DNMT1 IC_{50} values of 2 and 497 nM, respectively). From the viewpoint of G9a activity, in general, the cyclohexyl group of **23a** can be replaced by diverse substituents (small groups, alkyl rings, aromatic rings, heteroaromatic rings and heterocycles), most of them resulting in low nanomolar G9a inhibitors (IC_{50} < 50 nM). Analysis of the basicity of the N1 nitrogen can only partially explain SAR results: decreased potency for electron-withdrawing groups such as –CF3 (compound **23f**, 637 nM). However, it does not explain the reduced activity of other small electron-donating groups such as the methoxy group of compound **23e** (136 nM). Here, lipophilic interactions of 6-membered rings with Val1096 (Figure 1A) seem to confer G9a potency, as solely an explicit potential hydrogen-bond interaction was predicted for compound **23m** (between the NH of its methylpyrrole group and Asp1088, Figure S2). Interestingly, this compound **23m** is the most potent against G9a in Table 1 (IC_{50} = 0.5 nM). As for compound **11**, a substrate competitive mechanism was observed for **23m** (Figure S3), indicating binding site conservation in both targets.

Considering DNMT1 activity, a clear SAR trend was not observed for the diverse substituents in Table 1. Small substituents such as methyl (**23d**), methoxy (**23e**) and –CF_3 (**23f**) resulted in low micromolar (**23d**, **23e**) or inactive (IC_{50} > 10 μM, **23f**) compounds against DNMT1. Alkyl rings (**23a**, **23b**) tended to be more potent (IC_{50} below or around 500 nM) than non-aromatic heterocycles such as N-methylpiperazine (**23c**) and oxygen-containing rings (**31**, **23p**, **23q**) with DNMT1 inhibitory activity in the low micromolar range (~ 1 μM) (Table 1). Regarding aromatic and heteroaromatic rings, the introduction of 5-membered heteroaromatic rings such as 5-methyl-2-furyl

(**12**), 5-methyl-2-thienyl (**23l**) and 5-methyl-1*H*-pyrrol-2-yl (**23m**) resulted in a slightly increased DNMT1 inhibition compared with the cyclohexyl **23a** (0.1-0.5 log units). Analysis of the DNMT1 cavity around the 2-position of the quinoline core did not reveal any clue to interpret the SAR, probably due to the missing CXXC domain. However, comparative analysis of the electrostatic potential of these compounds suggests a preference for negative potentials surrounding the 2-position of the quinolines, as shown in Figure 3 for derivatives **12** (IC_{50} = 382 nM) and **23m** (IC_{50} = 232 nM). However, as highlighted by compound **23b** (IC_{50} = 494 nM), this is not a strict mandatory requirement.

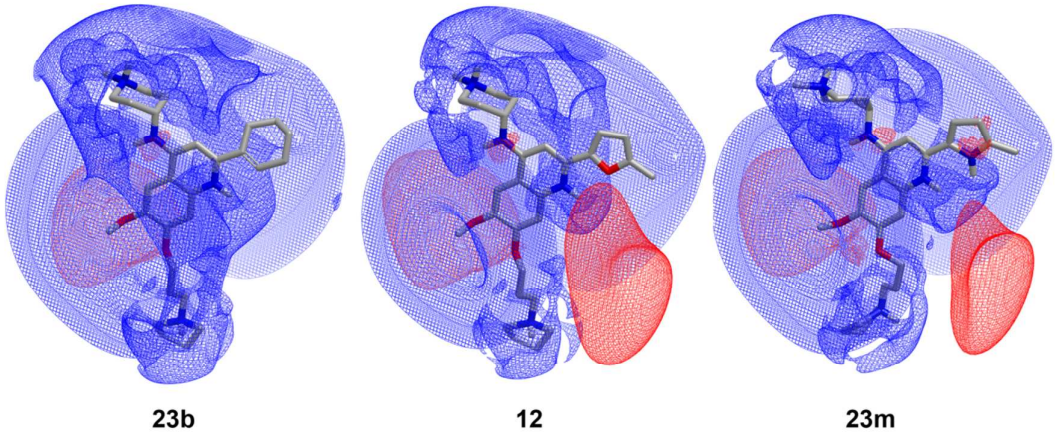

Figure 3. Electrostatic maps of potent DNMT1 inhibitors **23b**, **12** and **23m**. The blue and red grids correspond to positive and negative potentials, respectively.

Concerning the anti-proliferative effect of the most biochemically potent compounds in Table 1 against ALL cell lines (CEMO-1 and primary culture LAL-CUN-2), DLBCL (OCI-Ly3 and OCI-Ly10) and AML (MV4-11) cell lines, only compound **12** showed GI_{50} values lower than 1 μM against all five cell lines, indicating that 5-substituted-2-furyl groups at the 2-position are optimal for cellular activity. Other compounds with both, similar *in vitro* inhibitory profile and moderate PAMPA permeability (10 < Pe <

30 nm/s)[67] to that of **12**, had either no effect on proliferation (**23a**) or were poorer responders (**23b**, **23l**). Even compound **23m**, which displayed high activity in the *in vitro* assay against G9a and DNMT1, had minor effect on cellular viability than **12**. It remains to be seen if differences in active transport may account for this difference. For passive permeability, compounds with predicted LogD values at pH =7.4[65] ranging between 1 and 3 (**23a**, **23b**, **23g**, **12**, **23l**), exhibited better permeability (moderate) compared to more hydrophilic compounds (e.g. **23i**, **23o**, **23p**, **23q**), with Pe PAMPA values less than 10 nm/s). Cytotoxicity of selected compounds in the healthy hepatic cell line THLE-2 allowed for a therapeutic window (absolute difference between pLC_{50} and pGI_{50}) of around 0.8 – 1 log units against their corresponding most responsive hematological neoplasia cell line (compounds **12**, **23b**, **23g**, **23l** and **23m**), or even higher (1.8 log units for compound **23k** in OCI-Ly10 cell line).

Table 1. Exploration of the 2-position

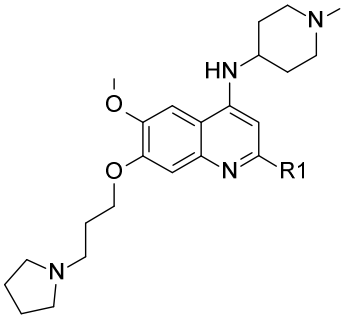

Cpd	R1	G9a IC_{50} nM[c]	DNMT1 IC_{50} nM[c]	PAMPA Pe (nm/s) [d]	CEMO-1 GI_{50} nM[e]	LAL-CUN-2 GI_{50} nM[e]	OCI-Ly3 GI_{50} nM[e]	OCI-Ly10 GI_{50} nM[e]	MV4-11 GI_{50} nM[e]	THLE-2 LC_{50} nM[f]

23a		2	497	19.8	20%[a]				>10000	34800
23b		6	494	20.9	1175	4290				7580
23c		42	945		14%[b]					
23d	Me	6	929		14%[b]					
23e	OMe	136	2290		1%[a]					
23f	CF_3	637	>10000		24%[a]					
23g		15	1050	16.9	658	7%[a]	717	420	2595	5620
23h		52	582							
23i		40	1410	2.2	0%[a]	16%[a]	12%[a]	17%[a]		
23j		142	1250							
12[53]		8	382	12.9	218	664	409	455	269	1780
23k		7	978	2.2	4560	54%[b]	>4000	386		22300
23l		43	230	29.1	555		21%[a]	42%[a]	3095	4060

23m	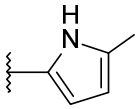	0.5	232		1650	12%[a]	896	915		7680
23n	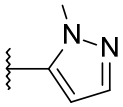	1080	>10000	0.9						
23o	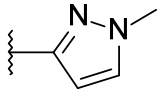	44	969		10%[a]	16%[a]	16%[a]	0%[a]		
31[g]	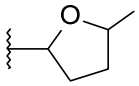	27	1370							
23p	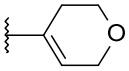	12	957	3.7	8%[a]	0%[a]	6%[a]	16%[a]		
23q	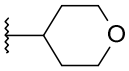	17	4420	2.2	20%[a]	6%[a]	0%[a]	3%[a]		

[a] Percentage of growth inhibition at 1 μM of the compound; [b] percentage of growth inhibition at 10 μM of the compound. For data in Tables 1-3 and Charts 1-3: [c] all biochemical results are the average of at least two independent replicates performed at different days. If absolute pIC_{50} difference was higher than 0.3 log units, additional replicates were performed until satisfying the experimental error (by discarding individual results with values outside 2 MADs of the mean value). [d] The PAMPA assay was performed in triplicate. [e] Proliferation assays are the average of three replicates at different days. [f] THLE-2 cytotoxicity results after 72 hours of incubation are the average of at least two independent experiments performed at different days. If absolute pLC_{50} difference was higher than 1 log unit, additional replicates were performed until satisfying the experimental error (by discarding individual results with values outside 3 MADs of the mean value). [g] racemic mixture.

Subsequent SAR exploration of the 2-position was centered on studying the effects of the replacement of the methyl fragment of the 5-methyl-2-furyl group of compound **12**

by diverse chemical moieties having representative potential ligand-receptor interaction patterns.[68]

Thus, compounds **34a-f** and **36** in Table 2 were synthesized according to Scheme 4 from compound **16**. 4-Chloroquinolines **33a**, **33f** and **35** were directly prepared by Suzuki coupling from this intermediate, while compounds **33b-e** were afforded from aldehyde **32**. Next, the desired 4-aminoquinolines **34a-f** and **36** were isolated by Buchwald-Hartwig amination.

Scheme 4.

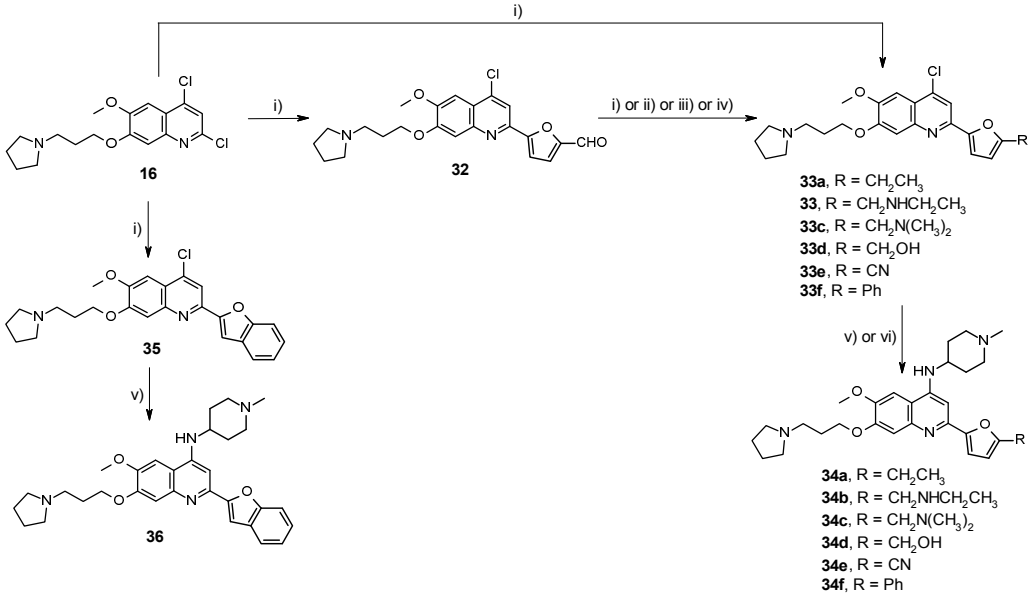

Conditions: i) corresponding boronic acid or ester, K_2CO_3 or Na_2CO_3, $Pd(PPh_3)_4$, 1,4-dioxane/H_2O (5:1, 10:1 or 15:1), 80-120 ºC, MW or conventional heating, 1-12 h; ii) ethylamine or dimethyl amine hydrochloride, MeOH, rt, 90 minutes, followed by $NaBH_3CN$, rt, 12 h; iii) $NaBH_4$, MeOH, rt, 2 h; iv) phenylphosphonic dichloride, pyridine, $NH_2OH{\cdot}HCl$, MeOH/CH_2Cl_2 (1:4), rt, 15 h, then $NaBH_3CN$, rt, 12 h; v) Cs_2CO_3, BINAP, $Pd_2(dba)_3$, 1-methylpiperidin-4-amine, 1,4-dioxane, 120-130 ºC, MW, 2-5 h; vi) 1-methylpiperidin-4-amine, *t*-BuOK, xantphos, $Pd_2(dba)_3$, toluene, 130 ºC, MW, 2-3 h.

Table 2. Focused exploration on 5-substituted-2-furyl groups

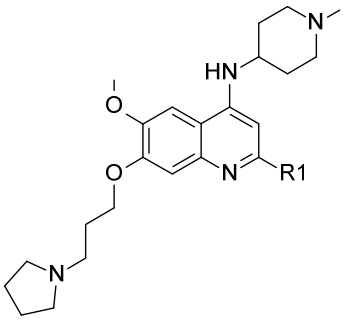

Cpd	R1	G9a IC_{50} nM[b]	DNMT1 IC_{50} nM[b]	PAMPA Pe (nm/s)	CEMO-1 GI_{50} nM	LAL-CUN-2 GI_{50} nM	OCI-Ly3 GI_{50} nM	OCI-Ly10 GI_{50} nM
34a	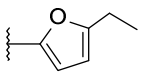	2	234	23.9	56	577	95	64
34b	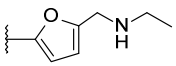	48	618	1.3	0%[a]	3%[a]	0%[a]	0%[a]
34c	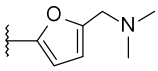	148	1270					
34d	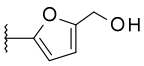	15	759	0.5	0%[a]	19%[a]	26%[a]	1%[a]
34e	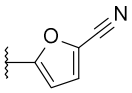	264	1600					
34f	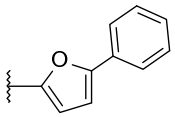	2720	1050					
36	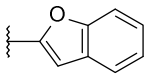	3140	1070					

[a] Percentage of growth inhibition at 1 μM of the compound. For compound **34a**, GI_{50} and LC_{50} values in MV4-11 and THLE-2 cell lines are 679 nM and 2320 nM, respectively.

Except for the 5-ethyl-2-furyl (compound **34a**), the introduction of different polar substituents with either hydrogen bond donors (compounds **34b**, **34c**) or hydrogen bond acceptors (compound **34e**) or both (compound **34d**) had a detrimental impact on both biochemical activities, emphasizing a stronger preference for hydrophobic groups. Bulky aromatic substituents (**34f**, **36**) were not well tolerated, especially for G9a, probably caused by steric clashes with Val1096. Because no significant improvement was observed, no further exploration was performed.

Compound **34a**, with similar biochemical profile and slightly higher PAMPA permeability than **12**, showed higher anti-tumour activity against all cell lines, except for MV4-11. Especially, for CEMO-1, OCI-Ly3 and OCI-Ly10 lines (GI_{50} < 100 nM), an interesting therapeutic window of 1.4 – 1.6 log units was achieved. In summary, as a result of the exploration of the 2-position of the quinoline series, compounds **12** and **34a** were selected for further profiling (see below).

SAR and anti-proliferative response: Exploration of the 4-position (R_2)

Next, a small exploration of the N-capping group at the 4-position (cyclopropyl and isopropyl groups) was carried out by holding constant the two optimal groups (5-methyl-2-furyl and 5-ethyl-2-furyl) at the 2-position (Table 3). Our aim was two-fold: avoiding the potential N-demethylation *in vivo* of the 1-methylpiperidine ring and decreasing the basicity of the nitrogen of this piperidine to decrease potential hERG binding.

Compounds **38a** and **39a-d** were prepared as illustrated in Scheme 5. Starting from previously described 4-chloroquinolines **22r** and **33a**, BOC-protected piperidines **37a-b**

were isolated after Buchwald-Hartwig amination. Next, the BOC protecting group was removed under acidic conditions, and the desired isopropyl or cyclopropyl substituents were installed by reductive amination or cyclopropanation, respectively.

Scheme 5.

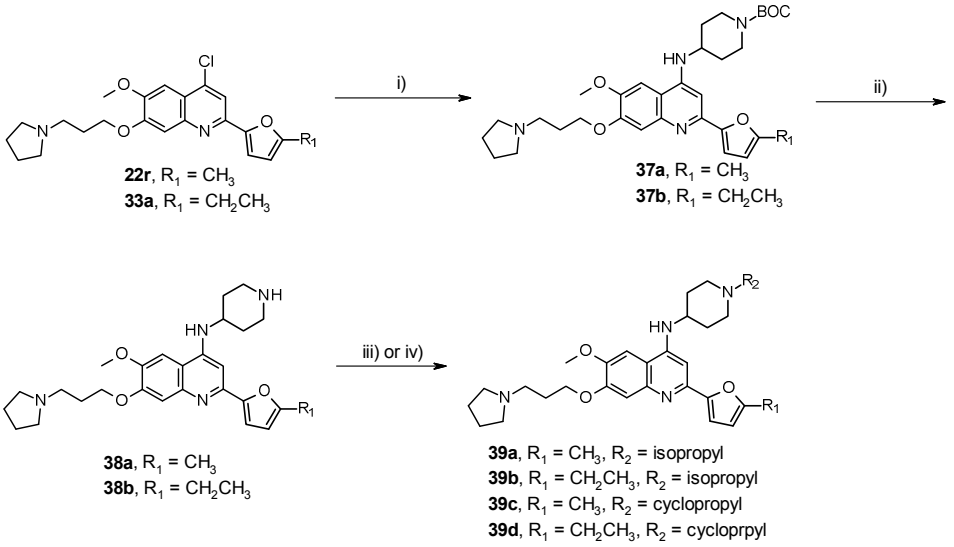

Conditions: i) *tert*-butyl 4-aminopiperidine-1-carboxylate, CS_2CO_3, BINAP, $Pd_2(dba)_3$, 1,4-dioxane, 80-130 ºC, 5-16 h; ii) HCl/EtOAc (1.0 M), 22-25 ºC, 2-3 h; iii) acetone, $NaBH_3CN$, AcOH, *i*-PrOH, 50 ºC, 15 h; iv) (1-ethoxycyclopropoxy)-trimethyl-silane, $NaBH_3CN$, AcOH, MeOH, 60 ºC, overnight.

Table 3. Exploration of the N-capping group at the 4-position

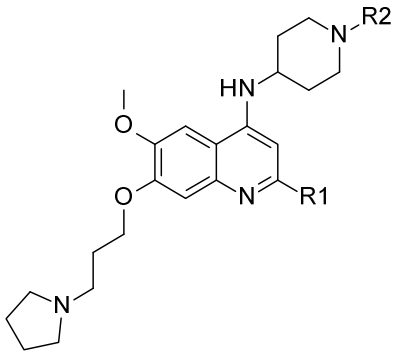

Cpd	R1	R2	G9a IC_{50} nM	DNMT1 IC_{50} nM	PAMPA Pe (nm/s)	CEMO-1 GI_{50} nM	LAL-CUN-2 GI_{50} nM	OCI-Ly3 GI_{50} nM	OCI-Ly10 GI_{50} nM	MV4-11 GI_{50} nM	THLE-2 LC_{50} nM
38a	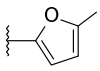	-H	6	137	2.0	1980	>5000	1270	>4000		8850
39a	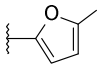		3	231	25.8	247		898	792	649	1340
39b	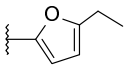		3	284	38.3	441				971	1720
39c	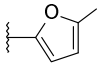		22	413	40.4	453	1380	187	94	1590	455
39d	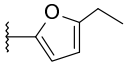		24	274	55.6	917		1560	236	3506	703

For DNMT1 activity, the replacement of the methyl group by an isopropyl or cyclopropyl group had a minor effect (IC_{50} between 200 and 500 nM, as for **12** and **34a**). For G9a, the introduction of the cyclopropyl ring diminished G9a activity (up to 1 log unit in the case of compound **39d**), emphasizing the impact of the basicity of the alkylated nitrogen for G9a inhibitory activity, predictably decreased by the vinylic character of the cyclopropyl moiety.[69] Considering the trend in improved permeability (cyclopropyl > isopropyl > methyl), this drop in G9a potency might be one factor to explain the reduced cellular potency against CEMO-1, OCI-Ly3 and MV4-11 cell lines of compound **39d** (low micromolar range) compared to **34a** (low to middle nanomolar range). Notably, compound **39c** retained an acceptable growth inhibitory profile and was even more potent against DLBCL cell lines than compound **12**; then, **39c** was

assayed at 10μM against a panel of 14 histone methyltransferases (Supplementary Table 1), no target was significantly inhibited (>50%). Surprisingly, compound **39c** was selective for G9a over GLP (IC_{50} > 20 μM). For DNMTs, DNMT3A but not DNMT3B was inhibited by **39c** (81% and 0%, respectively). Thus, based on all these results, **39c** was further progressed into ADME and PK studies despite its THLE-2 cytotoxicity. Overall, these data showed that the inhibition of G9a and DNMT has differential phenotypic effects depending on the cell type. Despite a general trend in increased cytotoxicity in both tumoral and healthy cell lines can be observed (e.g. for compounds in Tables 2 and 3), this tendency was not confirmed for all molecules and, in some cases, adequate therapeutic windows are achieved (e.g. >1.5 log units for **23k** and **34a**).

Finally, and as also reported for compound **12**,[53] the functional cellular potency of selected compounds was assessed by quantifying the global levels of H3K9me2 (Western Blot) and 5-methylcytosine (5mC) (LC-MS/MS) in the MV4-11 cell line following 48 h of exposure. As an additional example of this chemical series, compound **39c** (Figure 4), with potent anti-proliferative effects (Table 3) and slightly worse biochemical profile than **12**, reduced significantly ($p \leq 0.05$) the H3K9me2 levels in a concentration-dependent manner from 50 nM (Figure 4A). In the case of the measurement of global DNA methylation by LC-MS/MS in the MV4-11 cell line, we detected that compound **39c** results in a subtle decrease, around 10%, of the overall DNA methylation in the genome at 50 nM (Figure 4B). Higher doses of **39c** did not result in reduced global DNA methylation levels; this seems to be a common fact to DNMT inhibitors Decitabine[70] and Azacitidine.[71] In our opinion, these effects are because at high concentrations the majority of the cells are dead and we are only analyzing the epigenetic marks in those cells that are resistant to the treatment. This is a

key point; we have to work at lower doses than their IC_{50} values, and long incubation periods, to avoid killing cells and thus to be able to monitor their impact on the epigenetic marks. To better verify the importance of the overall decrease in DNA methylation detected by LC-MS/MS, we conducted a study using MethylationEPIC BeadChip, which interrogate quantitatively over 850,000 methylation sites across the genome at single-nucleotide resolution. We performed this analysis in MV4-11 cells, controls as well as treated with 10nM and 50nM of **39c**. As identified by LC-MS/MS, both concentrations led to a subtle but very consistent change in the level of global DNA methylation (changes are greater than 5%); in fact, more than 15,000 CpGs are hypomethylated and there is a significant overlap between results obtained with both concentrations (Supplementary Information, Figure S4). The results obtained using LC-MS/MS and the methylation array show that the changes in the level of global and specific DNA methylation mediated by compound **39c** are small but in turn very consistent with all the techniques used and in all experiments carried out. In summary, these results demonstrate the functional dual effect of compound **39c** against the methyltranferase activity of G9a and DNMTs.

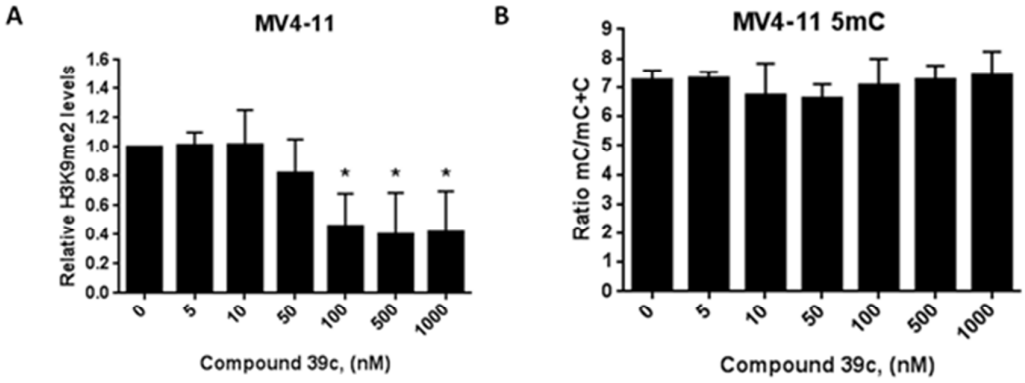

Figure 4. H3K9me2 and 5mC hallmarks in the MV4-11 cell line after treatment with compound **39c** for 48 hours. A) Densitometry quantification of H3K9me2 levels. B) Global DNA methylation measurement by LC-MS/MS in MV4-11 cell line after

treatment with different doses of compound **39c**. Asterisks show the P value of a one-tailed Mann-Whitney U test (* $p \leq 0.05$). Error bars indicate s.d. from three replicates.

ADME and PK Profile

As shown in Table 4, the selected compounds **12**, **34a, 39a** and **39c** exhibited low inhibition of the five major cytochrome P450 isoforms (1A2, 2C9, 2C19, 2D6, and 3A4); in fact, the percentage inhibition values, at 10 μM, were less than 30% for all tested compounds. The metabolic stability of these three compounds at a concentration of 1 μM was evaluated in human and mouse liver microsomes after 20 min of incubation. A species difference in metabolism was observed. In human microsomes, 5-methyl-2-furyl substituted compounds **12** and **39c** displayed excellent stability (>95% remaining), in contrast to the moderate stability of compound **34a** with the 5-ethyl-2-furyl side chain. In mice, only compound **12** had good stability (>70% remaining) and, in contrast to our initial expectations, the introduction of the cyclopropyl ring of compound **39c** did not improve its metabolic stability (<20% remaining), at least in mice.

The low metabolic stability in mouse microsomes of compounds **34a** and **39c** translated in a high clearance (**34a**) and a reduced half-life (**39c**, in comparison to **12**) when administered to BALB/c-RAG2$^{-/-}$γc$^{-/-}$ mice for PK profiling (Table 5 and Supplementary Tables S2 and S3); thus, precluding their use in *in vivo* efficacy assays. Only compound **12** dosed at 2.5 mg/kg intravenously (i.v.) revealed an acceptable profile with a good half-life (24.2 h) and an acceptable exposure ($AUC_{0\text{-}24h}$ = 1494 nM), optimal for once-daily dosing, to achieve *in vivo* efficacy *versus* cell lines with GI_{50} values around 200-450 nM.[53]

Table 4. ADME Profile of selected compounds

Cpd	1A2 (%)[a]	2C9 (%)[a]	2C19 (%)[a]	2D6 (%)[a]	3A4 (%)[a]	HLM (%)[b]	HLM ($t_{1/2}$)[c]	MLM (%)[b]	MLM ($t_{1/2}$)[c]
12[53]	2.8	0.56	2.5	4.9	0.0	99.7	>2.4	70.9	0.6
34a	0.0	0.0	0.0	26.7	0.07	67.1	1.6	16.9	0.2
39c	28.6	8.0	4.0	27.6	4.6	97	>2.4	15	0.1
39a	4.3	6.1	0	11.4	0	64	1.7	36.9	0.3

[a] % inhibition at 10 μM. [b] % compound remaining after a 20-min incubation in human or mouse liver microsomes (HLM and MLM respectively), [c] media time (h) in HML and MLM. All assays were performed in duplicate.

Table 5. PK Profile of selected compounds

Cpd	Route	Dose (mg/kg)	AUC_{0-24h} (nM * h)	$t_{1/2}$ (h)	Cl (L/h/kg)	Vss (L/kg)
12[53]	i.v.	2.5	1494	24.2	0.91	29.3
34a	i.v.	1.9	505	13.2	5.90	88.5
39c	i.v.	5	8789	10.4	0.90	11.9

Species: BALB/c-RAG2$^{-/-}$γc$^{-/-}$ mice; Vehicle: saline (NaCl 0.9%); n=4 and time points: 0.25, 1, 2, 4, 8 and 24 h (the time point after 1 h was not collected for compound **12**).

Compared with the PK profile of **4** (intraperitoneal administration, at 5mg/kg),[22] the first G9a chemical probe suitable for *in vivo* testing, compound **12** (as reported in Table 5, i.v. at 2.5 mg/kg), reached a lower area under the curve (AUC_{0-24h}): 1494 nM versus 2314 nM, for **12** and **4**, respectively. Considering that intraperitoneal administration may lead to first pass clearance and the lower AUC_{0-24h} for **12**, one could assume (leaving aside the dose difference), that compound **4** exhibits a better PK profile than **12**. However, the once-daily administration of **12** at 2.5 mg/kg (i.v.) is optimal to reach

an adequate sustained plasmatic concentration for *in vivo* treatment, in terms of efficacy and safety (within the therapeutic window), and to achieve our initial aim: *in-vivo* proof-of-concept (PoC). Additional medicinal chemistry efforts are required to optimize this molecule.

***In Vivo* Efficacy of CM-272 in human AML xenografts in a mouse model**

Given the potent anti-proliferative response of compound **12** against the AML MV4-11 cell line, with a GI_{50} value of 269 nM (Table 1),[53] we decided to test its *in vivo* efficacy in terms of tumor growth in a mouse model using human AML xenografts.

This mouse model using human AML xenografts showed, for the first time, that tumor growth is prevented using these reversible inhibitors, in tumors induced by subcutaneously injecting 10×10^6 MV4-11 cells in $Rag2^{-/-}\gamma c^{-/-}$ mice. These mice were then treated with 2.5 mg/kg (i.v.) of compound **12** starting one day after leukemic cell inoculation, administered daily during 21 consecutive days and sacrificed at day 23 after cell inoculation. The mice were controlled for signs of morbidity (behavior and body weight loss), and the tumor volume was monitored weekly (Figure 5). As shown in Figure 5, treatment with **12** produced a significant (p value < 0.05) 70% overall tumor growth inhibition (average tumor volumes at day 23 of 940 ± 435 mm^3 and 3096 ± 1399 mm^3 for treated and control groups, respectively). For comparison, when treating a AML flank xenograft model using MV4-11 cells with compound **5**, administered via osmotic mini-pump at 30 mg/kg/day for two weeks (to achieve a projected efficacious exposure while mitigating the presumed C_{max}-driven toxicity), a modest 45% tumor growth inhibition was observed.[26]

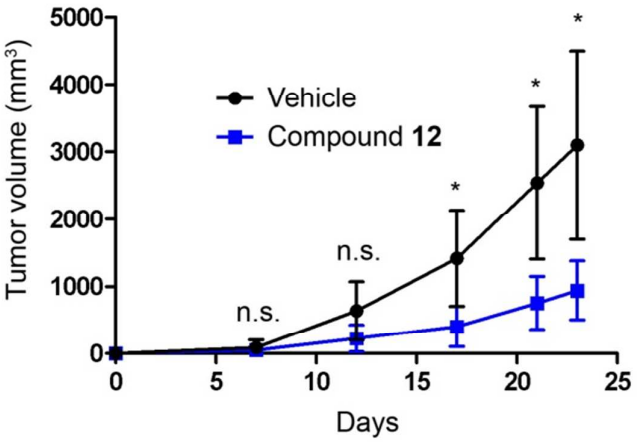

Figure 5. Compound **12** has *in vivo* activity in a MV4-11 tumor progression model. Average volume (mm^3) ± SD values of both groups, control and treated mice (n=6), during treatment. n.s. = non-statistically significant. * p value ≤ 0.05.

DISCUSSION AND CONCLUSIONS

We presented a detailed account of the ligand- and structure-based design of a novel 4-aminoquinoline series of potent molecules that simultaneously inhibit G9a and DNMT1 methyltransferase activities in a reversible manner. Exploration around the 2- and 4-amino positions of the quinoline scaffold led us to evolve from the initial hit compound **11** and achieve a pharmacological tool compound, **12**, for *in vivo* proof-of-concept. Interestingly, the corresponding quinazoline-based pair of **12**, compound **40** (Chart 5 and synthesis in the Supporting Information), exhibited reduced biochemical potency, thereby validating the quinoline scaffold for the blocking of both targets, while quinazolines were extensively examined for G9a inhibition.

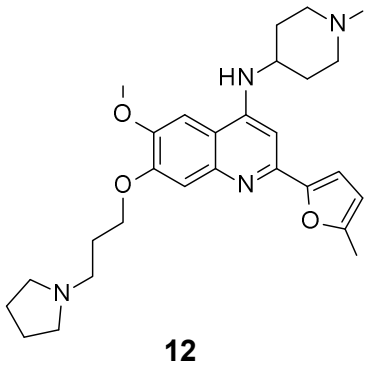

12

IC_{50} G9a = 8 nM
IC_{50} DNMT1 = 382 nM

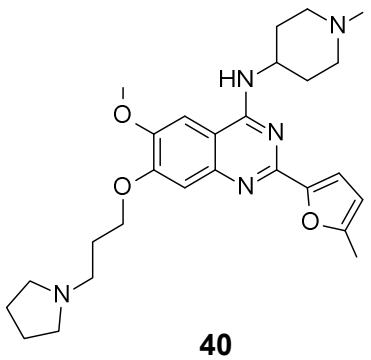

40

IC_{50} G9a = 336 nM
IC_{50} DNMT1 = 2250 nM

Chart 5. Lead compound **12** and its corresponding quinoline matched pair **40**.

Methyl-2-furyl and 5-ethyl-2-furyl rings at the 2-position were prioritized because the groups conferred a good biochemical potency against both targets as well as the highest antiproliferative response. Optimizations at the 4-position to reduce the basicity yielded potent biochemical and cellular compounds with improved permeability over **12**, but, unexpectedly, reduced the therapeutic window as well as the microsomal stability and showed poor PK. Together with previously reported data in overall survival mouse models, where impact on both epigenetic marks was shown,[53] we present new evidence of the *in vivo* efficacy of compound **12** in an AML tumor progression model. This result, compared to **5** (selective G9a inhibitor), suggests that DNMT1 inhibition may contribute to the improved *in-vivo* efficacy of compound **12**.

Additional characterization of the *in vivo* efficacy of compound **12** to treat different solid tumors, focused on unmet medical needs, will be described in due course. On the other hand, a detailed SAR analysis describing the exploration around those growing vectors from our chemical series (4-aminoquinoline) and the corresponding impact on

selectivity profiling against the targets of interest (G9a and DNMTs: equally potent, G9a selective and DNMT1 selective) has been also reported.[72]

EXPERIMENTAL SECTION

Chemistry. General Procedure.

Unless otherwise noted, all reagents and solvents were of the highest commercial quality and used without further purification. All experiments dealing with moisture sensitive compounds were conducted under N_2. Flash column chromatography was performed on silica gel, particle size 60 Å, mesh = 230-400 (Merck) under standard techniques. Automated flash column chromatography was performed using ready-to-connect cartridges from Varian, on irregular silica gel, particle size 15-40 µm (normal phase disposable flash columns) on a Biotage SPX flash purification system. Microwave-assisted reactions were performed in a Biotage Smith Synthesis microwave reactor. The NMR spectroscopic data were recorded on a Bruker AV400 or VARIAN 400MR spectrometer with standard pulse sequences, operating at 400 MHz. Chemical shifts (δ) are reported in parts per million (ppm) downfield from tetramethylsilane (TMS), which was used as internal standard. The abbreviations used to explain multiplicities are s = singlet, d = doublet, t = triplet, m = multiplet. Coupling constants (J) are in hertz. HPLC-analysis was performed using a Shimadzu LC-20AB or LC-20AD with a Luna-C18(2), 5 µm, 2.0*50 mm column at 40 ºC and UV detection at 215, 220 and 254 nm. Flow from the column was split to a MS spectrometer. The MS detector (Agilent 1200, 6110MS or Agilent 1200, 6120MS Quadropole) was configured with an electrospray source or API/APCI. N_2 was used as the nebulizer gas. The source temperature was maintained at 50 ºC. Data acquisition was accomplished with ChemStation LC/MSD quad software. All tested compounds possessed a purity of at

least 95% established by HPLC or LCMS unless otherwise noted. Reported yields were not optimized, the emphasis being on purity of product rather than quantity.

2-Cyclohexyl-*N*-(1-isopropyl-4-piperidyl)-6-methoxy-7-(3-pyrrolidin-1-ylpropoxy)quinolin-4-amine (11)

To a mixture of compound **20** (90 mg, 0.19 mmol) and acetone (6 mg, 1.07 mmol) in THF (30 mL) were added AcOH (65 mg, 1.08 mmol) and $NaBH_3CN$ (67 mg, 1.07 mmol) in one portion at 16 °C under N_2 and the mixture was stirred at 50 °C for 15 hours. Then, the reaction mixture was cooled to 16 °C, filtered and concentrated in vacuum. The residue was purified by preparative HPLC (method 1 described in supporting information) to obtain pure compound **11** (38 mg, 39%) as a yellow syrup. ^{1}H NMR (MeOD, 400 MHz): δ 7.81 (s, 1H), 7.31 (s, 1H), 6.75 (s, 1H), 4.37-4.30 (m, 2H), 4.27-4.21 (m, 1H), 4.03 (s, 3H), 3.87-3.80 (m, 2H), 3.64-3.55 (m, 3H), 3.52-3.45 (m, 2H), 3.37-3.28 (m, 2H), 3.17-3.07 (m, 2H), 2.91-2.82 (m, 1H), 2.41-2.34 (m, 4H), 2.22-1.92 (m, 10H), 1.86-1.68 (m, 4H), 1.56-1.46 (m, 2H), 1.42 (d, J = 8 Hz, 6H). ESI-MS *m/z* 509.5 $[M+H]^+$ calc. for $C_{31}H_{48}N_4O_2$.

1-[3-(2-Methoxy-5-nitro-phenoxy)propyl]pyrrolidine (14)

To a solution of commercially available 2-methoxy-5-nitro-phenol (**13**) (49.0 g, 0.29 mol) in THF (500 mL) was added PPh_3 (152 g, 0.58 mol), 3-pyrrolidin-1-yl-propan-1-ol (38 g, 0.29 mol) and DEAD (101 g 0.58 mol) at 0 ºC and the solution was stirred at room temperature for 5 hours. Then, the reaction mixture was concentrated and extracted with EtOAc. The combined organic layers were washed with brine, dried over anhydrous Na_2SO_4, filtered and concentrated to give the crude product which was purified by column chromatography to obtain pure compound **14** (50 g, 62%) as yellow

solid. ^{1}H NMR ($CDCl_3$, 400 MHz): δ 7.88 (dd, *J* = 8.8 Hz, 1H), 7.76 (d, *J* = 6.4 Hz, 1H), 6.88 (d, *J* = 8.8 Hz, 1H), 4.16 (t, *J* = 6.8 Hz, 2H), 3.95 (s, 3H), 2.65 (t, *J* = 7.2 Hz, 2H), 2.60-2.45 (m, 4H), 2.10-2.04 (m, 2H), 1.85-1.75 (m, 4H). ESI-MS *m/z* 281 $[M+H]^+$ calc. for $C_{14}H_{20}N_2O_4$.

4-Methoxy-3-(3-pyrrolidin-1-ylpropoxy)aniline (15)

To a solution of compound **14** (14 g, 0.05 mol) in MeOH (200 mL) was added Pd/C (3 g) and the solution was stirred at 25 ºC for 3 hours under H_2 atmosphere (1 atm). Then, the mixture was filtrated and concentrated to give compound **15** (12 g, 96%) as yellow oil. ^{1}H NMR ($CDCl_3$, 400 MHz): δ 6.69 (d, *J* = 8.4 Hz, 1H), 6.33 (d, *J* = 6.4 Hz, 1H), 6.21 (dd, *J* = 8.4 Hz, 1H), 4.02 (t, *J* = 6.8 Hz, 2H), 3.76 (s, 3H), 2.65 (t, *J* = 7.2 Hz, 2H), 2.60-2.45 (m, 4H), 2.05-2.00 (m, 2H), 1.75-1.60 (m, 4H). ESI-MS *m/z* 251 $[M+H]^+$ calc. for $C_{14}H_{22}N_2O_2$.

2,4-Dichloro-6-methoxy-7-(3-pyrrolidin-1-ylpropoxy)quinoline (16)

To a solution of compound **15** (12.4 g, 0.049 mol) in $POCl_3$ (200 mL) was added malonic acid (5.67 g, 0.055 mol) at room temperature. After stirring for 4 hours, the solution was heated to 90 ºC overnight. Then, the solution was concentrated and the residue was poured into ice-water. The mixture was extracted with EtOAc and the combined organic layers were washed with brine, dried over anhydrous Na_2SO_4, filtered and concentrated to give compound **16** (10 g, 57%) as pale yellow solid. ^{1}H NMR ($CDCl_3$, 400 MHz): δ 7.36 (s, 1H), 7.35 (s, 1H), 7.34 (s, 1H) 4.24 (t, *J* = 6.8 Hz, 2H), 4.02 (s, 3H), 2.66 (t, *J* = 7.2 Hz, 2H), 2.60-2.45 (m, 4H), 2.14 (t, *J* = 6.8 Hz, 2H), 1.87-1.75 (m, 4H). ESI-MS *m/z* 355 $[M+H]^+$ calc. for $C_{17}H_{20}Cl_2N_2O_2$.

4-Chloro-2-(cyclohexen-1-yl)-6-methoxy-7-(3-pyrrolidin-1-ylpropoxy)quinoline (17)

To a solution of compound **16** (708 mg, 2 mmol) in 1,4-dioxane/H_2O (5:1, 18 mL) was added K_2CO_3 (27 mg, 0.20 mmol), $Pd(PPh_3)_4$ (233 mg, 0.2 mmol) and 2-(cyclohex-1-en-1-yl)-4,4,5,5-tetramethyl-1,3,2-dioxaborolane (416 mg, 2 mmol) and the solution was heated to 120 ºC under microwave irradiation for 1 hour. Then, the mixture was concentrated and extracted with EtOAc. The combined organic layers were washed with brine, dried over anhydrous Na_2SO_4, filtered and concentrated to give the crude product which was purified by column chromatography to obtain pure compound **17** (0.4 g, 50%) as yellow solid. ESI-MS *m/z* 401 $[M+H]^+$ calc. for $C_{23}H_{29}ClN_2O_2$. This intermediate was used in the next step without further characterization.

***Tert*-butyl 4-[[2-(cyclohexen-1-yl)-6-methoxy-7-(3-pyrrolidin-1-ylpropoxy)-4-quinolyl]amino]piperidine-1-carboxylate (18)**

To a solution of compound **17** (150 mg, 0.38 mmol) and *tert*-butyl 4-aminopiperidine-1-carboxylate (375 mg, 1.87 mmol) in 1,4-dioxane (30 mL) were successively added $Pd_2(dba)_3$ (68 mg, 0.074 mmol), BINAP (93 mg, 0.15 mmol) and Cs_2CO_3 (305 mg, 0.94 mmol) and the resulting mixture was stirred at 130 °C for 36 hours under N_2. Then, the mixture was diluted with water and extracted with EtOAc. The combined organic phase was washed with brine, dried with Na_2SO_4, filtered, concentrated and purified by preparative TLC to give pure compound **18** (156 mg, 73%) as a yellow solid. ESI-MS *m/z* 565.4 $[M+H]^+$ calc. for $C_{33}H_{48}N_4O_4$. This intermediate was used in the next step without further characterization.

Tert-butyl 4-[[2-cyclohexyl-6-methoxy-7-(3-pyrrolidin-1-ylpropoxy)-4-quinolyl]amino]piperidine-1-carboxylate (19)

A stirred suspension of compound **18** (156 mg, 0.28 mmol) in absolute MeOH (30 mL) containing Pd/C (250 mg) was placed under H_2 (15 Psi) at 15 °C for 10 hours. Then, the mixture was filtered through Celite and washed with MeOH (30 mL). The filtrate was concentrated to dryness to give compound **19** (158 mg, 99% crude) as a yellow solid. ESI-MS *m/z* 567.5 $[M+H]^+$ calc. for $C_{33}H_{50}N_4O_4$. This intermediate was used in the next step without further characterization.

2-Cyclohexyl-6-methoxy-*N*-(4-piperidyl)-7-(3-pyrrolidin-1-ylpropoxy)quinolin-4-amine (20)

A solution of compound **19** (95 mg, 0.17 mmol) in HCl/EtOAc (1.0 M, 15 mL) was stirred at 16 °C for 4 hours. Then, the reaction mixture was concentrated to dryness to give compound **20** (90 mg, 99% crude) as a yellow solid. ESI-MS *m/z* 467.4 $[M+H]^+$ calc. for $C_{28}H_{42}N_4O_2$. This intermediate was used in the next step without further characterization.

6-Methoxy-7-(3-pyrrolidin-1-ylpropoxy)-2-(trifluoromethyl)quinolin-4-ol (21)

Phenylpropanolamine (50 mL) was heated to 80 ºC with stirring in round-bottomed flask, then compound **15** (5 g, 0.02 mol) was added at 80-100 ºC. After addition, ethyl 4,4,4-trifluoro-3-oxobutanoate (3.68 g, 0.02 mol) was added into the reaction mixture over 15-20 minutes. The reaction mixture was stirred vigorously at 120 ºC for 12 hours. The reaction mixture was poured into ice-water and adjusted pH to 8 by Na_2CO_3, then concentrated and extracted with CH_2Cl_2/MeOH (3:1). The combined organic layer was concentrated to give the desired compound **21** (2.5 g, 33%). ESI-MS *m/z* 371 $[M+H]^+$

calc. for $C_{18}H_{21}F_3N_2O_3$. This intermediate was used in the next step without further characterization.

4-Chloro-6-methoxy-2-(4-methylpiperazin-1-yl)-7-(3-pyrrolidin-1-ylpropoxy)quinoline (22c)

To a solution of compound **16** (1.38 g, 3.9 mmol) in 1,4-dioxane (15 mL) was added Cs_2CO_3 (2.56 g, 7.86 mmol), BINAP (0.244 g, 0.39 mmol), $Pd_2(dba)_3$ (0.302 , 0.33 mmol) and 1-methyl-piperazine (0.6 g, 5.3 mmol) and the mixture was heated to 110 ºC for 12 hours. Then, the solution was concentrated and extracted with EtOAc. The combined organic layers were washed with brine, dried over anhydrous Na_2SO_4, filtered and concentrated to give the crude product which was purified by column chromatography to obtain pure compound **22c** (0.3 g, 18%) as a yellow solid. ESI-MS *m/z* 419 $[M+H]^+$ calc. for $C_{22}H_{31}ClN_4O_2$. This intermediate was used in the next step without further characterization.

4-Chloro-6-methoxy-2-methyl-7-(3-pyrrolidin-1-ylpropoxy)quinoline (22d)

To a solution of compound **16** (2.78 g, 7.87 mmol) in 1,4-dioxane (30 mL) was added $MeB(OH)_2$ (0.52 g, 8.66 mmol), K_2CO_3 (2.17 g, 15.7 mmol) and $Pd(PPh_3)_4$ (0.91 g, 0.78 mmol) and the mixture was heated to 110 ºC for 12 hours. Then, the solution was concentrated and extracted with EtOAc. The combined organic layers were washed with brine, dried over anhydrous Na_2SO_4, filtered and concentrated to give the crude product which was purified by column chromatography to obtain pure compound **22d** (0.5 g, 19%) as yellow solid. ^{1}H NMR ($CDCl_3$, 400 MHz): δ 7.27 (s, 1H), 7.16 (s, 1H), 7.14 (s, 1H), 4.15 (t, *J* = 6.8Hz, 2H), 3.92 (s, 3H), 2.60-2.51 (m, 5H), 2.50-2.41 (m, 4H), 2.10-2.01 (m, 2H) 1.75-1.65 (m, 4H). ESI-MS *m/z* 335 $[M+H]^+$ calc. for $C_{18}H_{23}ClN_2O_2$.

4-Chloro-2,6-dimethoxy-7-(3-pyrrolidin-1-ylpropoxy)quinoline (22e)

Compound **16** (1.5 g, 4.24 mmol) was dissolved in NaOMe (25 mL, 25%) and stirred at room temperature overnight. Then, the reaction mixture was quenched with water and extracted with EtOAc. The combined organic phase was concentrated to give the crude product which was purified by preparative HPLC (method 1 described in supporting information) to obtain pure compound **22e** (0.5 g, 34%). ESI-MS *m/z* 351 $[M+H]^+$ calc. for $C_{18}H_{23}ClN_2O_3$. This intermediate was used in the next step without further characterization.

4-Chloro-6-methoxy-7-(3-pyrrolidin-1-ylpropoxy)-2-(trifluoromethyl)quinoline (22f)

Compound **21** (370 mg, 1 mmol) was dissolved in $POCl_3$ (30 mL) and stirred at 110 ºC for 2 hours. Then, the reaction mixture was concentrated, quenched by ice-water and extracted with EtOAc. The organic phase was dried with Na_2SO_4, filtered and concentrated to give the desired compound **22f** (200 mg, 52%). ESI-MS *m/z* 389 $[M+H]^+$ calc. for $C_{18}H_{20}ClF_3N_2O_2$. This intermediate was used in the next step without further characterization.

4-Chloro-6-methoxy-2-phenyl-7-(3-pyrrolidin-1-ylpropoxy)quinoline (22g)

To a solution of compound **16** (300 mg, 0.85 mmol) in 1,4-dioxane/H_2O (5:1, 18 mL) was added Na_2CO_3 (180 mg, 1.7 mmol), $Pd(PPh_3)_4$ (98 mg, 0.085 mmol) and phenylboronic acid (93 mg, 0.76 mmol) and the solution was heated to 110 ºC for 4 hours under microwave irradiation. Then, the mixture was concentrated and extracted with EtOAc. The combined organic layers were washed with brine, dried over

anhydrous Na_2SO_4, filtered and concentrated to give the crude product which was purified by preparative TLC to obtain pure compound **22g** (0.1 g, 30%) as pale yellow solid. ESI-MS *m/z* 397 $[M+H]^+$ calc. for $C_{23}H_{25}ClN_2O_2$. This intermediate was used in the next step without further characterization.

4-Chloro-6-methoxy-2-(o-tolyl)-7-(3-pyrrolidin-1-ylpropoxy)quinoline (22h)

To a solution of compound **16** (200 mg, 0.56 mmol) in 1,4-dioxane/H_2O (5:1, 18 mL) was added K_2CO_3 (78 mg, 0.56 mmol), $Pd(PPh_3)_4$ (65 mg, 0.056 mmol) and o-tolylboronic acid (103 mg, 0.76 mmol) and the solution was heated to 110 ºC for 4 hours under microwave irradiation. Then, the mixture was concentrated and extracted with EtOAc. The combined organic layers were washed with brine, dried over anhydrous Na_2SO_4, filtered and concentrated to give the crude product which was purified by preparative TLC to obtain pure compound **22h** (0.11 g, 48%) as pale yellow solid. ESI-MS *m/z* 411 $[M+H]^+$ calc. for $C_{24}H_{27}ClN_2O_2$. This intermediate was used in the next step without further characterization.

4-Chloro-6-methoxy-2-(3-pyridyl)-7-(3-pyrrolidin-1-ylpropoxy)quinoline (22i)

To a solution of compound **16** (354 mg, 1 mmol) in 1,4-dioxane/H_2O (15:1, 16 mL) was added Na_2CO_3 (212 mg, 2 mmol), $Pd(PPh_3)_4$ (40 mg, 0.03 mmol) and pyridin-3-ylboronic acid (123 mg, 1 mmol) and the solution was heated to 110 ºC for 2 hours under microwave irradiation. Then, the reaction was quenched with water and extracted with EtOAc. The organic layer was washed with brine, dried over anhydrous Na_2SO_4, filtered and concentrated to give the crude product which was purified by preparative HPLC (method 2 described in supporting information) to obtain pure compound **22i** (200 mg, 50%) as a yellow solid. ^{1}H NMR (MeOD, 400 MHz): δ 9.67 (s, 1H), 9.41 (d, *J*

= 8.4 Hz, 1H), 8.93 (d, *J* = 8.4 Hz, 1H), 8.33 (s, 1H), 8.26-8.22 (m, 1H), 7.63 (s, 1H), 7.60 (s, 1H), 4.45-4.35 (m, 2H), 4.09 (s, 3H), 3.88-3.78 (m, 2H), 3.54-3.48 (m, 2H), 3.22-3.10 (m, 2H), 2.45-2.35 (m, 2H), 2.26-2.15 (m, 2H), 2.11-2.02 (m, 2H). ESI-MS *m/z* 398.2 $[M+H]^+$ calc. for $C_{22}H_{24}ClN_3O_2$.

4-[4-Chloro-6-methoxy-7-(3-pyrrolidin-1-ylpropoxy)-2-quinolyl]-1*H*-pyridin-2-one (22j)

To a solution of compound **16** (354 mg, 1 mmol) in 1,4-dioxane/H_2O (15:1, 16 mL) was added K_2CO_3 (278 mg, 2 mmol), $Pd(PPh_3)_4$ (50 mg, 0.04 mmol) and 4-(4,4,5,5-tetramethyl-1,3,2-dioxaborolan-2-yl)-1*H*-pyridin-2-one (**Int. 1**) (freshly prepared, 1.25 mmol in 10 mL of 1,4-dioxane, synthesis described in supporting information) and the solution was heated to 120 ºC for 4 hours under microwave irradiation. Then, the mixture was quenched with water and extracted with EtOAc. The organic layer was washed with brine, dried over anhydrous Na_2SO_4 and concentrated to give the crude product which was purified by preparative HPLC (method 3 described in supporting information) to obtain pure compound **22j** (207 mg, 50%). ^{1}H NMR (MeOD, 400 MHz): δ 8.12 (s, 1H), 7.72 (s, 1H), 7.58-7.55 (m, 2H), 7.37 (br s, 2H), 4.43-4.35 (m, 2H), 4.10 (s, 3H), 3.89-9.78 (m, 2H), 3.55-3.45 (m, 2H), 3.25-3.15 (m, 2H), 2.45-2.35 (m, 2H), 2.25-2.15 (m, 2H), 2.12-2.02 (m, 2H). ESI-MS *m/z* 414.2 $[M+H]^+$ calc. for $C_{22}H_{24}ClN_3O_3$.

4-Chloro-2-(3-furyl)-6-methoxy-7-(3-pyrrolidin-1-ylpropoxy)quinoline (22k)

To a solution of compound **16** (354 mg, 1 mmol) in 1,4-dioxane/H_2O (15:1, 16 mL) was added Na_2CO_3 (212 mg, 2 mmol), $Pd(PPh_3)_4$ (40 mg, 0.03 mmol) and furan-3-ylboronic acid (159 mg, 1.43 mmol) and the solution was heated to 110 ºC for 2 hours under

microwave irradiation. Then, the reaction was quenched with water and extracted with EtOAc. The organic layer was washed with brine, dried over anhydrous Na_2SO_4, filtered and concentrated to give the crude product which was purified by preparative HPLC (method 2 described in supporting information) to obtain pure compound **22k** (120 mg, 31%) as a yellow solid. ^{1}H NMR (DMSO-d_6, 400 MHz): δ 8.51 (s, 1H), 8.00 (s, 1H), 7.81 (s, 1H), 7.43-3.37 (m, 2H), 7.15 (s, 1H), 4.33-4.24 (m, 2H), 3.97 (s, 3H), 3.68-3.58 (m, 2H), 3.35-3.25 (m, 2H), 3.10-3.00 (m, 2H), 2.25-2.15 (m, 2H), 2.06-1.95 (m, 2H), 1.90-1.78 (m, 2H). ESI-MS *m/z* 387.2 $[M+H]^+$ calc. for $C_{21}H_{23}ClN_2O_3$.

4-Chloro-6-methoxy-2-(5-methyl-2-thienyl)-7-(3-pyrrolidin-1-ylpropoxy)quinoline (22l)

To a solution of compound **16** (200 mg, 0.56 mmol) in 1,4-dioxane/H_2O (5:1, 18 mL) was added K_2CO_3 (116 mg, 0.84 mmol), $Pd(PPh_3)_4$ (65 mg, 0.056 mmol) and 4,4,5,5-tetramethyl-2-(5-methyl-2-thienyl)-1,3,2-dioxaborolane (126 mg, 0.56 mmol) and the solution was heated to 110 ºC for 4 hours under microwave irradiation. Then, the mixture was concentrated and extracted with EtOAc. The combined organic layers were washed with brine, dried over anhydrous Na_2SO_4, filtered and concentrated to give the crude product which was purified by preparative TLC to obtain pure compound **22l** (0.12 g, 51%) as pale yellow solid. ESI-MS *m/z* 417 $[M+H]^+$ calc. for $C_{22}H_{25}ClN_2O_2S$. This intermediate was used in the next step without further characterization.

4-Chloro-6-methoxy-2-(5-methyl-1*H*-pyrrol-2-yl)-7-(3-pyrrolidin-1-ylpropoxy)quinoline (22m)

To a solution of compound **16** (354 mg, 1 mmol) in 1,4-dioxane/H_2O (15:1, 16 mL) was added K_2CO_3 (278 mg, 2 mmol), $Pd(PPh_3)_4$ (50 mg, 0.04 mmol) and 2-methyl-5-

(4,4,5,5-tetramethyl-1,3,2-dioxaborolan-2-yl)-1*H*-pyrrole (**Int. 2**, synthesis described in supporting information) (207 mg, 1 mmol) and the solution was heated to 120 ºC for 4 hours under microwave irradiation. Then, the mixture was quenched with water and extracted with EtOAc. The organic layer was washed with brine, dried over anhydrous Na_2SO_4, filtered and concentrated to give the crude product which was purified by preparative HPLC (method 3 described in supporting information) to obtain pure compound **22m** (150 mg, 38%) as a yellow solid. ^{1}H NMR (MeOD, 400 MHz): δ 8.13 (s, 1H), 7.67 (s, 1H), 7.60 (s, 1H), 7.41 (d, *J* = 4 Hz, 1H), 6.28 (d, *J* = 4 Hz, 1H), 4.48-4.40 (m, 2H), 4.10 (s, 3H), 3.90-3.80 (m, 2H), 3.56-3.48 (m, 2H), 3.26-3.10 (m, 2H), 2.50-2.35 (m, 5H), 2.30-2.18 (m, 2H), 2.11-2.02 (m, 2H). ESI-MS *m/z* 400.2 $[M+H]^+$ calc. for $C_{22}H_{26}ClN_3O_2$.

4-Chloro-6-methoxy-2-(2-methylpyrazol-3-yl)-7-(3-pyrrolidin-1-ylpropoxy)quinoline (22n)

To a solution of compound **16** (270 mg, 0.76 mmol) in 1,4-dioxane/H_2O (15:1, 16 mL) was added Na_2CO_3 (322 mg, 3.04 mmol), $Pd(PPh_3)_4$ (87.7 mg, 0.07 mmol) and commercially available 1-methyl-5-(4,4,5,5-tetramethyl-1,3,2-dioxaborolan-2-yl)-1*H*-pyrazole (159 mg, 0.76 mmol). The solution was heated to 110 ºC for 2 hours under microwave irradiation. The mixture was quenched with water and extracted with EtOAc. The organic layer was washed with brine, dried over anhydrous Na_2SO_4, filtered and concentrated to give the crude product which was purified by preparative HPLC (method 2 described in supporting information) to obtain pure compound **22n** (120 mg, 40%) as a yellow solid. ESI-MS *m/z* 401 $[M+H]^+$ calc. for $C_{21}H_{25}ClN_4O_2$. This intermediate was used in the next step without further characterization.

4-Chloro-6-methoxy-2-(1-methylpyrazol-3-yl)-7-(3-pyrrolidin-1-ylpropoxy)quinoline (22o)

To a solution of compound **16** (354 mg, 1 mmol) in 1,4-dioxane/H_2O (15:1, 16 mL) was added K_2CO_3 (278 mg, 2 mmol), $Pd(PPh_3)_4$ (50 mg, 0.05 mmol) and 1-methyl-3-(4,4,5,5-tetramethyl-1,3,2-dioxaborolan-2-yl)pyrazole (207 mg, 1 mmol) and the solution was heated to 120 ºC for 4 hours under microwave irradiation. Then, the mixture was quenched with water and extracted with EtOAc. The organic layer was washed with brine, dried over anhydrous Na_2SO_4, filtered and concentrated to give the crude product which was purified by preparative HPLC (method 3 described in supporting information) to obtain pure compound **22o** (130 mg, 33%) as a yellow solid. ^{1}H NMR (MeOD, 400 MHz): δ 8.30 (s, 1H), 7.83 (s, 1H), 7.68 (s, 1H), 7.63 (s, 1H), 7.17 (s, 1H), 4.48-4.38 (m, 2H), 4.14-4.03 (m, 6H), 3.85-3.75 (m, 2H), 3.56-3.47 (m, 2H), 3.26-3.15 (m, 2H), 2.48-2.35 (m, 2H), 2.30-2.15 (m, 2H), 2.15-2.03 (m, 2H). ESI-MS *m/z* 401.2 $[M+H]^+$ calc. for $C_{21}H_{25}ClN_4O_2$.

4-Chloro-2-(3,6-dihydro-2*H*-pyran-4-yl)-6-methoxy-7-(3-pyrrolidin-1-ylpropoxy)quinoline (22p)

To a solution of compound **16** (354 mg, 1 mmol) in 1,4-dioxane/H_2O (15:1, 16 mL) was added Na_2CO_3 (212 mg, 2 mmol), $Pd(PPh_3)_4$ (50 mg, 0.04 mmol) and 2-(3,6-dihydro-2*H*-pyran-4-yl)-4,4,5,5-tetramethyl-1,3,2-dioxaborolane (210 mg, 1 mmol) and the solution was heated to 110 ºC for 4 hours under microwave irradiation. Then, the reaction was quenched with water and extracted with EtOAc. The organic layer was washed with brine, dried over anhydrous Na_2SO_4, filtered and concentrated to give the crude product which was purified by preparative HPLC (method 2 described in supporting information) to obtain pure compound **22p** (250 mg, 62%) as a yellow solid.

^{1}H NMR (MeOD, 400 MHz): δ 7.92 (s, 1H), 7.59 (s, 1H), 7.57 (s, 1H), 6.90 (s, 1H), 4.43-4.37 (m, 4H), 4.07 (s, 3H), 3.99-3.91 (m, 2H), 3.87-3.77 (m, 2H), 3.51-3.45 (m, 2H), 3.20-3.10 (m, 2H), 2.75-2.70 (m, 2H), 2.55-2.30 (m, 2H), 2.25-2.15 (m, 2H), 2.11-2.03 (m, 2H). ESI-MS *m/z* 403.2 $[M+H]^+$ calc. for $C_{22}H_{27}ClN_2O_3$.

4-Chloro-6-methoxy-2-(5-methyl-2-furyl)-7-(3-pyrrolidin-1-ylpropoxy)quinoline (22r)

To a mixture of **16** (10.00 g, 28.15 mmol) and 4,4,5,5-tetramethyl-2-(5-methyl-2-furyl)-1,3,2-dioxaborolane (6.44 g, 30.97 mmol,) in 1,4-dioxane (100 mL), was added K_2CO_3 (7.78 g, 56.30 mmol) and $Pd(PPh_3)_4$ (2.00 g, 1.73 mmol) in one portion at 25 ºC under N_2 and the mixture was stirred at 25 ºC for 10 minutes. Then, the reaction mixture was heated to 120 ºC for 12 hours. Then, the mixture was cooled to 25 ºC and extracted with EtOAc. The combined organic phase was washed with saturated brine, dried with anhydrous Na_2SO_4, filtered and concentrated in vacuum to give a residue which was purified by column chromatography to afford pure compound **22r** (8.00 g, 71%) as yellow solid. ^{1}H NMR (DMSO-d_6, 400 MHz): δ 7.83 (s, 1H), 7.47 (s, 1H), 7.36 (s, 1H), 7.19 (d, J = 3.2 Hz, 1H), 6.31 (d, J = 3.2 Hz, 1H), 4.32-4.23 (m, 2H), 3.96 (s, 3H), 3.65-3.55 (m, 2H), 3.36-3.26 (m, 2H), 3.10-3.00 (m, 2H), 2.39 (s, 3H), 2.25-2.15 (m, 2H), 2.06-1.95 (m, 2H), 1.90-1.80 (m, 2H). ESI-MS *m/z* 401.2 $[M+H]^+$ calc. for $C_{22}H_{25}ClN_2O_3$.

2-Cyclohexyl-6-methoxy-*N*-(1-methyl-4-piperidyl)-7-(3-pyrrolidin-1-ylpropoxy)quinolin-4-amine (23a)

To a solution of compound **23b** (47.8 mg, 0.1 mmol) in EtOH (10 mL) was added Pd/C (15 mg) under H_2 (1 atm) and the mixture was stirred at 25 ºC for 15 hours. Then, the

reaction mixture was filtered and the filtrate was concentrated to give the desired compound **23a** (48 mg, 99%) as yellow solid; m.p. 101-102 ºC. ^{1}H NMR (MeOD, 400 MHz): δ 7.82 (s, 1H), 7.35 (s, 1H), 6.76 (s, 1H), 4.40-4.30 (m, 3H), 4.04 (s, 3H), 3.90-3.80 (m, 2H), 3.75-3.66 (m, 2H), 3.55-3.45 (m, 2H), 3.35-3.25 (m, 2H), 3.21-3.12 (m, 2H), 2.96 (s, 3H), 2.91-2.85 (m, 1H), 2.43-2.31 (m, 4H), 2.22-1.90 (m, 10H), 1.90-1.70 (m, 3H), 1.58-1.37 (m, 3H). ESI-MS *m/z* 482.5 $[M+H]^+$ calc. for $C_{29}H_{44}N_4O_2$.

2-(Cyclohexen-1-yl)-6-methoxy-*N*-(1-methyl-4-piperidyl)-7-(3-pyrrolidin-1-ylpropoxy)quinolin-4-amine (23b)

To a solution of compound **17** (0.33 g, 0.83 mmol) in 1,4-dioxane (15 mL) was added Cs_2CO_3 (1.7 g, 5.2 mmol), BINAP (0.154 g, 0.25 mmol), $Pd_2(dba)_3$ (0.14 g, 0.15 mmol) and 1-methylpiperidin-4-amine (0.282 g, 2.48 mmol) and the solution was heated to 110 ºC for 1 hour under microwave irradiation. Then, the reaction mixture was concentrated and extracted with EtOAc. The combined organic layers were washed with brine, dried over anhydrous Na_2SO_4, filtered and concentrated to give the crude product which was purified by preparative HPLC (method 1 described in supporting information) to obtain pure compound **23b** (80 mg, 20%) as yellow solid; m.p. 189-190 ºC. ^{1}H NMR (MeOD, 400 MHz): δ 7.82 (s, 1H), 7.43 (s, 1H), 6.81 (s, 1H), 6.73 (s, 1H), 4.34-4.25 (m, 3H), 4.05 (s, 3H), 3.85-3.75 (m, 2H), 3.70-3.60 (m, 2H), 3.60-3.40 (m, 2H), 3.30-3.20 (m, 2H), 3.19-3.10 (m, 2H), 2.99 (s, 3H), 2.62-2.55 (m, 2H), 2.40-2.30 (m, 6H), 2.20-2.10 (m, 6H), 1.91-1.79 (m, 4H). ESI-MS *m/z* 479.6 $[M+H]^+$ calc. for $C_{29}H_{42}N_4O_2$.

6-Methoxy-2-(4-methylpiperazin-1-yl)-*N*-(1-methyl-4-piperidyl)-7-(3-pyrrolidin-1-ylpropoxy)quinolin-4-amine (23c)

To a solution of compound **22c** (0.2 g, 0.48 mmol) in 1,4-dioxane (10 mL) was added Cs_2CO_3 (0.7 g, 2.15 mmol), BINAP (0.059 g, 0.096 mmol), $Pd_2(dba)_3$ (0.087 g, 0.096 mol) and 1-methylpiperidin-4-amine (0.272 , 2.39 mmol) and the mixture was heated to 120 ºC for one hour under microwave irradiation. Then, the solution was concentrated and extracted with EtOAc. The combined organic layers were washed with brine, dried over anhydrous Na_2SO_4, filtered and concentrated to give the crude product which was purified by preparative HPLC (method 1 described in supporting information) to obtain pure compound **23c** (0.02 g, 9%) as yellow solid; m.p. 107-108 ºC. ^{1}H NMR (MeOD, 400 MHz): δ 7.70 (s, 1H), 7.37 (s, 1H), 6.17 (s, 1H), 4.34-4.25 (m, 3H), 4.25-4.05 (m, 3H), 3.97 (s, 3H), 3.85-3.75 (m, 3H), 3.70-3.60 (m, 2H), 3.60-3.40 (m, 6H), 3.20-3.10 (m, 3H), 2.99 (s, 3H), 2.92 (s, 3H), 2.40-2.30 (m, 4H), 2.25-2.15 (m, 3H), 2.12-2.00 (m, 4H). ESI-MS *m/z* 497.4 $[M+H]^+$ calc. for $C_{28}H_{44}N_6O_2$.

6-Methoxy-2-methyl-*N*-(1-methyl-4-piperidyl)-7-(3-pyrrolidin-1-ylpropoxy)quinolin-4-amine (23d)

To a solution of compound **22d** (100 mg, 0.30 mmol) in DME (5 mL) was added K_3PO_4 (0.11 g, 0.5 mmol), biphenyl-2-yl-dicyclohexyl-phosphane (0.052 g, 0.15 mmol), $Pd_2(dba)_3$ (0.14 g, 0.015 mmol) and 1-methylpiperidin-4-amine (0.17 g, 1.5 mmol) and the mixture was heated to 110 ºC for 3 hours under microwave irradiation. Then, the solution was concentrated and extracted with EtOAc. The combined organic layers were washed with brine, dried over anhydrous Na_2SO_4, filtered and concentrated to give the crude product which was purified by preparative HPLC (method 1 described in supporting information) to obtain pure compound **23d** (25 mg, 20%) as a yellow syrup. ^{1}H NMR (MeOD, 400 MHz): δ 7.78 (s, 1H), 7.21 (s, 1H), 6.78 (s, 1H), 4.32 (t, J = 5.2 Hz, 2H), 4.20-4.17 (m, 1H), 4.00 (s, 3H), 3.82-3.78 (m, 2H), 3.70-3.63 (m, 2H), 3.48 (

t, J = 6.8 Hz, 2H), 3.29-3.21 (m, 2H), 3.19-3.11 (m, 2H), 2.95-2.93 (s, 3H), 2.66 (s, 3H), 2.38-2.32 (m, 4H), 2.21-2.16 (m, 2H), 2.11-2.03 (m, 4H). ESI-MS *m/z* 413.3 $[M+H]^+$ calc. for $C_{24}H_{36}N_4O_2$.

2,6-Dimethoxy-*N*-(1-methyl-4-piperidyl)-7-(3-pyrrolidin-1-ylpropoxy)quinolin-4-amine (23e)

To a solution of compound **22e** (0.28 g, 0.8 mmol) in 1,4-dioxane (15 mL) was added Cs_2CO_3 (1.04 g, 3.2 mmol), BINAP (150 mg, 0.24 mmol), $Pd_2(dba)_3$ (218 mg, 0.24 mmol) and 1-methylpiperidin-4-amine (216 mg, 1.9 mmol) and the solution was heated to 110 ºC for 1 hour under microwave irradiation. Then, the solution was concentrated and extracted with EtOAc. The combined organic layer was washed with brine, dried over anhydrous Na_2SO_4, filtered and concentrated to give the crude product which was purified by preparative HPLC (method 1 described in supporting information) to obtain pure compound **23e** (53 mg, 16%) as yellow solid; m.p. 129-130 ºC. ^{1}H NMR (MeOD, 400 MHz): δ 7.81 (s, 1H), 7.10 (s, 1H), 6.32 (s, 1H), 4.32-4.24 (m, 2H), 4.20 (s, 3H), 4.07 (s, 3H), 3.89-3.78 (m, 2H), 3.75-3.63 (m, 2H), 3.53-3.45 (m, 2H), 3.35-3.23 (m, 3H), 3.20-3.10 (m, 2H), 2.96 (s, 3H), 2.45-2.30 (m, 4H), 2.25-2.03 (m, 6H). ESI-MS *m/z* 429.5 $[M+H]^+$ calc. for $C_{24}H_{36}N_4O_3$.

6-Methoxy-*N*-(1-methyl-4-piperidyl)-7-(3-pyrrolidin-1-ylpropoxy)-2-(trifluoromethyl)quinolin-4-amine (23f)

To a solution of compound **22f** (194 mg, 0.5 mmol) in 1,4-dioxane (15 mL) was added Cs_2CO_3 (488 mg, 1.5 mmol), BINAP (94 mg, 0.15 mmol), $Pd_2(dba)_3$ (78 mg, 0.08 mmol) and 1-methylpiperidin-4-amine (171 mg, 1.5 mmol) and the mixture was heated to 110 ºC for 3 hours under microwave irradiation. Then the solution was concentrated

and extracted with EtOAc. The combined organic layer was washed with brine, dried over anhydrous Na_2SO_4, filtered and concentrated to give the crude product which was purified by preparative HPLC (method 1 described in supporting information) to obtain pure compound **23f** (52 mg, 22%) as yellow syrup. ^{1}H NMR (MeOD, 400 MHz): δ 7.92 (s, 1H), 7.42 (s, 1H), 7.31 (s, 1H), 4.42-3.34 (m, 3H), 4.08 (s, 3H), 3.90-3.80 (m, 2H), 3.75-3.68 (m, 2H), 3.55-3.45 (m, 2H), 3.35-3.24 (m, 2H), 3.22-3.12 (m, 2H), 2.92 (s, 3H), 2.45-2.34 (m, 4H), 2.27-2.12 (m, 4H), 2.10-2.02 (m, 2H). ESI-MS *m/z* 467.3 $[M+H]^+$ calc. for $C_{24}H_{33}F_3N_4O_2$.

6-methoxy-*N*-(1-methyl-4-piperidyl)-2-phenyl-7-(3-pyrrolidin-1-ylpropoxy)quinolin-4-amine (23g)

To a solution of compound **22g** (100 mg, 0.25 mmol) in toluene (10 mL) was added *t*-BuOK (1.0 M in THF, 0.37 mL, 0.37 mmol), xantphos (24 mg, 0.04 mmol), $Pd_2(dba)_3$ (69 mg, 0.075 mmol) and 1-methylpiperidin-4-amine (167 mg, 1.4 mmol) and the solution was heated to 130 ºC for 5 hours under microwave irradiation. Then, the mixture was quenched with water and extracted with EtOAc. The organic layer was washed with brine, dried over anhydrous Na_2SO_4, filtered and concentrated to give the crude product which was purified by preparative HPLC (method 1 described in supporting information) to obtain pure compound **23g** (18.2 mg, 15%) as a yellow solid; m.p. 186-187 ºC. ^{1}H NMR (MeOD, 400 MHz): δ 7.95-7.93 (m, 2H), 7.88 (s, 1H), 7.67-7.65 (m, 3H), 7.43 (s, 1H), 7.10 (s, 1H), 4.41-4.32 (m, 3H), 4.06 (s, 3H), 3.85-3.75 (m, 3H), 3.70-3.62 (m, 2H), 3.52-3.47 (m, 2H), 3.30-3.20 (m, 1H), 3.20-3.10 (m, 2H), 2.93 (s, 3H), 2.45-2.35 (m, 4H), 2.23-2.02 (m, 6H). ESI-MS *m/z* 475.3 $[M+H]^+$ calc. for $C_{29}H_{38}N_4O_2$.

6-Methoxy-*N*-(1-methyl-4-piperidyl)-2-(o-tolyl)-7-(3-pyrrolidin-1-ylpropoxy)quinolin-4-amine (23h)

To a solution of compound **22h** (98 mg, 0.24 mmol) in 1,4-dioxane (5 mL) was added BINAP (15 mg, 0.024 mmol), $Pd_2(dba)_3$ (22 mg, 0.024 mmol), Cs_2CO_3 (157 mg, 0.48 mmol) and 1-methylpiperidin-4-amine (54 mg, 0.48 mmol) and the solution was heated to 130 ºC for 5 hours under microwave irradiation. Then, the mixture was quenched with water and extracted with EtOAc. The organic layer was washed with brine, dried over anhydrous Na_2SO_4, filtered and concentrated to give the crude product which was purified by preparative HPLC (method 1 described in supporting information) to obtain pure compound **23h** (16.4 mg, 14%) as a yellow solid; m.p. 98-99 ºC. ^{1}H NMR (MeOD, 400 MHz): δ 7.90 (s, 1H), 7.51-7.48 (m, 2H), 7.45-7.40 (m, 2H), 7.23 (s, 1H), 6.91 (s, 1H), 4.35-4.15 (m, 3H), 4.07 (s, 3H), 3.87-3.77 (m, 2H), 3.67-3.58 (m, 2H), 3.49-3.42 (m, 2H), 3.19-3.14 (m, 4H), 2.89 (s, 3H), 2.42-2.32 (m, 7H), 2.25-2.12 (m, 4H), 2.10-2.06 (m, 2H). ESI-MS *m/z* 489.3 $[M+H]^+$ calc. for $C_{30}H_{40}N_4O_2$.

6-Methoxy-*N*-(1-methyl-4-piperidyl)-2-(3-pyridyl)-7-(3-pyrrolidin-1-ylpropoxy)quinolin-4-amine (23i)

To a solution of compound **22i** (80 mg, 0.2 mmol) in toluene (10 mL) was added *t*-BuOK (1.0 M in THF, 0.4 mL, 0.4 mmol), xantphos (9 mg, 0.02 mmol), $Pd_2(dba)_3$ (30 mg, 0.03 mmol) and 1-methylpiperidin-4-amine (34 mg, 0.3 mmol) and the solution was heated to 130 ºC for 3 hours under microwave irradiation. Then, the solution was concentrated and extracted with EtOAc. The combined organic layer was washed with brine, dried over anhydrous Na_2SO_4, filtered and concentrated to give the crude product which was purified by preparative HPLC (method 2 described in supporting information) to obtain pure compound **23i** (30 mg, 31%) as yellow solid; m.p. 157-158

ºC. ^{1}H NMR (MeOD, 400 MHz): δ 9.18 (br s, 1H), 8.88 (br s, 1H), 8.49-8.47 (m, 1H), 7.92 (s, 1H), 7.78 (br s, 1H), 7.45 (s, 1H), 7.21 (s, 1H), 4.44-4.35 (m, 2H), 4.09 (s, 3H), 3.90-3.80 (m, 2H), 3.75-3.67 (m, 2H), 3.55-3.45 (m, 2H), 3.38-3.25 (m, 3H), 3.24-3.15 (m, 2H), 2.96 (s, 3H), 2.47-2.35 (m, 4H), 2.26-2.05 (m, 6H). ESI-MS *m/z* 476.3 $[M+H]^+$ calc. for $C_{28}H_{37}N_5O_2$.

4-[6-Methoxy-4-[(1-methyl-4-piperidyl)amino]-7-(3-pyrrolidin-1-ylpropoxy)-2-quinolyl]-1*H*-pyridin-2-one (23j)

To a solution of compound **22j** (100 mg, 0.24 mmol) in toluene (10 mL) was added *t*-BuOK (1.0 M in THF, 0.5 mL, 0.5 mmol), xantphos (9 mg, 0.02 mmol), $Pd_2(dba)_3$ (30 mg, 0.03 mmol) and 1-methylpiperidin-4-amine (57 mg, 0.5 mmol) and the mixture was heated to 130 ºC for 10 hours. Then, the solution was concentrated and extracted with EtOAc. The combined organic layer was washed with brine, dried over anhydrous Na_2SO_4, filtered and concentrated to give the crude product which was purified by preparative HPLC (method 3 described in supporting information) to obtain pure compound **23j** (10 mg, 9%) as yellow solid; m.p. 173-174 ºC. ^{1}H NMR (MeOD, 400 MHz): δ 7.91 (s, 1H), 7.73-7.71 (m, 1H), 7.42 (s, 1H), 7.16 (s, 1H), 7.05 (s, 1H), 6.88-6.86 (m, 1H), 4.42-4.33 (m, 3H), 4.09 (s, 3H), 3.90-3.80 (m, 2H), 3.77-3.66 (m, 2H), 3.55-3.47 (m, 2H), 3.35-3.13 (m, 4H), 2.96 (s, 3H), 2.45-2.33 (m, 4H), 2.26-2.05 (m, 6H). ESI-MS *m/z* 492.3 $[M+H]^+$ calc. for $C_{28}H_{37}N_5O_3$.

2-(3-Furyl)-6-methoxy-*N*-(1-methyl-4-piperidyl)-7-(3-pyrrolidin-1-ylpropoxy)quinolin-4-amine (23k)

To a solution of compound **22k** (120 mg, 0.3 mmol) in 1,4-dioxane (10 mL) was added Cs_2CO_3 (325 mg, 1 mmol), BINAP (67 mg, 0.1 mmol), $Pd_2(dba)_3$ (30 mg, 0.03 mmol)

and 1-methylpiperidin-4-amine (114 mg, 1 mmol) and the mixture was heated to 120 ºC for 3 hours under microwave irradiation. Then, the solution was concentrated and extracted with EtOAc. The combined organic layer was washed with brine, dried over anhydrous Na_2SO_4, filtered and concentrated to give the crude product which was purified by preparative HPLC (method 2 described in supporting information) to obtain pure compound **23k** (20 mg, 15%) as yellow solid; m.p. 108-109 ºC. ^{1}H NMR (MeOD, 400 MHz): δ 8.57 (s, 1H), 7.84-7.81 (m, 2H), 7.45 (s, 1H), 7.25 (s, 1H), 7.07 (s, 1H), 4.40-4.30 (m, 2H), 4.04 (s, 3H), 3.85-3.75 (m, 2H), 3.72-3.64 (m, 2H), 3.51-3.45 (m, 2H), 3.30-3.25 (m, 3H), 3.24-3.10 (m, 2H), 2.95 (s, 3H), 2.41-2.34 (m, 4H), 2.23-2.05 (m, 6H). ESI-MS *m/z* 465.2 $[M+H]^+$ calc. for $C_{27}H_{36}N_4O_3$.

6-Methoxy-*N*-(1-methyl-4-piperidyl)-2-(5-methyl-2-thienyl)-7-(3-pyrrolidin-1-ylpropoxy)quinolin-4-amine (23l)

To a solution of compound **22l** (100 mg, 0.24 mmol) in 1,4-dioxane (5 mL) was added BINAP (15 mg, 0.024 mmol), $Pd_2(dba)_3$ (22 mg, 0.024 mmol), Cs_2CO_3 (157 mg, 0.48 mmol) and 1-methylpiperidin-4-amine (54 mg, 0.48 mmol) and the solution was heated to 130 ºC for 5 hours under microwave irradiation. Then, the mixture was quenched with water and extracted with EtOAc. The organic layer was washed with brine, dried over anhydrous Na_2SO_4, filtered and concentrated to give the crude product which was purified by preparative HPLC (method 1 described in supporting information) to obtain pure compound **23l** (13.4 mg, 11%) as a yellow solid; m.p. 110-111 ºC. ^{1}H NMR (MeOD, 400 MHz): δ 7.86-7.83 (m, 2H), 7.44 (s, 1H), 7.04-7.02 (m, 1H), 6.95 (s, 1H), 4.40-4.25 (m, 3H), 4.04 (s, 3H), 3.85-3.78 (m, 2H), 3.72-3.63 (m, 2H), 3.51-3.44 (m, 2H), 3.21-3.10 (m, 2H), 2.97-2.92 (m, 3H), 2.62 (s, 3H), 2.40-2.32 (m, 4H), 2.21-2.07 (m, 8H). ESI-MS *m/z* 495.3 $[M+H]^+$ calc. for $C_{28}H_{38}N_4O_2S$.

6-Methoxy-*N*-(1-methyl-4-piperidyl)-2-(5-methyl-1*H*-pyrrol-2-yl)-7-(3-pyrrolidin-1-ylpropoxy)quinolin-4-amine (23m)

To a solution of compound **22m** (100 mg, 0.25 mmol) in toluene (10 mL) was added *t*-BuOK (1.0 M in THF, 0.5 mL, 0.5 mmol), xantphos (9 mg, 0.02 mmol), $Pd_2(dba)_3$ (30 mg, 0.03 mmol) and 1-methylpiperidin-4-amine (57 mg, 0.5 mmol) and the solution was heated to 130 ºC for 3 hours under microwave irradiation. Then, the solution was concentrated and extracted with EtOAc. The combined organic layer was washed with brine, dried over anhydrous Na_2SO_4, filtered and concentrated to give the crude product which was purified by preparative HPLC (method 3 described in supporting information) to obtain pure compound **23m** (15 mg, 13%) as yellow syrup. ^{1}H NMR (MeOD, 400 MHz): δ 7.78 (s, 1H), 7.42 (br s, 2H), 7.18 (br s, 1H), 6.98 (s, 1H), 6.14 (s, 1H), 4.40-4.30 (m, 2H), 4.10-3.97 (m, 4H), 3.51-3.40 (m, 8H), 2.80-2.55 (m, 5H), 2.50 (s, 3H), 2.48-2.30 (m, 2H), 2.29-2.21 (m, 2H), 2.20-1.95 (m, 6H). ESI-MS *m/z* 478.3 $[M+H]^+$ calc. for $C_{28}H_{39}N_5O_2$.

6-Methoxy-*N*-(1-methyl-4-piperidyl)-2-(2-methylpyrazol-3-yl)-7-(3-pyrrolidin-1-ylpropoxy)quinolin-4-amine (23n)

To a solution of compound **22n** (95 mg, 0.24 mmol) in 1,4-dioxane (5 mL) was added Cs_2CO_3 (406 mg, 1.25 mmol), BINAP (34 mg, 0.05 mmol), $Pd_2(dba)_3$ (27 mg, 0.03 mmol), and 1-methylpiperidin-4-amine (143 mg, 1.25 mmol) and the solution was heated to 120 ºC for 3 hours under microwave irradiation. Then, the solution was concentrated and extracted with EtOAc. The combined organic layer was washed with brine, dried over anhydrous Na_2SO_4, filtered and concentrated to give the crude product which was purified by preparative HPLC (method 2 described in supporting

information) to obtain pure compound **23n** (40 mg, 35%) as yellow solid; m.p. 80-81 ºC. ^{1}H NMR (MeOD, 400 MHz): δ 7.89 (s, 1H), 7.68 (d, *J* = 2.4 Hz, 1H), 7.32 (s, 1H), 7.05 (s, 1H), 6.83 (d, *J* = 2.4 Hz, 1H), 4.40-4.30 (m, 2H), 4.06 (s, 3H), 4.03 (s, 3H), 3.85-3.77 (m, 2H), 3.70-3.62 (m, 2H), 3.51-3.48 (m, 2H), 3.32-3.10 (m, 5H), 2.92 (s, 3H), 2.44-2.30 (m, 4H), 2.25-2.02 (m, 6H). ESI-MS *m/z* 479.2 $[M+H]^+$ calc. for $C_{27}H_{38}N_6O_2$.

6-Methoxy-*N*-(1-methyl-4-piperidyl)-2-(1-methylpyrazol-3-yl)-7-(3-pyrrolidin-1-ylpropoxy)quinolin-4-amine (23o)

To a solution of compound **22o** (100 mg, 0.25 mmol) in toluene (10 mL) was added *t*-BuOK (1.0 M in THF, 0.5 mL, 0.5 mmol), xantphos (9 mg, 0.02 mmol), $Pd_2(dba)_3$ (30 mg, 0.03 mmol) and 1-methylpiperidin-4-amine (57 mg, 0.5 mmol) and the solution was heated to 130 ºC for 3 hours under microwave irradiation. Then, the solution was concentrated and extracted with EtOAc. The combined organic layer was washed with brine, dried over anhydrous Na_2SO_4, filtered and concentrated to give the crude product which was purified by preparative HPLC (method 3 described in supporting information) to obtain pure compound **23o** (25 mg, 21%) as yellow solid; m.p. 139-140 ºC. ^{1}H NMR (MeOD, 400 MHz): δ 7.84 (br s, 2H), 7.55 (s, 1H), 7.25-7.21 (m, 2H), 4.40-4.30 (m, 3H), 4.07 (s, 3H), 4.05 (s, 3H), 3.86-3.76 (m, 2H), 3.75-3.65 (m, 2H), 3.53-3.46 (m, 2H), 3.20-3.08 (m, 4H), 2.95 (s, 3H), 2.45-2.30 (m, 4H), 2.25-2.00 (m, 6H). ESI-MS *m/z* 479.3 $[M+H]^+$ calc. for $C_{27}H_{38}N_6O_2$.

2-(3,6-Dihydro-2*H*-pyran-4-yl)-6-methoxy-*N*-(1-methyl-4-piperidyl)-7-(3-pyrrolidin-1-ylpropoxy)quinolin-4-amine (23p)

To a solution of compound **22p** (200 mg, 0.5 mmol) in 1,4-dioxane (10 mL) was added Cs_2CO_3 (500 mg, 1.5 mmol), BINAP (67.5 mg, 0.1 mmol), $Pd_2(dba)_3$ (40 mg, 0.04 mmol) and 1-methylpiperidin-4-amine (114 mg, 1 mmol) and the solution was heated to 120 ºC for 3 hours under microwave irradiation. Then, the solution was concentrated and extracted with EtOAc. The combined organic layer was washed with brine, dried over anhydrous Na_2SO_4, filtered and concentrated to give the crude product which was purified by preparative HPLC (method 2 described in supporting information) to obtain pure compound **23p** (100 mg, 42%) as yellow solid; m.p. 182-183 ºC. ^{1}H NMR (MeOD, 400 MHz): δ 7.84 (s, 1H), 7.43 (s, 1H), 6.86 (s, 1H), 6.82 (s, 1H), 4.45-4.20 (m, 5H), 4.03 (s, 3H), 4.02-3.97 (m, 2H), 3.85-3.78 (m, 2H), 3.74-3.68 (m, 2H), 3.53-3.48 (m, 2H), 3.25-3.10 (m, 4H), 2.97 (s, 3H), 2.75-2.70 (m, 2H), 2.45-2.33 (m, 4H), 2.30-2.05 (m, 6H). ESI-MS *m/z* 481.3 $[M+H]^+$ calc. for $C_{28}H_{40}N_4O_3$.

6-Methoxy-*N*-(1-methyl-4-piperidyl)-7-(3-pyrrolidin-1-ylpropoxy)-2-tetrahydropyran-4-yl-quinolin-4-amine (23q)

To a solution of compound **23p** (48 mg, 0.1 mmol) in MeOH (15 mL) was added Pd/C (10 mg) under H_2 (1 atm) and the solution was heated to 35 ºC for 4 hours. Then, the mixture was filtrated and the filtrate was concentrated to give compound **23q** (30 mg, 62%) as a yellow solid; m.p. 120-121 ºC. ^{1}H NMR (MeOD, 400 MHz): δ 7.84 (s, 1H), 7.33 (s, 1H), 6.80 (s, 1H), 4.45-4.10 (m, 5H), 4.03 (s, 3H), 3.90-3.78 (m, 2H), 3.75-3.60 (m, 4H), 3.53-3.48 (m, 2H), 3.30-3.15 (m, 5H), 2.97 (s, 3H), 2.41-2.33 (m, 4H), 2.28-1.90 (m, 10H). ESI-MS *m/z* 483.3 $[M+H]^+$ calc. for $C_{28}H_{42}N_4O_3$.

Ethyl 3-(3-benzyloxy-4-methoxy-anilino)-3-oxo-propanoate (25)

To a mixture of commercially available 3-benzyloxy-4-methoxy-aniline (**24**) (35 g, 0.153 mol) and Et_3N (30.87 g, 0.306 mol) in CH_2Cl_2 (1 L) was added dropwise ethyl 3-chloro-3-oxo-propanoate (25.245 g, 0.168 mol) at 0 °C and the mixture was stirred at room temperature for 12 hours. Then, the reaction mixture was poured into water (2 L) and extracted with CH_2Cl_2. The combined the organic phase was dried over anhydrous Na_2SO_4, filtered and concentrated to afford compound **25** (40 g, 76%). ESI-MS *m/z* 344.2 $[M+H]^+$ calc. for $C_{19}H_{21}NO_5$. This intermediate was used in the next step without further characterization.

3-(3-Benzyloxy-4-methoxy-anilino)-3-oxo-propanoic acid (26)

To a mixture of **25** (20.40 g, 59.41 mmol) in THF/MeOH/H_2O (3:3:2, 267 mL) was added LiOH·H_2O (3.74 g, 89.12 mmol) in one portion at 25 °C and the mixture was stirred at room temperature for 16 hours. Then, the mixture was concentrated by rotary evaporation under vacuum at 45 °C. The residue was poured into ice-water (200 mL) and stirred for 10 minutes. The resulting slurry was filtered and the filter cake was dried under vacuum to afford compound **26** (19.30 g, 99% crude) as a white solid. ESI-MS *m/z* 316.2 $[M+H]^+$ calc. for $C_{17}H_{17}NO_5$. This intermediate was used in the next step without further characterization.

7-Benzyloxy-2,4-dichloro-6-methoxy-quinoline (27)

Compound **26** (7.00 g, 22.20 mmol) was suspended in $POCl_3$ (68.08 g, 443.99 mmol) in a 500 mL single-necked round bottom flask and the mixture was stirred at 90 °C for 2 hours under N_2. Then, the reaction mixture was cooled to 25 °C and concentrated to remove $POCl_3$. The residue was further purified by silica gel column chromatography to

obtain pure compound **27** (2.50 g, 34%). ^{1}H NMR ($CDCl_3$, 400 MHz): δ 7.49-7.36 (m, 8H), 5.30 (s, 2H), 4.06 (s, 3H). ESI-MS *m/z* 334.2 $[M+H]^+$ calc. for $C_{17}H_{13}Cl_2NO_2$.

7-Benzyloxy-4-chloro-6-methoxy-2-(5-methyl-2-furyl)quinoline (28)

Compound **27** (900 mg, 2.69 mmol), 4,4,5,5-tetramethyl-2-(5-methyl-2-furyl)-1,3,2-dioxaborolane (588 mg, 2.83 mmol), K_2CO_3 (558 mg, 4.04 mmol) and $Pd(PPh_3)_4$ (311 mg, 0.26 mmol) were dissolved in 1,4-dioxane (10 mL) and heated to 100 °C for 16 hours under N_2. Then, the reaction mixture was poured into H_2O and was extracted with EtOAc. The organic phase was washed with saturated brine, dried over anhydrous Na_2SO_4, filtered and concentrated in vacuum to give a residue, which was purified by column chromatography to afford pure compound **28** (500 mg, 49%). ESI-MS *m/z* 380.1 $[M+H]^+$ calc. for $C_{22}H_{18}ClNO_3$. This intermediate was used in the next step without further characterization.

7-Benzyloxy-6-methoxy-2-(5-methyl-2-furyl)-*N*-(1-methyl-4-piperidyl)quinolin-4-amine (29)

Compound **28** (500 mg, 1.32 mmol), 1-methylpiperidin-4-amine (301 mg, 2.63 mmol), $Pd_2(dba)_3$ (121 mg, 0.13 mmol), BINAP (82 mg, .013 mmol) and Cs_2CO_3 (858 mg, 2.63 mmol) were dissolved in 1,4-dioxane (10 mL) and heated at 110 °C for 16 hours under N_2. Then, the reaction mixture was purified by column chromatography to afford pure compound **29** (400 mg, 66%). ESI-MS *m/z* 458.2 $[M+H]^+$ calc. for $C_{28}H_{31}N_3O_3$. This intermediate was used in the next step without further characterization.

6-Methoxy-4-[(1-methyl-4-piperidyl)amino]-2-(5-methyltetrahydrofuran-2-yl)quinolin-7-ol (30)

A mixture of **29** (400 mg, 0.87 mmol) and Pd/C (100 mg) in MeOH (20 mL) was stirred at 50 °C under H_2 (50 Psi) for 16 hours. Then, catalyst was removed by filtration and the filtrate was concentrated to dryness to give compound **30** (300 mg, 93%) as a yellow solid. ^{1}H NMR (MeOD, 400 MHz): δ 7.83 (s, 1H), 7.31 (s, 1H), 6.81 (s, 1H), 5.11-5.07 (m, 1H), 4.32-4.15 (m, 2H), 4.06 (s, 3H), 3.65-3.54 (m, 2H), 3.35-3.20 (m, 2H), 2.89 (s, 3H), 2.79-2.52 (m, 1H), 2.35-2.10 (m, 5H), 2.06-1.95 (m, 1H), 1.70-1.60 (m, 1H), 1.43 (d, *J* = 6 Hz, 3H). ESI-MS *m/z* 372.3 $[M+H]^+$ calc. for $C_{21}H_{29}N_3O_3$.

6-Methoxy-*N*-(1-methyl-4-piperidyl)-2-(5-methyltetrahydrofuran-2-yl)-7-(3-pyrrolidin-1-ylpropoxy)quinolin-4-amine (31)

A mixture of **30** (200 mg, 0.53 mmol), 1-(3-chloropropyl)pyrrolidine (95 mg, 064 mmol) and Cs_2CO_3 (351 mg, 1.08 mmol) in DMF (5 mL) was degassed and purged with N_2 for 3 times. Then, the mixture was stirred at 100 °C for 16 hours under N_2. Then, the mixture was concentrated to give a residue which was purified by preparative HPLC (method 1 described in supporting information) to obtain pure compound **31** (50 mg, 19%) as a yellow syrup (racemic mixture). ^{1}H NMR (MeOD, 400 MHz): δ 7.82 (s, 1H), 7.50 (s, 1H), 6.84 (s, 1H), 5.13-5.05 (m, 1H), 4.37-4.12 (m, 4H), 4.03 (s, 3H), 3.86-3.76 (m, 2H), 3.71-3.65 (m, 2H), 3.52-3.44 (m, 2H), 3.31-3.20 (m, 2H), 3.18-3.10 (m, 2H), 2.94 (s, 3H), 2.63-2.56 (m, 1H), 2.39-2.30 (m, 4H), 2.25-2.13 (m, 4H), 2.08-2.00 (m, 4H), 1.70-1.60 (m, 1H), 1.45 (d, *J* = 6.4 Hz, 3H). ESI-MS *m/z* 483.4 $[M+H]^+$ calc. for $C_{28}H_{42}N_4O_3$.

5-[4-Chloro-6-methoxy-7-(3-pyrrolidin-1-ylpropoxy)-2-quinolyl]furan-2-carbaldehyde (32)

To a solution of compound **16** (0.2 g, 0.56 mmol) in 1,4-dioxane/H_2O (5:1, 12 mL) was added Na_2CO_3 (65 mg, 0.6 mmol), $Pd(PPh_3)_4$ (65 mg, 0.056 mmol) and (5-formylfuran-2-yl)boronic acid (69 mg, 0.50 mmol) and the solution was heated to 110 ºC for 2 hours under microwave irradiation. Then, the mixture was concentrated and extracted with EtOAc. The combined organic layers were washed with brine, dried over anhydrous Na_2SO_4, filtered and concentrated to give the crude product which was purified by preparative TLC to obtain pure compound **32** (100 mg, 43%) as pale yellow solid. ESI-MS *m/z* 415 $[M+H]^+$ calc. for $C_{22}H_{23}ClN_2O_4$. This intermediate was used in the next step without further characterization.

4-Chloro-2-(5-ethyl-2-furyl)-6-methoxy-7-(3-pyrrolidin-1-ylpropoxy)quinoline (33a)

To a solution of compound **16** (8.80 g, 24.77 mmol) in 1,4-dioxane/H_2O (10:1, 110 mL) were successively added 2-(5-ethyl-2-furyl)-4,4,5,5-tetramethyl-1,3,2-dioxaborolane (5.78 g, 26.01 mmol), $Pd(PPh_3)_4$ (2.86 g, 2.48 mmol) and K_2CO_3 (8.56 g, 61.93 mmol) and the resulting mixture was stirred at 80 °C for 12 hours under N_2. Then, the mixture was diluted with water and extracted with EtOAc. The combined organic phase was washed with brine, dried over anhydrous Na_2SO_4, filtered, concentrated and purified by silica gel column chromatography to obtain pure compound **33a** (9.36 g, 91%) as a yellow solid. ESI-MS *m/z* 415.2 $[M+H]^+$ calc. for $C_{23}H_{27}ClN_2O_3$. This intermediate was used in the next step without further characterization.

***N*-[[5-[4-chloro-6-methoxy-7-(3-pyrrolidin-1-ylpropoxy)-2-quinolyl]-2-furyl]methyl]ethanamine (33b)**

To a solution of compound **32** (180 mg, 0.43 mmol) in MeOH (5 mL) was added ethylamine hydrochloride (105 mg, 1.30 mmol) and the solution was stirred at room temperature for 90 minutes. Then, $NaBH_3CN$ (135 mg, 2.15 mmol) was added to the solution and the mixture was stirred at room temperature for 12 hours. Then, the reaction was quenched with water and extracted with EtOAc. The organic layer was washed with brine, dried over anhydrous Na_2SO_4, filtered and concentrated to give the crude product which was purified by preparative HPLC (method 1 described in supporting information) to obtain pure compound **33b** (80 mg, 42%) as a yellow solid. ESI-MS *m/z* 444.2 $[M+H]^+$ calc. for $C_{24}H_{30}ClN_3O_3$. This intermediate was used in the next step without further characterization.

1-[5-[4-Chloro-6-methoxy-7-(3-pyrrolidin-1-ylpropoxy)-2-quinolyl]-2-furyl]-*N*,*N*-dimethyl-methanamine (33c)

To a solution of compound **32** (180 mg, 0.43 mmol) in MeOH (5 mL) was added dimethylamine hydrochloride (105 mg, 1.30 mmol) and the solution was stirred at room temperature for 90 minutes. Then, $NaBH_3CN$ (135 mg, 2.15 mmol) was added and the mixture was stirred at room temperature for 12 hours. Then, the reaction was quenched with water and extracted with EtOAc. The organic layer was washed with brine, dried over anhydrous Na_2SO_4, filtered and concentrated to give the crude product which was purified by preparative HPLC (method 1 described in supporting information) to obtain pure compound **33c** (100 mg, 52%) as a yellow solid. ESI-MS *m/z* 444.2 $[M+H]^+$ calc. for $C_{24}H_{30}ClN_3O_3$. This intermediate was used in the next step without further characterization.

[5-[4-Chloro-6-methoxy-7-(3-pyrrolidin-1-ylpropoxy)-2-quinolyl]-2-furyl]methanol (33d)

To a solution of compound **32** (200 mg, 0.48 mmol) in MeOH (5 mL) was added $NaBH_4$ (91.2 mg, 2.4 mmol) and the solution was stirred at room temperature for 2 hours. Then, the mixture was concentrated to give the crude product which was purified by preparative TLC to obtain pure compound **33d** (0.1 g, 50%) as pale yellow solid. ESI-MS *m/z* 417 $[M+H]^+$ calc. for $C_{22}H_{25}ClN_2O_4$. This intermediate was used in the next step without further characterization.

5-[4-Chloro-6-methoxy-7-(3-pyrrolidin-1-ylpropoxy)-2-quinolyl]furan-2-carbonitrile (33e)

To a solution of compound **32** (100 mg, 0.24 mmol) in $MeOH/CH_2Cl_2$ (1:4, 10 mL) was added phenylphosphonic dichloride (94 mg, 0.48 mmol), pyridine (76 mg, 0.96 mmol) and $NH_2OH{\cdot}HCl$ (17 mg, 0.24 mmol) and the solution was stirred at room temperature for 15 hours. Then, $NaBH_3CN$ (135 mg, 2.15 mol) was added to the solution and the mixture was stirred at room temperature for 12 hours. Then, the mixture was concentrated and extracted with EtOAc. The organic layer was washed with aqueous $NaHCO_3$ and brine, dried over anhydrous Na_2SO_4, filtered and concentrated to give the crude product which was purified by column chromatography to obtain pure compound **33e** (50 mg, 51%) as a yellow solid. ESI-MS *m/z* 412 $[M+H]^+$ calc. for $C_{22}H_{22}ClN_3O_3$. This intermediate was used in the next step without further characterization.

4-Chloro-6-methoxy-2-(5-phenyl-2-furyl)-7-(3-pyrrolidin-1-ylpropoxy)quinoline (33f)

To a solution of compound **16** (354 mg, 1 mmol) in 1,4-dioxane/H_2O (15:1, 16 mL) was added K_2CO_3 (278 mg, 2 mmol), $Pd(PPh_3)_4$ (50 mg, 0.05 mmol) and 4,4,5,5-tetramethyl-2-(5-phenyl-2-furyl)-1,3,2-dioxaborolane (**Int. 3**, synthesis described in supporting information) (272 mg, 1 mmol) and the solution was heated to 120 ºC for 4 hours under microwave irradiation. Then, the mixture was quenched with water and extracted with EtOAc. The organic layer was washed with brine, dried over anhydrous Na_2SO_4, filtered and concentrated to give the crude product which was purified by preparative HPLC (method 3 described in supporting information) to obtain pure compound **33f** (150 mg, 33%) as a yellow solid. ^{1}H NMR (MeOD, 400 MHz): δ 8.09 (s, 1H), 7.95-7.92 (m, 2H), 7.48 (m, 6H), 7.07 (s, 1H), 4.38-4.28 (m, 2H), 4.06 (s, 3H), 3.86-3.77 (m, 2H), 3.55-3.45 (m, 2H), 3.21-3.10 (m, 2H), 2.45-2.35 (m, 2H), 2.30-2.15 (m, 2H), 2.11-2.01 (m, 2H). ESI-MS *m/z* 463.2 $[M+H]^+$ calc. for $C_{27}H_{27}ClN_2O_3$.

2-(5-Ethyl-2-furyl)-6-methoxy-*N*-(1-methyl-4-piperidyl)-7-(3-pyrrolidin-1-ylpropoxy)quinolin-4-amine (34a)

To a solution of compound **33a** (207 mg, 0.5 mmol) in 1,4-dioxane (15 mL) was added Cs_2CO_3 (325 mg, 1 mmol), BINAP (34 mg, 0.05 mmol), $Pd_2(dba)_3$ (30 mg, 0.03 mmol) and 1-methylpiperidin-4-amine (114 mg, 1.0 mmol) and the solution was heated to 130 ºC for 4 hours under microwave irradiation. Then, the solution was concentrated and extracted with EtOAc. The combined organic layer was washed with brine, dried over anhydrous Na_2SO_4, filtered and concentrated to give the crude product which was purified by preparative HPLC (method 2 described in supporting information) to obtain pure compound **34a** (35 mg, 14%) as yellow solid; m.p. 133-134 ºC. ^{1}H NMR (MeOD, 400 MHz): δ 7.79 (s, 1H), 7.57 (d, *J* = 3.2 Hz, 1H), 7.49 (s, 1H), 7.08 (s, 1H), 6.46 (d, *J* = 3.2 Hz, 1H), 4.38-4.25 (m, 3H), 4.05 (s, 3H), 3.87-3.77 (m, 2H), 3.75-3.65 (m, 2H),

3.51-3.45 (m, 2H), 3.25-3.10 (m, 4H), 2.94 (s, 3H), 2.90-2.80 (m, 2H), 2.45-2.30 (m, 4H), 2.26-2.02 (m, 6H), 1.40-1.32 (m, 3H). ESI-MS *m/z* 493.3 $[M+H]^+$ calc. for $C_{29}H_{40}N_4O_3$.

2-[5-(ethylaminomethyl)-2-furyl]-6-methoxy-*N*-(1-methyl-4-piperidyl)-7-(3-pyrrolidin-1-ylpropoxy)quinolin-4-amine (34b)

To a solution of compound **33b** (70 mg, 0.16 mmol) in toluene (5 mL) was added *t*-BuOK (1.0 M in THF, 0.24 mL, 0.24 mmol), xantphos (15 mg, 0.026 mmol), $Pd_2(dba)_3$ (44 mg, 0.048 mmol) and 1-methylpiperidin-4-amine (106 mg, 0.9 mmol) and the solution was heated to 130 ºC for 2 hours under microwave irradiation. Then, the mixture was quenched with water and extracted with EtOAc. The organic layer was washed with brine, dried over anhydrous Na_2SO_4, filtered and concentrated to give the crude product which was purified by preparative HPLC (method 1 described in supporting information) to obtain pure compound **34b** (9.7 mg, 11%) as a yellow syrup. ^{1}H NMR (MeOD, 400 MHz): δ 7.84 (s, 1H), 7.72-7.71 (m, 1H), 7.66 (s, 1H), 7.22 (s, 1H), 6.97-6.96 (m, 1H), 4.46 (s, 2H), 4.40-4.30 (m, 3H), 4.05 (s, 3H), 3.86-3.76 (m, 2H), 3.74-3.65 (m, 2H), 3.52-3.44 (m, 2H), 3.32-3.23 (m, 2H), 3.21-3.12 (m, 4H), 2.96 (s, 3H), 2.45-2.33 (m, 4H), 2.25-2.15 (m, 4H), 2.15-2.00 (m, 2H), 1.40-1.34 (m, 3H). ESI-MS *m/z* 522.3 $[M+H]^+$ calc. for $C_{30}H_{43}N_5O_3$.

2-[5-[(Dimethylamino)methyl]-2-furyl]-6-methoxy-*N*-(1-methyl-4-piperidyl)-7-(3-pyrrolidin-1-ylpropoxy)quinolin-4-amine (34c)

To a solution of compound **33c** (80 mg, 0.18 mmol) in toluene (5 mL) was added *t*-BuOK (1.0 M in THF, 0.27 mL, 0.27 mmol), xantphos (17 mg, 0.03 mmol), $Pd_2(dba)_3$ (49 mg, 0.054 mmol) and 1-methylpiperidin-4-amine (119 mg, 1 mmol) and the

solution was heated to 130 ºC for 2 hours under microwave irradiation. Then, the mixture was quenched with water and extracted with EtOAc. The organic layer was washed with brine, dried over anhydrous Na_2SO_4, filtered and concentrated to give the crude product which was purified by preparative HPLC (method 1 described in supporting information) to obtain pure compound **34c** (20.7 mg, 22%) as a yellow syrup. ^{1}H NMR (MeOD, 400 MHz): δ 7.84 (s, 1H), 7.74 (s, 1H), 7.65 (s, 1H), 7.23 (s, 1H), 7.07-7.06 (m, 1H), 4.58 (s, 2H), 4.40-4.30 (m, 3H), 4.05 (s, 3H), 3.85-3.75 (m, 2H), 3.75-3.60 (m, 2H), 3.50-3.42 (m, 2H), 3.36-3.28 (m, 2H), 3.19-3.08 (m, 2H), 2.97-2.95 (m, 6H), 2.94 (s, 3H), 2.43-2.35 (m, 4H), 2.25-2.15 (m, 4H), 2.15-2.02 (m, 2H). ESI-MS *m/z* 522.3 $[M+H]^+$ calc. for $C_{30}H_{43}N_5O_3$.

[5-[6-Methoxy-4-[(1-methyl-4-piperidyl)amino]-7-(3-pyrrolidin-1-ylpropoxy)-2-quinolyl]-2-furyl]methanol (34d)

To a solution of compound **33d** (90 mg, 0.21 mmol) in 1,4-dioxane (4 mL) was added Cs_2CO_3 (0.21 g, 0.65 mmol), BINAP (27 mg, 0.043 mmol), $Pd_2(dba)_3$ (59 mg, 0.065 mmol) and 1-methylpiperidin-4-amine (86 mg, 0.75 mmol) and the solution was heated to 120 ºC for 5 hours under microwave irradiation. Then, the mixture was quenched with water and extracted with EtOAc. The organic layer was washed with brine, dried over anhydrous Na_2SO_4, filtered and concentrated to give the crude product which was purified by preparative HPLC (method 1 described in supporting information) to obtain pure compound **34d** (10 mg, 10%) as a yellow solid; m.p. 104-105 ºC. ^{1}H NMR (MeOD, 400 MHz): δ 7.83 (s, 1H), 7.64-7.63 (m, 1H), 7.49 (s, 1H), 7.17 (s, 1H), 6.68-6.67 (m, 1H), 4.71 (s, 2H), 4.43-4.28 (m, 3H), 4.04 (s, 3H), 3.88-3.78 (m, 2H), 3.75-3.65 (m, 2H), 3.52-3.43 (m, 2H), 3.30-3.25 (m, 2H), 3.20-3.08 (m, 2H), 2.95 (s, 3H),

2.43-2.34 (m, 4H), 2.25-2.16 (m, 4H), 2.15-2.02 (m, 2H). ESI-MS *m/z* 495.3 $[M+H]^+$ calc. for $C_{28}H_{38}N_4O_4$.

5-[6-Methoxy-4-[(1-methyl-4-piperidyl)amino]-7-(3-pyrrolidin-1-ylpropoxy)-2-quinolyl]furan-2-carbonitrile (34e)

To a solution of compound **33e** (80 mg, 0.19 mmol) in 1,4-dioxane (5 mL) was added Cs_2CO_3 (127 mg, 0.39 mmol), BINAP (12 mg, 0.019 mmol), $Pd_2(dba)_3$ (18 mg, 0.019 mmol) and 1-methylpiperidin-4-amine (44 mg, 0.38 mmol) and the solution was heated to 130 ºC for 2 hours under microwave irradiation. Then, the mixture was quenched with water and extracted with EtOAc. The organic layer was washed with brine, dried over anhydrous Na_2SO_4, filtered and concentrated to give the crude product which was purified by preparative HPLC (method 1 described in supporting information) to obtain pure compound **34e** (11.4 mg, 12%) as a yellow solid; m.p. 172-174 ºC. ^{1}H NMR (MeOD, 400 MHz): δ 7.86 (s, 1H), 7.83-7.82 (m, 1H), 7.65-7.64 (m, 1H), 7.53 (s, 1H), 7.31 (s, 1H), 4.42-4.33 (m, 3H), 4.05 (s, 3H), 3.90-3.80 (m, 2H), 3.75-3.65 (m, 2H), 3.52-3.45 (m, 2H), 3.32-3.30 (m, 2H), 3.20-3.10 (m, 2H), 2.96 (s, 3H), 2.45-2.34 (m, 4H), 2.25-2.12 (m, 4H), 2.11-2.01 (m, 2H). ESI-MS *m/z* 490.2 $[M+H]^+$ calc. for $C_{28}H_{35}N_5O_3$.

6-Methoxy-*N*-(1-methyl-4-piperidyl)-2-(5-phenyl-2-furyl)-7-(3-pyrrolidin-1-ylpropoxy)quinolin-4-amine (34f)

To a solution of compound **33f** (100 mg, 0.22 mmol) in toluene (10 mL) was added *t*-BuOK (1.0 M in THF, 0.5 mL, 0.5 mmol), xantphos (9 mg, 0.02 mmol), $Pd_2(dba)_3$ (30 mg, 0.03 mmol) and 1-methylpiperidin-4-amine (57 mg, 0.5 mmol) and the mixture was heated to 130 ºC for 3 hours under microwave irradiation. Then, the solution was

concentrated and extracted with EtOAc. The combined organic layer was washed with brine, dried over anhydrous Na_2SO_4, filtered and concentrated to give the crude product which was purified by preparative HPLC (method 3 described in supporting information) to obtain pure compound **34f** (21 mg, 18%) as yellow solid; m.p. 207-208 ºC. ^{1}H NMR (MeOD, 400 MHz): δ 8.04-8.02 (m, 2H), 7.86-7.79 (m, 2H), 7.60-7.40 (m, 4H), 7.23-7.20 (m, 2H), 4.45-4.35 (m, 3H), 4.08 (s, 3H), 3.90-3.85 (m, 2H), 3.78-3.70 (m, 2H), 3.56-3.48 (m, 2H), 3.25-3.15 (m, 4H), 3.00 (s, 3H), 2.47-2.38 (m, 4H), 2.30-2.05 (m, 6H). ESI-MS *m/z* 541.3 $[M+H]^+$ calc. for $C_{33}H_{40}N_4O_3$.

2-(Benzofuran-2-yl)-4-chloro-6-methoxy-7-(3-pyrrolidin-1-ylpropoxy)quinoline (35)

To a solution of compound **16** (280 mg, 0.79 mmol) in 1,4-dioxane/H_2O (15:1, 16 mL) was added Na_2CO_3 (335 mg, 3.16 mmol), $Pd(PPh_3)_4$ (92 mg, 0.079 mmol) and benzofuran-2-ylboronic acid (128 mg, 0.79 mmol) and the solution was heated to 110 ºC for 1 hour under microwave irradiation. Then, the mixture was quenched with water and extracted with EtOAc. The organic layer was washed with brine, dried over anhydrous Na_2SO_4, filtered and concentrated to give the crude product which was purified by preparative HPLC (method 2 described in supporting information) to obtain pure compound **35** (250 mg, 73%) as a yellow solid. ^{1}H NMR (DMSO-d_6, 400 MHz): δ 9.52-9.45 (m, 1H), 8.18 (s, 1H), 7.80-7.65 (m, 2H), 7.57 (s, 1H), 7.45-7.35 (m, 2H), 7.32-7.25 (m, 1H), 4.35-4.28 (m, 2H), 3.99 (s, 3H), 3.38-3.30 (m, 2H), 3.10-3.02 (m, 2H), 2.27-2.18 (m, 2H), 2.09-1.98 (m, 2H), 1.90-180 (m, 2H), 1.60-1.50 (m, 2H).

2-(Benzofuran-2-yl)-6-methoxy-*N*-(1-methyl-4-piperidyl)-7-(3-pyrrolidin-1-ylpropoxy)quinolin-4-amine (36)

To a solution of compound **35** (210 mg, 0.5 mmol) in 1,4-dioxane (10 mL) was added Cs_2CO_3 (815 mg, 2.5 mmol), BINAP (62.5 mg, 0.1 mmol), $Pd_2(dba)_3$ (20 mg, 0.02 mmol) and 1-methylpiperidin-4-amine (285 mg, 2.5 mmol) and the mixture was heated to 120 ºC for 3 hours under microwave irradiation. Then, the solution was concentrated and extracted with EtOAc. The combined organic layer was washed with brine, dried over anhydrous Na_2SO_4, filtered and concentrated to give the crude product which was purified by preparative HPLC (method 2 described in supporting information) to obtain pure compound **36** (60 mg, 23%) as yellow solid; m.p. 191-192 ºC. ^{1}H NMR (MeOD, 400 MHz): δ 8.09 (s, 1H), 7.87 (s, 1H), 7.81 (d, *J* = 8.8 Hz, 1H), 7.72 (d, *J* = 8.8 Hz, 1H), 7.59-7.50 (m, 2H), 7.45-7.38 (m, 2H), 4.42-4.35 (m, 2H), 4.07 (s, 3H), 3.85-3.65 (m, 4H), 3.53-3.45 (m, 2H), 3.38-3.35 (m, 3H), 3.20-3.10 (m, 2H), 2.97 (s, 3H), 2.46-2.37 (m, 4H), 2.15-2.00 (m, 6H). ESI-MS *m/z* 515.3 $[M+H]^+$ calc. for $C_{31}H_{38}N_4O_3$.

***Tert*-butyl 4-[[6-methoxy-2-(5-methyl-2-furyl)-7-(3-pyrrolidin-1-ylpropoxy)-4-quinolyl]amino]piperidine-1-carboxylate (37a)**

To a solution of compound **22r** (2.2 g, 5.50 mmol) in 1,4-dioxane (150 mL) were added Cs_2CO_3 (3.58 g, 10.99 mmol), BINAP (342 mg, 0.55 mmol), $Pd_2(dba)_3$ (504 mg, 0.55 mmol) and *tert*-butyl 4-aminopiperidine-1-carboxylate (1.1 g, 5.50 mmol) in one portion at 25 °C under N_2 and the mixture was stirred at 130 °C for 5 hours under N_2. Then, the mixture was cooled to room temperature and poured into water (50 mL). The aqueous phase was extracted with EtOAc. The combined organic phase was washed with saturated brine, dried with anhydrous Na_2SO_4, filtered, concentrated under vacuum and purified by silica gel column chromatography to obtain pure compound **37a** (1.8 g, 58%) as a yellow solid. ESI-MS *m/z* 565.3 $[M+H]^+$ calc. for $C_{32}H_{44}N_4O_5$. This intermediate was used in the next step without further characterization.

***Tert*-butyl 4-[[2-(5-ethyl-2-furyl)-6-methoxy-7-(3-pyrrolidin-1-ylpropoxy)-4-quinolyl]amino]piperidine-1-carboxylate (37b)**

To a solution of compound **33a** (622 mg, 1.50 mmol) in 1,4-dioxane (15 mL) were successively added $Pd_2(dba)_3$ (137 mg, 0.15 mmol), BINAP (187 mg, 0.3 mmol), Cs_2CO_3 (977 mg, 3 mmol) and *tert*-butyl 4-aminopiperidine-1-carboxylate (451 mg, 2.25 mmol) and the resulting mixture was stirred at 80 °C for 36 hours. Then, the mixture was cooled to room temperature, diluted with water and then extracted with EtOAc. The combined organic phase was washed with brine, concentrated and purified by silica gel column chromatography to obtain pure compound **37b** (950 mg, 99% crude) as a yellow solid. ESI-MS *m/z* 579.1 $[M+H]^+$ calc. for $C_{33}H_{46}N_4O_5$. This intermediate was used in the next step without further characterization.

6-Methoxy-2-(5-methyl-2-furyl)-*N*-(4-piperidyl)-7-(3-pyrrolidin-1-ylpropoxy)quinolin-4-amine (38a)

A mixture of compound **37a** (1.80 g, 3.19 mmol) and HCl/EtOAc (1.0 M, 80 mL) was stirred at 25 °C for 2 hours under N_2. Then, the mixture was concentrated to dryness to give the crude product which was purified by preparative HPLC (method 2 described in supporting information) to afford pure compound **38a** (1.2 g, 85%) as yellow solid; m.p. 127-128 ºC. ^{1}H NMR (MeOD, 400 MHz): δ 7.92 (s, 1H), 7.71 (d, *J* = 3.3 Hz, 1H), 7.57 (s, 1H), 7.17 (s, 1H), 6.46 (d, *J* = 3 Hz, 1H), 4.40 (t, *J* = 5.4 Hz, 3H), 4.12-4.05 (m, 5H), 3.85-3.75 (m, 2H), 3.60 (d, *J* = 13.1 Hz, 2H), 3.52 (t, *J* = 7.2 Hz, 2H), 3.21-3.13 (m, 2H), 2.54 (s, 3H), 2.45-2.28 (m, 4H), 2.25-2.02 (m, 6H). ESI-MS *m/z* 465.3 $[M+H]^+$ calc. for $C_{27}H_{36}N_4O_3$.

2-(5-Ethyl-2-furyl)-6-methoxy-*N*-(4-piperidyl)-7-(3-pyrrolidin-1-ylpropoxy)quinolin-4-amine (38b)

A solution of compound **37b** (868 mg, 1.50 mmol) in HCl/EtOAc (1.0 M, 40 mL) was stirred at 22 °C for 3 hours. Then, the reaction mixture was concentrated to dryness to give compound **38b** (850 mg, 99% crude). ESI-MS *m/z* 479 $[M+H]^+$ calc. for $C_{28}H_{38}N_4O_3$. This intermediate was used in the next step without further characterization.

***N*-(1-isopropyl-4-piperidyl)-6-methoxy-2-(5-methyl-2-furyl)-7-(3-pyrrolidin-1-ylpropoxy)quinolin-4-amine (39a)**

To a mixture of compound **38a** (155 mg, 0.33 mmol) and acetone (108 mg, 1.86 mmol) in *i*-PrOH (40 mL) were added $NaBH_3CN$ (117 mg, 1.86 mmol) and AcOH (112 mg, 1.86 mmol) in one portion at 16 °C under N_2 and the mixture was stirred at 50 °C for 15 hours. Then, the mixture was cooled to 16 °C, filtered and concentrated in vacuum. The residue was purified by preparative HPLC (method 4 described in supporting information) to obtain pure compound **39a** (61.4 mg, 37%) as a yellow solid; m.p. 106-107 ºC. ^{1}H NMR (MeOD, 400 MHz): δ 7.82 (s, 1H), 7.59 (d, *J* = 3.2 Hz, 1H), 7.51 (s, 1H), 7.09-7.07 (m, 1H), 6.43 (d, *J* = 2.8 Hz, 1H), 4.36-4.33 (m, 3H), 4.04 (s, 3H), 3.86-3.76 (m, 2H), 3.65-3.57 (m, 3H), 3.51-3.47 (m, 2H), 3.36-3.31 (m, 2H), 3.20-3.10 (m, 2H), 2.50 (s, 3H), 2.45- 2.33 (m, 4H), 2.25-2.13 (m, 4H), 2.10-2.02 (m, 2H), 1.43 (d, *J* = 6.8 Hz, 6H). ESI-MS *m/z* 507.4 $[M+H]^+$ calc. for $C_{30}H_{42}N_4O_3$.

2-(5-Ethyl-2-furyl)-*N*-(1-isopropyl-4-piperidyl)-6-methoxy-7-(3-pyrrolidin-1-ylpropoxy)quinolin-4-amine (39b)

To a mixture of compound **38b** (120 mg, 0.25 mmol) and acetone (81 mg, 1.40 mmol) in *i*-PrOH (20 mL) were added $NaBH_3CN$ (88 mg, 1.40 mmol) and AcOH (84 mg, 1.4 mmol) in one portion at 16 °C under N_2 and the mixture was stirred at 50 °C for 15 hours. Then, the mixture was cooled to 16 °C, filtered and concentrated in vacuum. The residue was purified by preparative HPLC (method 4 described in supporting information) to obtain pure compound **39b** (32.9 mg, 25%) as a yellow solid; m.p. 105-106 ºC. ^{1}H NMR (MeOD, 400 MHz): δ 7.83 (s, 1H), 7.60 (d, *J* = 3.6 Hz, 1H), 7.52 (s, 1H), 7.10 (s, 1H), 6.45 (d, *J* = 3.6 Hz, 1H), 4.36-4.31 (m, 3H), 4.02 (s, 3H), 3.87-3.77 (m, 2H), 3.70-3.60 (m, 3H), 3.52-3.45 (m, 2H), 3.35-3.31 (m, 2H), 3.20-3.10 (m, 2H), 2.90-2.82 (m, 2H), 2.46-2.35 (m, 4H), 2.25-2.15 (m, 4H), 2.11-2.00 (m, 2H), 1.43 (d, *J* = 6.8 Hz, 6H), 1.36 (t, *J* = 7.6 Hz, 3H). ESI-MS *m/z* 521.4 $[M+H]^+$ calc. for $C_{31}H_{44}N_4O_3$.

_N_-(1-cyclopropyl-4-piperidyl)-6-methoxy-2-(5-methyl-2-furyl)-7-(3-pyrrolidin-1-ylpropoxy)quinolin-4-amine (39c)

To a solution of compound **38a** (1 g, 2.15 mmol) and (1-ethoxycyclopropoxy)-trimethyl-silane (2.09 g, 12 mmol) in MeOH (100 mL) were added $NaBH_3CN$ (750 mg, 11.98 mmol) and AcOH (719 mg, 11.98 mmol) in one portion at 25 °C under N_2 and the mixture was stirred at 25 °C for 10 minutes. Then, the mixture was heated to 60 °C overnight. Then, the reaction mixture was concentrated and purified by preparative HPLC (method 2 described in supporting information) to obtain pure compound **39c** (333 mg, 31%) as a yellow solid; m.p. 120-122 ºC. ^{1}H NMR (MeOD, 400 MHz): δ 7.82 (s, 1H), 7.58 (d, *J* = 3.5 Hz, 1H), 7.50 (s, 1H), 7.10 (s, 1H), 6.45 (dd, *J* = 3.5, 0.88 Hz, 1H), 4.35 (t, *J* = 5.51 Hz, 3H), 4.04 (s, 3H), 3.85-3.75 (m, 4H), 3.50 (t, *J* = 7.06 Hz, 3H), 3.21-3.11 (m, 3H), 2.85 (br s, 1H), 2.52 (s, 3H), 2.43-2.36 (m, 4H), 2.23-2.06 (m,

6H), 1.10-1.06 (m, 2H), 1.05-1.00 (m, 2H). ESI-MS *m/z* 505.4 $[M+H]^+$ calc. for $C_{30}H_{40}N_4O_3$.

_N_-(1-cyclopropyl-4-piperidyl)-2-(5-ethyl-2-furyl)-6-methoxy-7-(3-pyrrolidin-1-ylpropoxy)quinolin-4-amine (39d)

To a mixture of compound **38b** (185 mg, 0.39 mmol) and (1-ethoxycyclopropoxy)-trimethyl-silane (406 mg, 2.30 mmol) in MeOH (20 mL) were added $NaBH_3CN$ (146 mg, 2.33 mmol) and AcOH (140 mg, 2.6 mmol) in one portion under N_2 and the mixture was heated to 60 °C overnight. Then, the mixture was cooled and filtered. The filtrate was concentrated in vacuum and the residue was purified by preparative HPLC (method 1 described in supporting information) to obtain pure compound **39d** (46 mg, 23%) as a yellow solid; m.p. 113-115 ºC. ^{1}H NMR (MeOD, 400 MHz): δ 7.82 (s, 1H), 7.62 (d, *J* = 3.6 Hz, 1H), 7.52 (s, 1H), 7.09 (s, 1H), 6.45 (d, *J* = 3.2 Hz, 1H), 4.83-4.79 (m, 1H), 4.39-4.31 (m, 3H), 4.04 (s, 3H), 3.87-3.78 (m, 4H), 3.55-3.45 (m, 4H), 3.19-3.10 (m, 2H), 2.90-2.80 (m, 2H), 2.45-2.35 (m, 4H), 2.27-2.15 (m, 4H), 2.12-2.02 (m, 2H), 1.36 (t, *J* = 7.6 Hz, 3H), 1.11-1.04 (m, 2H), 1.02-0.95 (m, 2H). ESI-MS *m/z* 519.4 $[M+H]^+$ calc. for $C_{31}H_{42}N_4O_3$.

G9a and DNMT1 docking

Compound **11** was superposed to the conformation of UNC0638 in the cocrystal structure of the G9-UNC0638-SAH complex (Protein Data Bank, PDB, entry 3RJW) with the MOE program (Chemical Computing Group, http://www.chemcomp.com). Then, the overlaid conformation of the compound was translated into the G9a-UNC0638-SAH crystal in order to analyze the key interactions between the ligand and the methyltransferase.

The GoldSuite 5.2 program (Cambridge Crystallographic Data Centre, https://www.ccdc.cam.ac.uk/pages/Home.aspx) was used to carry out docking of compounds to DNMT1. The crystal structure of Mouse DNMT1 bound to hemimethylated CpG DNA (PDB entry 4DA4) was chosen. In order to explore both, different binding pockets and different binding modes, a range of docking set ups where considered with emphasis on keeping adequate volume occupancy of the different binding pockets and considering protein-ligand interactions, especially those involving conserved catalytic residues. The docking configuration was, when adequate, validated by reproducing the crystallographic binding mode of SAH. In the final selected set-up, the docking region used was a 20-Å sphere around the carboxylate oxygen of Glu1269. The PLP scoring function was used to rank docking poses, and protein hydrogen bond constraints for binding to carboxylate of Glu-1269 were imposed on the ligand. The top twenty best docked structures out of 100 independent genetic algorithm runs were retrieved and visually inspected. The high-scoring pose was finally chosen as it has a plausible binding mode with key interactions with DNMT1 and a high degree of convergence (rmsd < 2 Å) was observed among the top three ranked poses.

Comparative analysis of the electrostatic potential

Electrostatic maps for each compound where calculated with VIDA (OpenEye, http://www.eyesopen.com/vida). Previously, all compounds where overlaid to the reference compound **11**, translated into the protein cavity and relaxed to adapt their conformation to this cavity using MOE.

G9a enzyme activity assay

The biochemical assay to measure G9a enzyme activity relies on time-resolved fluorescence energy transfer (TR-FRET) between europium cryptate (donor) and XL665 (acceptor). TR-FRET is observed when biotinylated histone monomethyl-H3K9 peptide is incubated with cryptate-labeled anti- H3K9me2 antibody (CisBio Cat# 61KB2KAE) and streptavidin XL665 (CisBio Cat#610SAXLA), after enzymatic reaction of G9a.

The assay was carried out during 1 hour at room temperature, in a final volume of 20 μL, with 0.2 nM human G9a enzyme, 40nM biotinylated histone monomethyl-H3K9 peptide, 20 μM S-adenosylmethionine (SAM) and different final concentrations of tested compounds in assay buffer (50 mM Tris-HCl, 10 mM NaCl, 4 mM DTT, 0.01% Tween-20 pH 9). The final percentage of DMSO was 0.5%. After incubation time enzyme activity was stopped by adding 150 nM of cryptate-labeled anti-H3K9me2 antibody and 16 μM of streptavidin XL665 beads. After one hour of incubation at room temperature, fluorescence was measured at 620 nm and 665 nm. A ratio (665 nm / 620 nm) was then calculated in order to minimize medium interferences. Positive control was obtained in the presence of the vehicle of the compounds. Negative control was obtained in the absence of G9a enzyme activity. Calculated IC_{50} values were determined using GraphPrism using 4-parameters inhibition curve. Compounds were tested in duplicate at different days, within an experimental error of 0.3 log units. If absolute pIC50 difference was higher than 0.3 log units, additional replicates were performed until satisfying the experimental error (by discarding individual results with values outside 2 MADs of the mean value).

DNMT1 enzyme activity assay

The biochemical assay to measure DNMT1 enzyme activity relies on time-resolved fluorescence energy transfer (TR-FRET) between lumi4-Tb (donor) and d2 (acceptor) using the EPIgeneous methyltransferase assay (CisBio Cat#62SAHPEB). TR-FRET is observed when antibody specific to S-adenosylhomocysteine labeled with Lumi4-Tb is incubated with d2-labeled S-adenosylhomocysteine. TR-FRET signal is inversely proportional to the concentration of SAH, product of DNMT1 enzyme activity, in the sample.

The assay was carried out during 15 minutes at 37 ºC, in a final volume of 20 μL, with 20 nM human DNMT1enzyme, 1 μg/mL poly-deoxy inosine poly-deoxy cytosine (pdI-pdC) DNA, 1 μM S-adenosylmethionine (SAM) and different final concentrations of tested compounds in assay buffer (50 mM Tris-HCl, 1 mM EDTA, 1 mM DTT, 0.1% Triton X-100, 5% glycerol pH 7.5).The final percentage of DMSO was 0.5%. After incubation time enzyme activity was stopped by adding 2 μL of buffer one of the EPIgeneous methyltransferase kit assay. After 10 minutes at room temperature, it was added 4 μL of antibody specific to S-adenosylhomocysteine labeled with Lumi4-Tb 50 x and 4 μL of d2-labeled S-adenosylhomocysteine 31x both diluted in buffer two of the EPIgeneous methyltransferase kit. Fluorescence was measured at 620 nm and 665 nm one hour later. A ratio (665 nm / 620 nm) was then calculated in order to minimize medium interferences. Positive control was obtained in the presence of the vehicle of the compounds. Negative control was obtained in the absence of DNMT1 enzyme activity. Calculated IC_{50} values were determined using GraphPrism using 4-parameters inhibition curve. Compounds were tested in duplicate at different days, within an experimental error of 0.3 log units. If absolute pIC_{50} difference was higher than 0.3 log units, additional replicates were performed until satisfying the experimental error (by discarding individual results with values outside 2 MADs of the mean value).

Methyltransferase Selectivity Panel

Selectivity of **11** and **39c** against 14 methyltransferases (GLP, MLL1, SET7/9, SUV39H1, SUV39H2, PRMT1, PRMT3, PRMT4, PRMT5, PRMT6, PRMT8, EZH1, EZH2, SETD2) and DNMTs (DNMT1, DNMT3A, DNMT3B) was performed by BPS Bioscience (http://www.bpsbioscience.com/index.ph). Binding experiments were performed in duplicate at each concentration. GLP IC_{50} determination for **11** and **39c** was carried out at Eurofins (https://www.eurofins.com/) in duplicate.

Cell culture

CEMO-1, LAL-CUN-2 and MV4-11 cell lines were cultured with RPMI 1640 medium supplemented with 20% fetal bovine serum and OCI-Ly10 and OCI-Ly3 cells with IMDM supplemented with 20% human serum and 55 μM of β-mercaptoethanol. All cell lines were maintained in culture at 37 °C in a humid atmosphere containing 5% CO_2 and were tested for mycoplasma.

Cell Proliferation Assay – MTS

Cell proliferation was analyzed after 48 hours of *in vitro* treatment using the CellTiter 96 Aqueous One Solution Cell Proliferation Assay (Promega). This is a colorimetric method for determining the number of viable cells in proliferation. For the assay, cells were cultured by triplicate at a density of $1x10^6$ cells/mL in 96-well plates (100.000 cells/well, 100μL/well), except for OCI-Ly3 and OCI-Ly10 cell lines which were cultured at a density of $0.5x10^6$ cells/mL (50.000 cells/well, 100 μL/well). In all cases, only the 60 inner wells were used to avoid any border effects. After 48 hours of

treatment, plates were centrifuged at 800g for 10 minutes and medium was removed. Then, cells were incubated with 100 µL/well of medium and 20 µL/well of CellTiter 96 Aqueous One Solution reagent. After 1-3 hours of incubation at 37 ºC, absorbance was measured at 490 nm in a 96-well plate reader. The background absorbance was measured in wells with only cell line medium and solution reagent. Data was calculated as a percentage of total absorbance of treated cell / absorbance of non-treated cells.

Cytotoxicity in THLE-2 cells

Cytotoxic effects of assayed compounds were tested using the immortalized human liver cell line THLE-2 (ATCC CRL-2706), cultured in BEGM medium (Clonetics #CC-4175). Medium was completed by adding 0.7µg/mL phosphoethanolamine, 0.5 ng/mL epidermal growth factor, antibiotics (penicillin and streptomycin) and 10% fetal bovine serum (FBS). Cells were plated in 96-well black microplates at 10,000 cells/well and incubated at 37 ºC (5% CO_2, 95% humidity) for 24 h. Test compounds were solubilized in 100% DMSO and then diluted with cell culture medium containing 10% DMSO. The final concentrations of the test compounds (1% DMSO) ranged from 0-100µM in a final volume of 200 µL. After 72 h, cell viability in each well was determined by measuring the concentration of cellular adenosine triphosphate (ATP) using the ViialightTM Plus Cell Proliferation/Cytotoxicity Kit as described by the manufacturer (Cambrex, East Rutherford, NJ). After addition of cell lysis buffer, test plate was incubated for 45 min at room temperature (orbital shaker). ATP monitoring solution was added and ATP concentration determined by reading luminescence using a Envision plate reader (PerkinElmer). The percentage of viable cells relative to the non-drug treated controls was determined for each well and LC_{50} values were calculated as concentrations

projected to kill 50% of the cells following a 72 h exposure. Results are the average of at least two independent experiments.

Western blot

After 48 hours of treatment, CEMO-1 cells were washed twice with PBS, being the last centrifugation of 4000 rpm for 10 min at 4 ºC. Histone extraction was performed as recommended by Upstate Biotechnology. Briefly, cells were homogenized in 5 volumes of lysis buffer (10 mM HEPES, pH 7.9; 1.5 mM $MgCl_2$; 10 mM KCl; 0.5 mM DTT; protease inhibitor cocktail (Complete Mini, Cat No 11836153301, Roche) and HCl was added to a final concentration of 0.2 M. After incubation on ice for 30 min, the homogenate was centrifuged at 11000 g for 10 min at 4 ºC, and the supernatant was first dialyzed twice against 0.1 M glacial acetic acid (1 hour each time) and then three times against water for 1 hour, 3 hours and overnight, respectively. The histone concentration in the extract was measured using the dye-binding assay of Bradford. 10 µg of histone was separated on 15 % SDS-PAGE gel and transferred to a nitrocellulose membrane. The membrane, after being blocked with Tropix I-block blocking reagent (Cat No AI300, Tropix) in PBS with 0.1 % of Tween-20 and 0.02 NaN_3, was incubated with the primary antibody against H3K9me2 (Mouse monoclonal antibody to Histone H3 dimethyl K9, Cat No ab1220, Abcam) diluted 1:2000 overnight at 4 ºC and then with alkaline phosphatase-conjugated secondary antibodies. Bound antibodies were revealed by a chemiluminiscent reagent (Tropix) and detected using HyperfilmTM enhanced chemilumincescence. Total H3 was used as a loading control (diluted 1:50000 overnight at 4 ºC or for 1 hour at rt) (Anti-Histone H3, CT, pan, rabbit polyclonal, Cat No 07-690, Millipore).

Liquid chromatography tandem-mass spectrometry (LC-MS/MS)

After 48 h of treatment, cells were washed twice with PBS and genomic DNA was extracted using a DNA kit (Nucleo Spin Tissue, Cat No 74095250, Macherey-Nagel) following the manufacturer's instructions. DNA purity and concentration was measured using a NanoDrop spectrophotometer (Thermo Scientific). For the analysis of methylation by mass-spectrometry, 1 μg of genomic DNA was digested with DNA degradase plus (ZYMO RESEARCH) and subjected to mass spectrometry (liquid chromatography electrospray ionization tandem mass spectrometry). All samples were analyzed using an Agilent 1200 liquid chromatograph (Agilent Technologies, Wilmington, DE, USA). An Agilent Zorbax Eclipse XDB-C18 column (2.1 × 150 mm, 3.5 μm particle size, Agilent Technologies, Wilmington, DE, USA) was used.

DNA methylation analysis with Human Methylation array

After 48 h of treatment, cells were washed twice with PBS and genomic DNA was extracted using a DNA kit (Nucleo Spin Tissue, Cat No 74095250, Macherey-Nagel) following the manufacturer's instructions. DNA purity and concentration was measured using a NanoDrop spectrophotometer (Thermo Scientific). 500ng of genomic DNA of MV4-11 controll cell lines and these cells treated with 10nM and 50nM of compound **39c** were bisulfite converted. Converted DNA was hybridized onto the MethylationEPIC BeadChip (Illumina), which interrogate over 850,000 methylation sites quantitatively across the genome at single-nucleotide resolution, as previously described.[73]

CYP Inhibition

The inhibitory effect of the compounds on five human cytochrome P450s (1A2, 2C9, 2C19, 2D6, and 3A4) was evaluated in human liver microsomes at WuXi (http://www.wuxi.com/). Compounds were prepared at 10 μM, and the corresponding substrates for each P450 isoform (20 μL) were incubated with 140 μL of liver microsomes (0.286 mg/mL; BD Gentest) and NADPH cofactor (20 μL, 1 mM) for 10 min at 37 °C. The reaction was terminated by adding 400 μL of cold stop solution (200 ng/mL tolbutamide in ACN), and samples were centrifuged at 1500g for 20min. Supernatants were analyzed by LC-MS/MS (Shimadzu LC 20-AD−API 4000) using the peak area ratio of the analyte/internal standard. Compounds and positive controls were tested in duplicate. The percentage of inhibition was calculated as the ratio of substrate metabolite detected in treated and non-treated wells.

Metabolic Stability

Test compounds (1 μM, 5% MeOH in potassium phosphate buffer) were incubated with human (catalogue no. 452161 from BD Gentest) and mouse (catalogue no. M1000, Xenotech) liver microsomes at 37 °C for 10 min. Liver microsomes were at a final assay concentration of 0.7 mg protein/mL. The reaction was started by the addition of 90 μL of NADP cofactor solution and stopped by the addition of 300 μL of stop solution (ACN at 4 °C, including 100 ng/mL tolbutamide as an internal standard) after 20 min of incubation. The samples were shaken for 5 min and then centrifuged for 20 min at 1500g. A 100 μL aliquot of the supernatant was transferred to eight new 96-well plates with 300 μL of HPLC water and centrifuged at 1500g for LC-MS/MS analysis (Shimadzu LC 10-AD−API 4000). An injection volume of 10 μL was added to a Phenomenex Synergi C18 column eluting with formic acid in water or ACN at a flow rate of 800 μL/min. The percent loss of parent compound was calculated from the peak

area ratio of the analyte/internal standard. Compounds and positive controls were tested in duplicate.

PAMPA Permeability

The permeability of compounds was evaluated with the parallel artificial membrane permeation assay (PAMPA) as an *in vitro* model of passive diffusion. Donor solutions of test compounds (180 µL. 50 µM in PBS/EtOH 70:30) were added to each well of the donor plate, whose PVDF membrane was precoated with 4 µL of a 20 mg×mL^{-1} PBL/dodecane mixture. PBS/EtOH (180 µL) was added to each well of the PTFE acceptor plate. The donor and acceptor plates were combined together and incubated for 18 h at 20 ºC without shaking. In each plate, compounds and controls were tested in duplicate. Drug concentration in the acceptor, the donor, and the reference wells was determined using the UV plate reader with 130 µL of acceptor and donor samples. Permeability rates (Pe in nm s^{-1}) were calculated with Equation (1). The permeability rate of each compound is the averaged value of three independent measurements.

Equation (1) $P_e = C \times \left(-ln\left(1 - \frac{[drug]_{acceptor}}{[drug]_{equilibrium}}\right)\right) \times 10^7$;

here $C = \frac{V_{D \times V_A}}{(V_D + V_A) \times Area \times time}$; V_D = 0.18 mL; V_A = 0.18 mL; Area = 0.32 cm^2; time = 64800 s; D_F = 180/130; $[drug]_{equilibrium} = ([drug]_{donor} \times V_D + [drug]_{acceptor} \times V_A) / (V_D + V_A)$; $[drug]_{donor} = (A_a/A_i*D_F)_{donor}$; $[drug]_{acceptor} = (A_a/A_i*D_F)_{acceptor}$; $A_{a\ donor} = Abs_{donor} - Abs_{vehicle}$; $A_{a\ acceptor} = Abs_{acceptor} - Abs_{vehicle}$, $Ai = Abs_{withoutPBL} - Abs_{vehicle}$.

Quantification of compounds in Plasma Samples (PK studies).

In vivo PK studies had previous approval from the Animal Care and Ethics Committee of the University of Navarra (protocol numbers: 158-12 and 009-16). Compounds were

measured in plasma samples using an Acquity UPLC (Waters, Manchester, UK) coupled to Xevo-TQ MS triple quadropole mass spectrometer with an electrospray ionization (ESI) source. Compound solutions were prepared by dissolving the solid in saline and drug dosages were administered as a single intravenous injection. Blood was collected at predetermined times into EDTA-containing tubes and plasma was obtained via centrifugation (4 ºC, 2500 rpm, 5 min) and stored at -80º C until analysis.

Chromatographic separation was performed by gradient elution at 0.6 mL/min using an Acquity UPLC BEH C18 column (50 x 2.1 mm, 1.7 µm particle size; Waters). Mobile phase consisted of A, water with 0.1% formic acid, and B, methanol with 0.08% formic acid. Autosampler temperature was set at 7 ºC and column temperature at 40 ºC. For detection and quantification, the electrospray ionization operated in the positive mode, and the collision gas used was ultra-pure argon at a flow rate of 0.15 mL min^{-1}. The compound was detected using multiple reaction monitoring (MRM).

Quantification was achieved by external calibration using matrix-matched standards. Concentrations were calculated using a weighted least-squares linear regression ($W = 1/x$). Calibration standards were prepared by adding the appropriate volume of diluted solutions of the compound (made in a mixture of methanol and water, 50:50, v:v) to aliquots of 25 uL of blank plasma. 3% formic acid in methanol was added to precipitate the proteins. The mixture was then agitated for 10 min and centrifuged at 13200 rpm for 20 min at 4º C. A 5 µL aliquot of the resulting supernatant was injected onto the LC-MS/MS system for analysis. Frozen plasma samples were thawed at room temperature, vortexed thoroughly, and subjected to the above described extraction procedure. PK parameters were obtained by fitting the blood concentration-time data to a non-compartmental model with the WinNonlin software (Pharsight, Mountain View, CA).

Parameters estimated included area under the curve (AUC), half-life of the product ($t_{1/2}$), clearance (Cl), and volume of distribution (V_{ss}).

***In vivo* experiments**

All animals studies had previous approval from the Animal Care and Ethics Committee of the University of Navarra (protocol number: 041-15). For the human subcutaneous MV4-11 AML model, $10x10^6$ MV4-11 cells diluted in 100 µL of saline solution were subcutaneously inoculated in the back left flank of BALB/cA- $Rag2^{-/-}\gamma c^{-/-}$ mice between 6 and 8 weeks of age (n=12). The treatment with 2.5 mg/kg (i.v.) of compound **12** was started 1 day after cell inoculation and was administered daily during 21 consecutive days (n=6). The control group (n=6) received only saline solution (diluents of compound **12**). Tumor size was analyzed every 5 days using the following method: V¼ D_d2/2, where D and d corresponding to the longest and shorter diameter, respectively. Mice were killed 23 days after cell inoculation.

Interference compound assessment

Potential PAINS (Pan Assay Interference Compounds) liability of reported compounds was assessed according to the structural filters defined by Baell & Holloway[74] (Charts 3 and 4 and Tables 1-3 of this reference) using a customized Pipeline Pilot protocol.[65] No compound reported in the manuscript matches any of these substructures.

ASSOCIATED CONTENT

SUPPORTING INFORMATION

Protocols for preparative HPLC purification methods (S1)

Synthesis of compound **40** (S2)

Synthesis of intermediates 1 to 3 (S3)

Method for High Resolution Mass Spectrometry of final compounds (S4)

Methods for LCMS, analytical HPLC and UHPLC (S5)

HRMS and purities of final compounds (S6)

HPLC traces of final compounds (S7)

Superposition of the autoinhibited crystal structure of hDNMT1 against the productive crystal structure of mDNMT1 (S8)

Binding mode of compound **23m** into G9a (S9)

Competition experiments performed with compound **23m** (S10)

Results of MethylationEPIC BeadChip assay (S11)

Selectivity profiling of compounds **11** and **39c** against a panel of 14 lysine and arginine methyltransferases and DNMTs (S12)

Plasmatic concentrations of compounds **34a** (S13) and **39c** (S14)

Molecular formula strings and some data.

This material is available free of charge via the Internet at http://pubs.acs.org.

PDB ID Codes:

2, 3K5K; **3**, 3RJW; 4DA4

AUTHOR INFORMATION

Corresponding author

*F. P.: phone, +34 948 194700, ext 825807. E-mail, fprosper@unav.es

*J. O.: phone, +34 948 19 47 00, ext 2044. E-mail, julenoyarzabal@unav.es

Notes

These authors declare no competing financial interest.

ACKNOWLEDGEMENTS

We thank the Foundation for Applied Medical Research (FIMA), University of Navarra (Pamplona, Spain), Asociación de Amigos of University of Navarra as well as to Fundación Fuentes Dutor for financial support. This work has been partially supported through Ministerio de Economía y Competitividad and grants from Instituto de Salud Carlos III PI10/01691, PI13/00862, PI13/01469, PI14/01867, PI16/02024, PI17/00701, RTICC RD12/0036/0068, CIBERONC (CB16/12/00489) (Co-finance with FEDER funds), ERA-NET programs TRANSCAN-2 JTC EPICA by the "Torres Quevedo" Subprogram (PTQ-11-04777 and PTQ-14-07320 I.D.M), Fundacio´ La Marato´ de TV3 (20132130-31-32), Gobierno de Navarra (40/2016, PT053/2016 and PT027/2017) and FSE (Inncorpora-Torres Quevedo grant), Plan Nacional de I+D+I 2013-2016/FEDER (PI15/00892 to M.F.F.), the Asturias Regional Government (GRUPIN14-052 to M.F.F.) and the IUOPA-Obra Social Liberbank-Cajastur. Finally, we would like to thank OpenEye Scientific Software for providing us with an academic license for use of its software.

ABBREVIATIONS

ACN; acetonitrile; AcOH, acetic acid; ADME, absorption, distribution, metabolism and excretion; ALL; acute lymphoblastic leukemia; AML; acute myeloid leukemia; AUC, area under the curve; BINAP, 2,2'-bis(diphenylphosphino)-1,1'-binaphthyl; BOC, *tert*-butoxycarbonyl; BPO, benzoyl peroxide; CDI, 1,1-carbonildiimidazol; Cl, clearance; Cpd, compound; DEAD, diisopropyl azodicarboxylate; DIEA, N,N-Diisopropylethylamine; DLBCL, diffuse large B-cell lymphoma; DME, dimethoxyethane; DMF, dimethylformamide; DMSO, dimethylsulfoxide; DNA, deoxyribonucleic Acid; DNMT, DNA methyltransferase; DTT, *dithiothreitol;* EDTA,

ethylenediaminetetraacetic acid; EHMT2, euchromatic histone methyltransferase 2; ESI-MS, electrospray ionisation mass spectrometry, Et_3N, triethylamine; EtOAc, ethyl acetate; EtOH, ethanol; FDA, food and drug administration; HDAC, histone deacetylase; HEPES, 4-(2-Hydroxyethyl)piperazine-1-ethanesulfonic acid; HIV, human immunodeficiency virus; HLM, human liver microsomes; HPLC, High-performance liquid chromatography; *i*-PrOH, propan-2-ol; iPSCs; inducible pluripotent stem cells; i.v., intravenous; KMT1C, lysine methyltransferase 1C; LCMS, liquid chromatography–mass spectrometry, MDR, multidrug resistance; MeOH, methanol; MLM, mouse liver microsome; m.p., melting point; MRM, multiple reaction monitoring; MST, microscale thermophoresis; MW, microwave; NADPH, nicotinamide adenine dinucleotide phosphate hydrogen; NaOMe, sodium methoxide; NMR, nuclear magnetic resonance; PAMPA, parallel artificial membrane permeability assay; PBS, *phosphate buffered* saline; $Pd_2(dba)_3$, tris(dibenzylideneacetone)dipalladium(0); PDB, protein data bank; pdI-pdC, poly-deoxy inosine poly-deoxy cytosine; Ph, phenyl; PK, pharmacokinetic; PMT, protein methyltransferase; PTFE, polytetrafluoroethylene; PVDF, polyvinylidene difluoride; RNA; ribonucleic acid; rt, room temperature; Rt, retention time; SAH, S-adenosyl-L-homocysteine; SAM, S-adenosyl methionine; SAR, structure-activity relationship; $t_{1/2}$, half-life of the product; *t*-BuOK, potassium *tert*-butoxide; THF, tetrahydrofuran; TLC, thin layer chromatography; TMS, tetramethylsilane; TR-FRET, time-resolved fluorescence resonance energy transfer; UPLC, ultra performance liquid chromatography; UV, ultraviolet; Vss, volume of distribution; xantphos, 4,5-bis(diphenylphosphino)-9,9-dimethylxanthene.

REFERENCES

(1) Helin, K.; Dhanak, D. Chromatin Proteins and Modifications as Drug Targets. *Nature* **2013**, *502* (7472), 480–488.

(2) Portela, A.; Esteller, M. Epigenetic Modifications and Human Disease. *Nat. Biotechnol.* **2010**, *28* (10), 1057–1068.

(3) Rathert, P.; Dhayalan, A.; Murakami, M.; Zhang, X.; Tamas, R.; Jurkowska, R.; Komatsu, Y.; Shinkai, Y.; Cheng, X.; Jeltsch, A. Protein Lysine Methyltransferase G9a Acts on Non-Histone Targets. *Nat. Chem. Biol.* **2008**, *4* (6), 344–346.

(4) Huang, J.; Dorsey, J.; Chuikov, S.; Pérez-Burgos, L.; Zhang, X.; Jenuwein, T.; Reinberg, D.; Berger, S. L. G9a and Glp Methylate Lysine 373 in the Tumor Suppressor p53. *J. Biol. Chem.* **2010**, *285* (13), 9636–9641.

(5) Casciello, F.; Windloch, K.; Gannon, F.; Lee, J. S. Functional Role of G9a Histone Methyltransferase in Cancer. *Front. Immunol.* **2015**, *6*, 487.

(6) Chen, M.-W.; Hua, K.-T.; Kao, H.-J.; Chi, C.-C.; Wei, L.-H.; Johansson, G.; Shiah, S.-G.; Chen, P.-S.; Jeng, Y.-M.; Cheng, T.-Y.; Lai, T.-C.; Chang, J.-S.; Jan, Y.-H.; Chien, M.-H.; Yang, C.-J.; Huang, M.-S.; Hsiao, M.; Kuo, M.-L. H3K9 Histone Methyltransferase G9a Promotes Lung Cancer Invasion and Metastasis by Silencing the Cell Adhesion Molecule Ep-CAM. *Cancer Res.* **2010**, *70* (20), 7830–7840.

(7) Hua, K.-T.; Wang, M.-Y.; Chen, M.-W.; Wei, L.-H.; Chen, C.-K.; Ko, C.-H.; Jeng, Y.-M.; Sung, P.-L.; Jan, Y.-H.; Hsiao, M.; Kuo, M.-L.; Yen, M.-L. The H3K9 Methyltransferase G9a Is a Marker of Aggressive Ovarian Cancer That Promotes Peritoneal Metastasis. *Mol. Cancer* **2014**, *13*, 189.

(8) Zhang, J.; He, P.; Xi, Y.; Geng, M.; Chen, Y.; Ding, J. Down-Regulation of G9a Triggers DNA Damage Response and Inhibits Colorectal Cancer Cells

Proliferation. *Oncotarget* **2015**, *6* (5), 2917–2927.

(9) Kondo, Y.; Shen, L.; Ahmed, S.; Boumber, Y.; Sekido, Y.; Haddad, B. R.; Issa, J.-P. J. Downregulation of Histone H3 Lysine 9 Methyltransferase G9a Induces Centrosome Disruption and Chromosome Instability in Cancer Cells. *PLoS One* **2008**, *3* (4), e2037.

(10) Goyama, S.; Nitta, E.; Yoshino, T.; Kako, S.; Watanabe-Okochi, N.; Shimabe, M.; Imai, Y.; Takahashi, K.; Kurokawa, M. EVI-1 Interacts with Histone Methyltransferases SUV39H1 and G9a for Transcriptional Repression and Bone Marrow Immortalization. *Leukemia* **2010**, *24* (1), 81–88.

(11) Watanabe, H.; Soejima, K.; Yasuda, H.; Kawada, I.; Nakachi, I.; Yoda, S.; Naoki, K.; Ishizaka, A. Deregulation of Histone Lysine Methyltransferases Contributes to Oncogenic Transformation of Human Bronchoepithelial Cells. *Cancer Cell Int.* **2008**, *8* (1), 15.

(12) Lehnertz, B.; Pabst, C.; Su, L.; Miller, M.; Liu, F.; Yi, L.; Zhang, R.; Krosl, J.; Yung, E.; Kirschner, J.; Rosten, P.; Underhill, T. M.; Jin, J.; Hebert, J.; Sauvageau, G.; Humphries, R. K.; Rossi, F. M. The Methyltransferase G9a Regulates HoxA9-Dependent Transcription in AML. *Genes Dev.* **2014**, *28* (4), 317–327.

(13) Imai, K.; Togami, H.; Okamoto, T. Involvement of Histone H3 Lysine 9 (H3K9) Methyltransferase G9a in the Maintenance of HIV-1 Latency and Its Reactivation by BIX01294. *J. Biol. Chem.* **2010**, *285* (22), 16538–16545.

(14) Antignano, F.; Burrows, K.; Hughes, M. R.; Han, J. M.; Kron, K. J.; Penrod, N. M.; Oudhoff, M. J.; Wang, S. K. H.; Min, P. H.; Gold, M. J.; Chenery, A. L.; Braam, M. J. S.; Fung, T. C.; Rossi, F. M. V; McNagny, K. M.; Arrowsmith, C. H.; Lupien, M.; Levings, M. K.; Zaph, C. Methyltransferase G9A Regulates T

Cell Differentiation during Murine Intestinal Inflammation. *J. Clin. Invest.* **2014**, *124* (5), 1945–1955.

(15) Benevento, M.; van de Molengraft, M.; van Westen, R.; van Bokhoven, H.; Nadif Kasri, N. The Role of Chromatin Repressive Marks in Cognition and Disease: A Focus on the Repressive Complex GLP/G9a. *Neurobiol. Learn. Mem.* **2015**, *124*, 88–96.

(16) Epsztejn-Litman, S.; Feldman, N.; Abu-Remaileh, M.; Shufaro, Y.; Gerson, A.; Ueda, J.; Deplus, R.; Fuks, F.; Shinkai, Y.; Cedar, H.; Bergman, Y. De Novo DNA Methylation Promoted by G9a Prevents Reprogramming of Embryonically Silenced Genes. *Nat. Struct. Mol. Biol.* **2008**, *15* (11), 1176–1183.

(17) Shi, Y.; Desponts, C.; Do, J. T.; Hahm, H. S.; Schöler, H. R.; Ding, S. Induction of Pluripotent Stem Cells from Mouse Embryonic Fibroblasts by Oct4 and Klf4 with Small-Molecule Compounds. *Cell Stem Cell* **2008**, *3* (5), 568–574.

(18) Kubicek, S.; O'Sullivan, R. J.; August, E. M.; Hickey, E. R.; Zhang, Q.; Teodoro, M. L.; Rea, S.; Mechtler, K.; Kowalski, J. A.; Homon, C. A.; Kelly, T. A.; Jenuwein, T. Reversal of H3K9me2 by a Small-Molecule Inhibitor for the G9a Histone Methyltransferase. *Mol. Cell* **2007**, *25* (3), 473–481.

(19) Liu, F.; Chen, X.; Allali-Hassani, A.; Quinn, A. M.; Wasney, G. A.; Dong, A.; Barsyte, D.; Kozieradzki, I.; Senisterra, G.; Chau, I.; Siarheyeva, A.; Kireev, D. B.; Jadhav, A.; Herold, J. M.; Frye, S. V; Arrowsmith, C. H.; Brown, P. J.; Simeonov, A.; Vedadi, M.; Jin, J. Discovery of a 2,4-Diamino-7-Aminoalkoxyquinazoline as a Potent and Selective Inhibitor of Histone Lysine Methyltransferase G9a. *J. Med. Chem.* **2009**, *52* (24), 7950–7953.

(20) Vedadi, M.; Barsyte-Lovejoy, D.; Liu, F.; Rival-Gervier, S.; Allali-Hassani, A.; Labrie, V.; Wigle, T. J.; Dimaggio, P. A.; Wasney, G. A.; Siarheyeva, A.; Dong,

A.; Tempel, W.; Wang, S.-C.; Chen, X.; Chau, I.; Mangano, T. J.; Huang, X.-P.; Simpson, C. D.; Pattenden, S. G.; Norris, J. L.; Kireev, D. B.; Tripathy, A.; Edwards, A.; Roth, B. L.; Janzen, W. P.; Garcia, B. A.; Petronis, A.; Ellis, J.; Brown, P. J.; Frye, S. V; Arrowsmith, C. H.; Jin, J. A Chemical Probe Selectively Inhibits G9a and GLP Methyltransferase Activity in Cells. *Nat. Chem. Biol.* **2011**, *7* (8), 566–574.

(21) Liu, F.; Chen, X.; Allali-Hassani, A.; Quinn, A. M.; Wigle, T. J.; Wasney, G. A.; Dong, A.; Senisterra, G.; Chau, I.; Siarheyeva, A.; Norris, J. L.; Kireev, D. B.; Jadhav, A.; Herold, J. M.; Janzen, W. P.; Arrowsmith, C. H.; Frye, S. V; Brown, P. J.; Simeonov, A.; Vedadi, M.; Jin, J. Protein Lysine Methyltransferase G9a Inhibitors: Design, Synthesis, and Structure Activity Relationships of 2,4-Diamino-7-Aminoalkoxy-Quinazolines. *J. Med. Chem.* **2010**, *53* (15), 5844–5857.

(22) Liu, F.; Barsyte-Lovejoy, D.; Li, F.; Xiong, Y.; Korboukh, V.; Huang, X.-P.; Allali-Hassani, A.; Janzen, W. P.; Roth, B. L.; Frye, S. V; Arrowsmith, C. H.; Brown, P. J.; Vedadi, M.; Jin, J. Discovery of an in Vivo Chemical Probe of the Lysine Methyltransferases G9a and GLP. *J. Med. Chem.* **2013**, *56* (21), 8931–8942.

(23) Kim, Y.; Lee, H.-M.; Xiong, Y.; Sciaky, N.; Hulbert, S. W.; Cao, X.; Everitt, J. I.; Jin, J.; Roth, B. L.; Jiang, Y. Targeting the Histone Methyltransferase G9a Activates Imprinted Genes and Improves Survival of a Mouse Model of Prader–Willi Syndrome. *Nat. Med.* **2017**, *23* (2), 213–222.

(24) Sweis, R. F.; Pliushchev, M.; Brown, P. J.; Guo, J.; Li, F.; Maag, D.; Petros, A. M.; Soni, N. B.; Tse, C.; Vedadi, M.; Michaelides, M. R.; Chiang, G. G.; Pappano, W. N. Discovery and Development of Potent and Selective Inhibitors

of Histone Methyltransferase g9a. *ACS Med. Chem. Lett.* **2014**, *5* (2), 205–209.

(25) Srimongkolpithak, N.; Sundriyal, S.; Li, F.; Vedadi, M.; Fuchter, M. J. Identification of 2,4-Diamino-6,7-Dimethoxyquinoline Derivatives as G9a Inhibitors. *Medchemcomm* **2014**, *5* (12), 1821–1828.

(26) Pappano, W. N.; Guo, J.; He, Y.; Ferguson, D.; Jagadeeswaran, S.; Osterling, D. J.; Gao, W.; Spence, J. K.; Pliushchev, M.; Sweis, R. F.; Buchanan, F. G.; Michaelides, M. R.; Shoemaker, A. R.; Tse, C.; Chiang, G. G. The Histone Methyltransferase Inhibitor A-366 Uncovers a Role for G9a/GLP in the Epigenetics of Leukemia. *PLoS One* **2015**, *10* (7), e0131716.

(27) UNC0638 Selective chemical probe for G9a/GLP methyltransferases. http://www.thesgc.org/chemical-probes/UNC0638 (accessed Dec 16, 2016).

(28) Kaniskan, H. Ü.; Konze, K. D.; Jin, J. Selective Inhibitors of Protein Methyltransferases. *J. Med. Chem.* **2015**, *58* (4), 1596–1629.

(29) Schapira, M. Chemical Inhibition of Protein Methyltransferases. *Cell Chem. Biol.* **2016**, *23* (9), 1067–1076.

(30) Lillico, R.; Stesco, N.; Khorshid Amhad, T.; Cortes, C.; Namaka, M. P.; Lakowski, T. M. Inhibitors of Enzymes Catalyzing Modifications to Histone Lysine Residues: Structure, Function and Activity. *Future Med. Chem.* **2016**, *8* (8), 879–897.

(31) Kondengaden, S. M.; Luo, L.-F.; Huang, K.; Zhu, M.; Zang, L.; Bataba, E.; Wang, R.; Luo, C.; Wang, B.; Li, K. K.; Wang, P. G. Discovery of Novel Small Molecule Inhibitors of Lysine Methyltransferase G9a and Their Mechanism in Leukemia Cell Lines. *Eur. J. Med. Chem.* **2016**, *122*, 382–393.

(32) Chen, W.-L.; Wang, Z.-H.; Feng, T.-T.; Li, D.-D.; Wang, C.-H.; Xu, X.-L.; Zhang, X.-J.; You, Q.-D.; Guo, X.-K. Discovery, Design and Synthesis of 6H-

anthra[1,9-Cd]isoxazol-6-One Scaffold as G9a Inhibitor through a Combination of Shape-Based Virtual Screening and Structure-Based Molecular Modification. *Bioorg. Med. Chem.* **2016**, *24* (22), 6102–6108.

(33) Jurkowska, R. Z.; Jurkowski, T. P.; Jeltsch, A. Structure and Function of Mammalian DNA Methyltransferases. *ChemBioChem* **2011**, *12* (2), 206–222.

(34) Baylin, S. B.; Jones, P. A. A Decade of Exploring the Cancer Epigenome - Biological and Translational Implications. *Nat. Rev. Cancer* **2011**, *11* (10), 726–734.

(35) Day, J. J.; Sweatt, J. D. DNA Methylation and Memory Formation. *Nat. Neurosci.* **2010**, *13* (11), 1319–1323.

(36) Di Francesco, A.; Arosio, B.; Falconi, A.; Micioni Di Bonaventura, M. V.; Karimi, M.; Mari, D.; Casati, M.; Maccarrone, M.; D'Addario, C. Global Changes in DNA Methylation in Alzheimer's Disease Peripheral Blood Mononuclear Cells. *Brain, Behav., Immun.* **2015**, *45*, 139–144.

(37) Oh, Y. S.; Kim, S. H.; Cho, G.-W. Functional Restoration of Amyotrophic Lateral Sclerosis Patient-Derived Mesenchymal Stromal Cells Through Inhibition of DNA Methyltransferase. *Cell. Mol. Neurobiol.* **2016**, *36* (4), 613–620.

(38) Grayson, D. R.; Guidotti, A. The Dynamics of DNA Methylation in Schizophrenia and Related Psychiatric Disorders. *Neuropsychopharmacology* **2013**, *38* (1), 138–166.

(39) Robison, A. J.; Nestler, E. J. Transcriptional and Epigenetic Mechanisms of Addiction. *Nat. Rev. Neurosci.* **2011**, *12* (11), 623–637.

(40) Friso, S.; Pizzolo, F.; Choi, S.-W.; Guarini, P.; Castagna, A.; Ravagnani, V.; Carletto, A.; Pattini, P.; Corrocher, R.; Olivieri, O. Epigenetic Control of 11 Beta-Hydroxysteroid Dehydrogenase 2 Gene Promoter Is Related to Human

Hypertension. *Atherosclerosis* **2008**, *199* (2), 323–327.

(41) Dunn, J.; Qiu, H.; Kim, S.; Jjingo, D.; Hoffman, R.; Kim, C. W.; Jang, I.; Son, D. J.; Kim, D.; Pan, C.; Fan, Y.; Jordan, I. K.; Jo, H. Flow-Dependent Epigenetic DNA Methylation Regulates Endothelial Gene Expression and Atherosclerosis. *J. Clin. Invest.* **2014**, *124* (7), 3187–3199.

(42) Williams, K. T.; Schalinske, K. L. Tissue-Specific Alterations of Methyl Group Metabolism with DNA Hypermethylation in the Zucker (Type 2) Diabetic Fatty Rat. *Diabetes/Metab. Res. Rev.* **2012**, *28* (2), 123–131.

(43) Chen, H.; Fan, J.; Shou, Q.; Zhang, L.; Ma, H.; Fan, Y. Hypermethylation of Glucocorticoid Receptor Gene Promoter Results in Glucocorticoid Receptor Gene Low Expression in Peripheral Blood Mononuclear Cells of Patients with Systemic Lupus Erythematosus. *Rheumatol. Int.* **2015**, *35* (8), 1335–1342.

(44) Neary, R.; Watson, C. J.; Baugh, J. A. Epigenetics and the Overhealing Wound: The Role of DNA Methylation in Fibrosis. *Fibrog. Tissue Repair* **2015**, *8* (1), 18.

(45) Foulks, J. M.; Parnell, K. M.; Nix, R. N.; Chau, S.; Swierczek, K.; Saunders, M.; Wright, K.; Hendrickson, T. F.; Ho, K.-K.; McCullar, M. V; Kanner, S. B. Epigenetic Drug Discovery: Targeting DNA Methyltransferases. *J. Biomol. Screen.* **2012**, *17* (1), 2–17.

(46) Issa, J.-P. J.; Roboz, G.; Rizzieri, D.; Jabbour, E.; Stock, W.; O'Connell, C.; Yee, K.; Tibes, R.; Griffiths, E. A.; Walsh, K.; Daver, N.; Chung, W.; Naim, S.; Taverna, P.; Oganesian, A.; Hao, Y.; Lowder, J. N.; Azab, M.; Kantarjian, H. Safety and Tolerability of Guadecitabine (SGI-110) in Patients with Myelodysplastic Syndrome and Acute Myeloid Leukaemia: A Multicentre, Randomised, Dose-Escalation Phase 1 Study. *Lancet. Oncol.* **2015**, *16* (9), 1099–1110.

(47) Erdmann, A.; Halby, L.; Fahy, J.; Arimondo, P. B. Targeting DNA Methylation with Small Molecules: What's Next? *J. Med. Chem.* **2015**, *58* (6), 2569–2583.

(48) Xu, P.; Hu, G.; Luo, C.; Liang, Z. DNA Methyltransferase Inhibitors: An Updated Patent Review (2012-2015). *Expert Opin. Ther. Pat.* **2016**, *26* (9), 1017–1030.

(49) Datta, J.; Ghoshal, K.; Denny, W. A.; Gamage, S. A.; Brooke, D. G.; Phiasivongsa, P.; Redkar, S.; Jacob, S. T. A New Class of Quinoline-Based DNA Hypomethylating Agents Reactivates Tumor Suppressor Genes by Blocking DNA Methyltransferase 1 Activity and Inducing Its Degradation. *Cancer Res.* **2009**, *69* (10), 4277–4285.

(50) Estève, P.-O.; Chin, H. G.; Smallwood, A.; Feehery, G. R.; Gangisetty, O.; Karpf, A. R.; Carey, M. F.; Pradhan, S. Direct Interaction between DNMT1 and G9a Coordinates DNA and Histone Methylation during Replication. *Genes Dev.* **2006**, *20* (22), 3089–3103.

(51) Tachibana, M.; Matsumura, Y.; Fukuda, M.; Kimura, H.; Shinkai, Y. G9a/GLP Complexes Independently Mediate H3K9 and DNA Methylation to Silence Transcription. *EMBO J.* **2008**, *27* (20), 2681–2690.

(52) Wozniak, R. J.; Klimecki, W. T.; Lau, S. S.; Feinstein, Y.; Futscher, B. W. 5-Aza-2'-deoxycytidine-Mediated Reductions in G9A Histone Methyltransferase and Histone H3 K9 Di-Methylation Levels Are Linked to Tumor Suppressor Gene Reactivation. *Oncogene* **2007**, *26* (1), 77–90.

(53) San José-Enériz, E.; Agirre, X.; Rabal, O.; Vilas-Zornoza, A.; Sánchez-Arias, J. A.; Miranda, E.; Ugarte, A.; Roa, S.; Paiva, B.; Estella-Hermoso de Mendoza, A.; Alvarez, R. M.; Casares, N.; Segura, V.; Martín-Subero, J. I.; Ogi, F.-X.; Soule, P.; Santiveri, C. M.; Campos-Olivas, R.; Castellano, G.; Garcia Fernandez de

Barrena, M.; Rodriguez-Madoz, J. R.; García-Barchino, M. J.; Lasarte, J. J.; Avila, M. A.; Martinez-Climent, J. A.; Oyarzabal, J.; Prosper, F. Discovery of First-in-Class Reversible Dual Small Molecule Inhibitors against G9a and DNMTs with in Vivo Activity in Hematological Malignancies. *Nat. Commun.* **2017**, *8*, 15424.

(54) Sharma, S.; Gerke, D. S.; Han, H. F.; Jeong, S.; Stallcup, M. R.; Jones, P. A.; Liang, G. Lysine Methyltransferase G9a Is Not Required for DNMT3A/3B Anchoring to Methylated Nucleosomes and Maintenance of DNA Methylation in Somatic Cells. *Epigenetics Chromatin* **2012**, *5* (1), 3.

(55) Chang, Y.; Zhang, X.; Horton, J. R.; Upadhyay, A. K.; Spannhoff, A.; Liu, J.; Snyder, J. P.; Bedford, M. T.; Cheng, X. Structural Basis for G9a-like Protein Lysine Methyltransferase Inhibition by BIX-01294. *Nat. Struct. Mol. Biol.* **2009**, *16* (3), 312–317.

(56) Rotili, D.; Tarantino, D.; Marrocco, B.; Gros, C.; Masson, V.; Poughon, V.; Ausseil, F.; Chang, Y.; Labella, D.; Cosconati, S.; Di Maro, S.; Novellino, E.; Schnekenburger, M.; Grandjenette, C.; Bouvy, C.; Diederich, M.; Cheng, X.; Arimondo, P. B.; Mai, A. Properly Substituted Analogues of BIX-01294 Lose Inhibition of G9a Histone Methyltransferase and Gain Selective Anti-DNA Methyltransferase 3A Activity. *PLoS One* **2014**, *9* (5), e96941.

(57) Rilova, E.; Erdmann, A.; Gros, C.; Masson, V.; Aussagues, Y.; Poughon-Cassabois, V.; Rajavelu, A.; Jeltsch, A.; Menon, Y.; Novosad, N.; Gregoire, J.-M.; Vispé, S.; Schambel, P.; Ausseil, F.; Sautel, F.; Arimondo, P. B.; Cantagrel, F. Design, Synthesis and Biological Evaluation of 4-Amino-N- (4-Aminophenyl)benzamide Analogues of Quinoline-Based SGI-1027 as Inhibitors of DNA Methylation. *ChemMedChem* **2014**, *9* (3), 590–601.

(58) Yoo, J.; Choi, S.; Medina-Franco, J. L. Molecular Modeling Studies of the Novel Inhibitors of DNA Methyltransferases SGI-1027 and CBC12: Implications for the Mechanism of Inhibition of DNMTs. *PLoS One* **2013**, *8* (4), e62152.

(59) Joshi, M.; Rajpathak, S. N.; Narwade, S. C.; Deobagkar, D. Ensemble Based Virtual Screening and Experimental Validation of Inhibitors Targeting a Novel Site of Human DNMT1. *Chem. Biol. Drug Des.* **2016**, *88* (1), 5–16.

(60) Valente, S.; Liu, Y.; Schnekenburger, M.; Zwergel, C.; Cosconati, S.; Gros, C.; Tardugno, M.; Labella, D.; Florean, C.; Minden, S.; Hashimoto, H.; Chang, Y.; Zhang, X.; Kirsch, G.; Novellino, E.; Arimondo, P. B.; Miele, E.; Ferretti, E.; Gulino, A.; Diederich, M.; Cheng, X.; Mai, A. Selective Non-Nucleoside Inhibitors of Human DNA Methyltransferases Active in Cancer Including in Cancer Stem Cells. *J. Med. Chem.* **2014**, *57* (3), 701–713.

(61) Medina-Franco, J. L.; Yoo, J. Molecular Modeling and Virtual Screening of DNA Methyltransferase Inhibitors. *Curr. Pharm. Des.* **2013**, *19* (12), 2138–2147.

(62) Song, J.; Teplova, M.; Ishibe-Murakami, S.; Patel, D. J. Structure-Based Mechanistic Insights into DNMT1-Mediated Maintenance DNA Methylation. *Science* **2012**, *335* (6069), 709–712.

(63) Song, J.; Rechkoblit, O.; Bestor, T. H.; Patel, D. J. Structure of DNMT1-DNA Complex Reveals a Role for Autoinhibition in Maintenance DNA Methylation. *Science* **2011**, *331* (6020), 1036–1040.

(64) Zhang, Z.-M.; Liu, S.; Lin, K.; Luo, Y.; Perry, J. J.; Wang, Y.; Song, J. Crystal Structure of Human DNA Methyltransferase 1. *J. Mol. Biol.* **2015**, *427* (15), 2520–2531.

(65) Accelrys Software Inc. Pipeline Pilot, Version 9.5. San Diego, CA 2015.

(66) Liu, F.; Barsyte-Lovejoy, D.; Allali-Hassani, A.; He, Y.; Herold, J. M.; Chen, X.;

Yates, C. M.; Frye, S. V.; Brown, P. J.; Huang, J.; Vedadi, M.; Arrowsmith, C. H.; Jin, J. Optimization of Cellular Activity of G9a Inhibitors 7-Aminoalkoxy-Quinazolines. *J. Med. Chem.* **2011**, *54* (17), 6139–6150.

(67) Rabal, O.; Sánchez-Arias, J. A.; Cuadrado-Tejedor, M.; de Miguel, I.; Pérez-González, M.; García-Barroso, C.; Ugarte, A.; Estella-Hermoso de Mendoza, A.; Sáez, E.; Espelosin, M.; Ursua, S.; Haizhong, T.; Wei, W.; Musheng, X.; Garcia-Osta, A.; Oyarzabal, J. Design, Synthesis, and Biological Evaluation of First-in-Class Dual Acting Histone Deacetylases (HDACs) and Phosphodiesterase 5 (PDE5) Inhibitors for the Treatment of Alzheimer's Disease. *J. Med. Chem.* **2016**, *59* (19), 8967–9004.

(68) Rabal, O.; Oyarzabal, J. Biologically Relevant Chemical Space Navigator: From Patent and Structure-Activity Relationship Analysis to Library Acquisition and Design. *J. Chem. Inf. Model.* **2012**, *52* (12), 3123–3137.

(69) Perrin, C. L.; Fabian, M. A.; Rivero, I. A. Basicities of Cycloalkylamines: Baeyer Strain Theory Revisited. *Tetrahedron* **1999**, *55* (18), 5773–5780.

(70) Klco, J. M.; Spencer, D. H.; Lamprecht, T. L.; Sarkaria, S. M.; Wylie, T.; Magrini, V.; Hundal, J.; Walker, J.; Varghese, N.; Erdmann-Gilmore, P.; Lichti, C. F.; Meyer, M. R.; Townsend, R. R.; Wilson, R. K.; Mardis, E. R.; Ley, T. J. Genomic impact of transient low-dose decitabine treatment on primary AML cells. *Blood* **2013**, *121* (9), 1633–1643.

(71) Hagemann, S.; Heil, O.; Lyko, F.; Brueckner, B. Azacytidine and decitabine induce gene-specific and non-random DNA demethylation in human cancer cell lines. *PLoS One* **2011**, *6* (3):e17388.

(72) Rabal, O.; Sánchez-Arias, J. A.; San José-Enériz, E.; Agirre, X.; de Miguel, I.; Garate, L.; Miranda, E.; Sáez, E.; Roa, S.; Martínez-Climent, J. Á.; Liu, Y.; Wei,

W.; Musheng, X.; Prosper, F.; Oyarzabal, J. Detailed Exploration around 4-Aminoquinolines Chemical Space to Navigate the Lysine Methyltransferase G9a and DNA Methyltransferase Biological Spaces. *Just Accepted in J Med Chem,* **DOI:** 10.1021/acs.jmedchem.7b01925

(73) Agirre, X.; Castellano, G.; Pascual, M.; Heath, S.; Kulis, M.; Segura, V.; Bergmann, A.; Esteve, A.; Merkel, A.; Raineri, E.; Agueda, L.; Blanc, J.; Richardson, D.; Clarke, L.; Datta, A.; Russiñol, N.; Queirós, A. C.; Beekman, R.; Rodríguez-Madoz, J. R.; San José-Enériz, E.; Fang, F.; Gutiérrez, N. C.; García-Verdugo, J. M.; Robson, M. I.; Schirmer, E. C.; Guruceaga, E.; Martens, J. H. A.; Gut, M.; Calasanz, M. J.; Flicek, P.; Siebert, R.; Campo, E.; Miguel, J. F. S.; Melnick, A.; Stunnenberg, H. G.; Gut, I. G.; Prosper, F.; Martín-Subero, J. I. Whole-Epigenome Analysis in Multiple Myeloma Reveals DNA Hypermethylation of B Cell-Specific Enhancers. *Genome Res.* **2015**, *25* (4), 478–487.

(74) Baell, J. B.; Holloway, G. A. New Substructure Filters for Removal of Pan Assay Interference Compounds (PAINS) from Screening Libraries and for Their Exclusion in Bioassays. *J. Med. Chem.* **2010**, *53* (7), 2719–2740.

Table of Contents Graphic